Lisa Steiner

Aging and Storage Stability
of Pyrolysis Oils

MASTER THESIS

For obtaining the Academic Degree of

Diplomingenieur

Master Studies
Chemical and Pharmaceutical Engineering

Graz University of Technology

Graz University of Technology

Supervisor:
Dipl.-Ing. Dr.techn. Nikolaus Schwaiger
Institute of Chemical Engineering and Environmental Technology

Graz, September 2013

EIDESSTATTLICHE ERKLÄRUNG

Ich erkläre an Eides statt, dass ich die vorliegende Arbeit selbstständig verfasst, andere als die angegebenen Quellen/Hilfsmittel nicht benutzt, und die den benutzten Quellen wörtlich und inhaltlich entnommene Stellen als solche kenntlich gemacht habe.

Graz, am ……………………………   …………………………………………………..
                                                                                        (Unterschrift)

STATUTORY DECLARATION

I declare that I have authored this thesis independently, that I have not used other than the declared sources / resources, and that I have explicitly marked all material which has been quoted either literally or by content from the used sources.

……………………………   …………………………………………………..
        date   (signature)

Abstract

The ever-depleting resources of oil have to be replaced by renewable, sustainable energy carriers as soon as possible. Before such bio-oils can be introduced into markets, it is of utmost importance to investigate their storage and aging behavior. For that reason, two topics were investigated in this thesis: firstly, the implementation of a gel permeation chromatography, GPC, measurement system, for the analysis of bio-oils and secondly, the investigation of the storage and aging behavior of bio-oils.

It is found out that bio-oils can be analyzed with GPC. However, various non-idealities are caused by substances contained in minor and major amounts in the bio-oils. Molecular mass distributions can be attributed to pyrolysis oils and hydrodeoxygenated pyrolysis oils via a calibration. However, molecular mass distributions cannot be attributed to coal liquefaction oils due to their high content in aromatic compounds. Furthermore, quantification is not possible for bio-oils because of non-valid assumptions concerning detection via a refractive index detector.

In order to investigate the storage stability of bio-oils, two pyrolysis experiments, one hydrodeoxygenation experiment and two coal liquefaction experiments were conducted. The products were stored in tightly closed glass bottles in a dark box at room temperature for 10 weeks. Analyses were carried out daily in the first week, then weekly and then fortnightly.

The dynamic viscosity of the pyrolysis oils increases within the first week of storage, then the increase rate becomes constant at a lower value. The viscosity of the hydrodeoxygenated pyrolysis oil increases strongly over time. Via GPC analyses, a shift to higher molecular masses is observed for the pyrolysis oils, the hydrodeoxygenated pyrolysis oil and the coal liquefaction oils. However, the shift is more pronounced in the pyrolysis oils than in the hydrodeoxygenated pyrolysis oil. Concerning gas chromatography-mass spectroscopy analysis, acid concentration measurements, pH-value measurements and water content measurements, no specific trends over storage time are observed for the pyrolysis oils and the hydrodeoxygenated pyrolysis oil. Furthermore, no phase separation occurs and neither a change in solubilites nor visual changes are observed.

Kurzfassung

Da die Rohölvorräte bald erschöpft sein werden, müssen so schnell wie möglich erneuerbare, nachhaltige Energieträger als Ersatz gefunden werden. Bevor solche Bioöle marktreif sind, ist es von größter Bedeutung, über deren Lagerungs- und Alterungsverhalten Bescheid zu wissen. Aus diesem Grund wurden in dieser Diplomarbeit zwei Themen untersucht: erstens die Untersuchung des Lagerungs- und Alterungsverhaltens der Bioöle, und zweitens die Inbetriebnahme und Verwendung eines Gelpermeationschromatographie-Messsystems, GPC, um die Bioöle zu analysieren.

Es zeigte sich, dass es möglich ist, Bioöle mit GPC zu analysieren. Allerdings treten verschiedene Nichtidealitäten auf, die durch Haupt- oder Nebenkomponenten verursacht werden. Molmassenverteilungen können mithilfe einer Kalibration den Pyrolyseölen und den hydrodeoxygenierten Pyrolyseölen zugeordnet werden. Aufgrund des hohen Gehalts an aromatischen Komponenten kann den Kohleverflüssigungsölen keine Molmassenverteilung zugeordnet werden. Außerdem ist keine Quantifizierung der Bioöle möglich, da einige Annahmen zur Detektion des Brechungsindex für die Komponenten der Bioöle nicht gültig sind.

Um das Lagerungsverhalten von Bioölen zu untersuchen wurden zwei Pyrolyseexperimente, ein Hydrodeoxygenierungsexperiment und zwei Kohleverflüssigungsexperimente durchgeführt. Die Produkte wurden für 10 Wochen in dicht verschlossenen Glasflaschen unter Lichtausschluss bei Raumtemperatur gelagert. Die Analysen wurden nach der Herstellung eine Woche lang täglich, danach wöchentlich und dann alle zwei Wochen durchgeführt.

Die dynamische Viskosität der Pyrolyseöle steigt innerhalb der ersten Lagerungswoche, danach bleibt die Zuwachsrate auf niedrigem Niveau konstant. Die Viskosität des hydrodeoxygenierten Pyrolyseöls steigt mit der Zeit stark an. Durch die GPC Analysen wird eine Verschiebung zu höheren Molmassen beobachtet und zwar für die Pyrolyseöle, für das hydrodeoxygenierte Pyrolyseöl und die Kohleverflüssigungsöle. Allerdings ist diese Verschiebung bei den Pyroylseölen viel ausgeprägter als bei dem hydrodeoxygenierten Pyrolyseöl. Bei der Gaschromatographie-Massenspektroskopie-Analyse, der Säurekonzentrationsmessung, der Messung des pH-Wertes und der Wassergehaltmessung der Pyrolyseöle und des hydrodeoxygenierten Pyrolyseöls werden keine Trends mit zunehmender Lagerungsdauer beobachtet. Außerdem kommt es zu keiner Phasentrennung, und weder Änderungen der Löslichkeiten, noch sichtbare Veränderungen werden beobachtet.

Acknowledgement

Contents

Contents

List of Figures

List of Tables

List of Abbreviations

ASTM	American Society for Testing and Materials
CL1, CL2	Liquid phase product of the coal liquefaction experiments 1 and 2
DCL	Direct coal liquefaction
DH1	Organic phase product of the deep hydrodeoxygenation experiment
DME	Dimethyl ether
E-VGO	Entrained vacuum gas oil
FID	Flame ionization detector
GPC	Gel permeation chromatography
HHV	Higher heating value
HOAc	Acetic acid
LPP	Liquid phase pyrolysis
n.d.	Not determined
OOT	Oxidation onset temperature
PAH	Polycyclic aromatic hydrocarbons
PCS	Process control system
PO	Pyrolysis oil
POww	Pyrolysis oil, water content reduced via thin-film-evaporation
PS	Polystyrene
PSS	Polymer Standard Service
PY1, PY2	heavy organic phase product of the pyrolysis experiments 1 and 2
RI	Refractive index
RID	Refractive index detector
SEC	Size exclusion chromatography
TFA	Trifluoroacetic acid
THF	Tetrahydrofuran
VGO	Vacuum gas oil

1. Introduction

It is long established that the resources of crude oil are finite. Furthermore, due to ever-increasing amounts of green house gases in the atmosphere, it is of paramount importance to replace crude oil by biogenic, renewable and sustainable fuels. Bio-oils produced by the biomass-to-liquid, BtL process, meet these demands. In this process, bio-oils are derived from the pyrolysis of wood.

In order to minimize harmful effects on the environment, many investigations have to be conducted. Efficient catalysts have to be found, as well as the lowest possible reaction temperature and the shortest possible reaction time. Thus, ecological as well as economical advantages can be achieved. Furthermore, by liquefying the bio-char, which is a by-product of the pyrolysis, the overall process efficiency can be increased. However, before these bio-oils are introduced into the markets, it is of utmost importance to know about the storage and aging behavior.

Although many publications exist about different pyrolysis processes, as well as about hydrodeoxygenation and coal liquefaction, surprisingly few literature exists about the long term stability. However, knowledge about possible changes during storage are essential: phase separation has to be avoided, the water content should be constant as well as the solubilities. Moreover, the viscosity should not change in order to design the pumps and injectors accordingly.

Another interesting aspect when monitoring the aging of bio-oils is the molecular mass distribution of the bio-oils. Gel permeation chromatography is a powerful technique for the determination of the molecular mass distribution. However, as it has originally been developed to investigate polymers, special aspects for the analysis of bio-oils have to be taken into account.

Astonishingly, these pitfalls are ignored in many publications. Assumptions that are true for the investigation of polymers are transferred to the interpretation of bio-oil elution chromatograms without questioning their validity. Polymers, which only vary in the number of monomer units and thus the chain length, are very similar in terms of chemical properties, functional groups, convolution in the eluent etc.

However, bio-oils contain many different substances belonging to various chemical classes like alkanes, aldehydes and ketones, alcohols, carboxylic acids etc. Hence these substances exhibit very different chemical properties. Precaution must be taken if the assumptions applied for the data processing of polymer analyses are adopted for the analysis of bio-oils. Further investigations regarding these assumptions have to be conducted. The behavior during the separation in the separation

columns has to be investigated as well as the behavior for the refractive index detection in order to see if the assumptions are valid.

This thesis is organized in three main chapters: the chapter **Basics**, chapter 2, the chapter **Experimental**, chapter 3 and the chapter **Results and Discussion**, chapter 4. Each of the three main chapters consists of the three processes of the BtL concept: the pyrolysis process, the hydrodeoxygenation process and the coal liquefaction process. Furthermore, a section about the aging is contained as well as a section about analytics.

In the first chapter, the basics chapter, a theoretical background is given along with a summary of the state-of-the-art in the respective fields. In the second chapter, the experimental chapter, all conducted experiments are described in detail. It is explained how the aging should be monitored. Furthermore, the applied analytical techniques are elucidated. Finally, in the third chapter, the results and discussion chapter, all results are presented and discussed and possible further investigation options are given.

2. Basics

2.1. Pyrolysis

Pyrolysis is the thermochemical decomposition of organic matter. In contrast to combustion, additional oxygen is excluded from the process. Both changes in chemical composition and in physical properties occur, which are irreversible. Three product groups are obtained: solids, condensible volatiles and non-condensible volatiles.

Various types of feedstock are used for pyrolysis: wood, bark, agricultural wastes/ residues, nuts and seeds, algae, grasses or forestry residues.[1] As this work only deals with the pyrolysis of wood, feedstock other than wood is not included in the theory part.

2.1.1. Wood

Hardwood and softwood are the two main types of wood, differing in density, cell dimensions, and the percentage of different cell types. Spruce wood (picea abies) is used for pyrolysis in this work, and since spruce is a softwood, the focus is put on softwood.
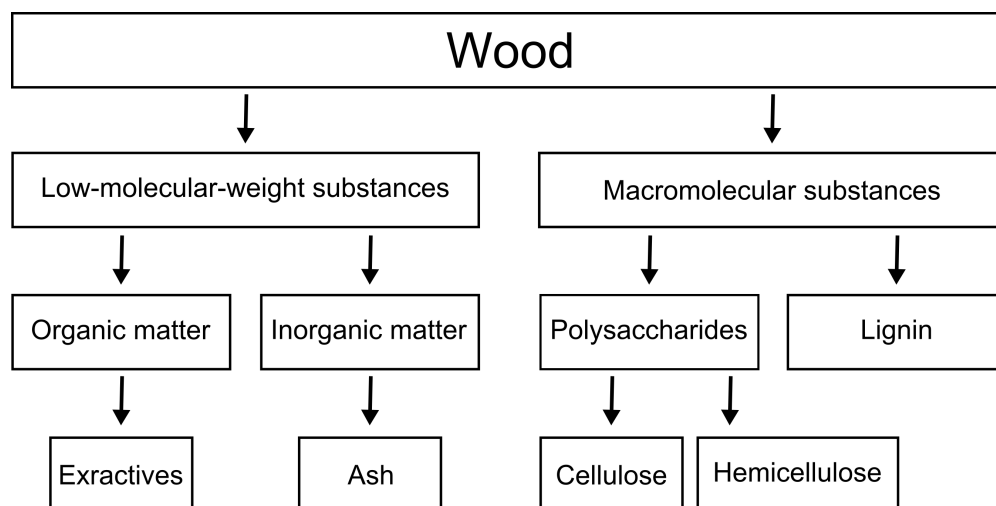
Figure 2.1.: Scheme of the wood components

Wood consists of approx. 50 wt% of carbon, 43 wt% of oxygen and 6 wt% of hydrogen, which corresponds to an average chemical formula of $CH_{1.68}O_{0.86}$[2]. In

general, wood consists mainly of three basic macromolecular units: lignin, cellulose and hemicellulose. Figure 2.1 depicts the composition.

By far the most abundant component is cellulose, as it constitutes approx. one half of the tissue. Besides the other two major macromolecular components, hemicellulose and lignin, minor macromolecular components are polymeric substances like starch, pectic substances and proteins. Furthermore, the low-molecular substances are divided into organic and inorganic low-molecular substances.

The organic low-molecular substances are also called extractives and comprise aromatic phenolic compounds, terpenes, aliphatic acids and alcohols. The inorganic low-molecular substances are called ash, the mineral components are mainly potassium, calcium and magnesium, only contained in very small amounts. The detailed composition of the European spruce is given in Table 2.1.

Table 2.1.: Composition of the European spruce[2], n.d.: not determined

Holocellulose	Cellulose	Polyoses	Pentosan	Lignin	Ash
80.9	46.0	15.3	8.3	27.3	n.d.
82.5	40.4	31.1	n.d.	28.2	0.3

The variations in the reported data arise not only from variations in the respective wood composition but also from different analysis methods, n.d. is short for not determined.

Holocellulose comprises all polysaccharides, thus cellulose and hemicellulose, while polyoses is another name for the hemicelluloses. Pentosan refers to polymers made up of pentoses, monosaccharides with five carbon atoms and ash consists of the inorganic material contained in wood.[2]

Cellulose

Cellulose consists of β-D-glucose. The glucose units are linked via β-(1→4)-glycosidic linkages, thus cellulose is a linear polymer. The stereochemical formula is shown in Figure 2.2.

The repeating unit of the chain is a cellobiose unit, two glycosidicly-linked glucose units. The reducing end is on the right, the non-reducing on the left. A sugar is a reducing sugar if it has an aldehyde group or is able to form one by isomerization[3].
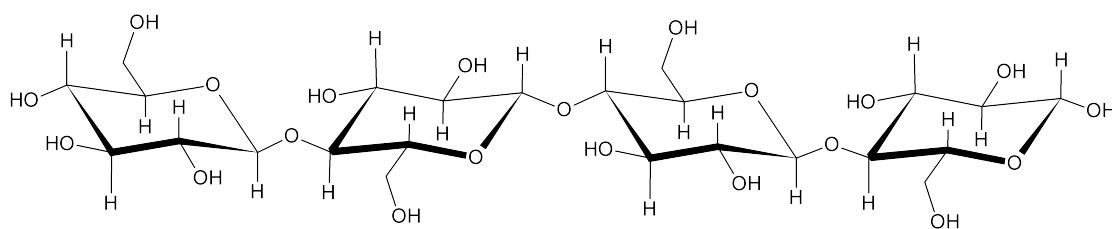
Figure 2.2.: Stereochemical formula of cellulose - two cellobiose units are shown

Hemicellulose

Hemicelluloses are also called polyoses. They consist mainly of five different neutral sugars, namely glucose, mannose, galactose, xylose and arabinose, see Figure 2.3.

(a) Glucose   (b) Mannose   (c) Galactose   (d) Xylose   (e) Arabinose
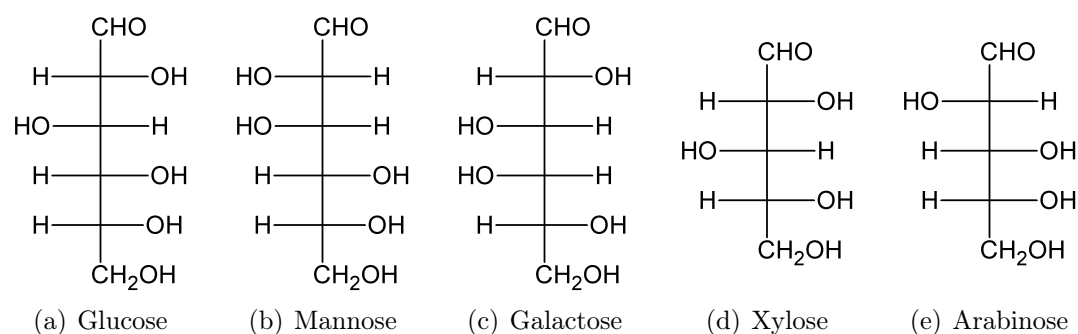
Figure 2.3.: Main sugars contained in hemicellulose

The amounts of the non-glucosic sugars in spruce hemicellulose are given in Table 2.2.

Table 2.2.: Non-glucosic sugars in spruce hemicellulose[4]

Mannose	Galactose	Xylose	Arabinose
[%]	[%]	[%]	[%]
13.6	2.8	5.6	1.2

The polyoses are in close association with the cellulose. However, the molecular chains are shorter than the chains of cellulose, and they may possess side-groups and branches. Due to the side-groups and branches, hydrogen bonds cannot be established easily. Thus, hemicellulose is more water-soluble than cellulose. The chains may consist of only one sugar unit, then the chain is a homopolymer, or of different sugar units, building a heteropolymer[4].

Lignin

The third main component of wood, lignin, differs from cellulose and hemicellulose as the main building units are not sugars but phenylpropane units, building an aromatic system. The most abundant building units of lignin are p-coumaryl alcohol, coniferyl alcohol and sinapyl alcohol, depicted in Figure 2.4.

(a) P-coumaryl alcohol   (b) Coniferyl alcohol   (c) Sinapyl alcohol
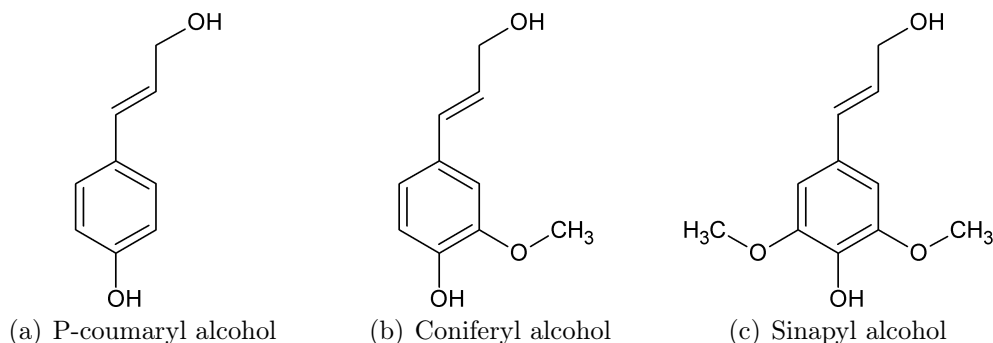
Figure 2.4.: Building units of lignin

The biosynthesis of lignin is very complex, the general reaction is a dehydrogenative polymerization. The coupling reactions of the different phenylpropane units are random, resulting in a non-linear polymer with many side-groups and branches.

The incorporation of the different units depends on their reactivity and frequency in the wood tissue. The most common linkage is the aryl ether β-O-4 linkage, but also carbon-carbon linkages exist.

The average elemental composition of spruce lignin is shown in Table 2.3, this corresponds to a chemical formula of $CH_{1.18}O_{0.42}$[5].

Table 2.3.: Elemental composition of spruce lignin[5]

C	H	O
%	%	%
62.3	5.7	32.0

Concerning the low-molecular substances, both organic and inorganic substances are only contained in minor amounts. The low protein content of wood is advantageous as the amount of nitrogen oxides formed during reaction is intrinsically low[2].

2.1.2. Pyrolysis

Various types of pyrolysis are found in the literature. However, exact definitions and consistent classifications do not exist. In general, it is distinguished between conventional pyrolysis, flash pyrolysis, and liquid phase pyrolysis, the main differences being the residence time in the reactor, the heating rate, the temperature and the target product[1].

2.1.2.1. Liquid Phase Pyrolysis

In liquid phase pyrolysis, LPP, a liquid heat carrier oil is used to transfer heat from the reactor walls to the wood chips. In detail, the heat carrier oil is heated in the reactor, when the temperature is attained, the wood chips are added. The obvious advantages are a fast heat transfer and a more uniform temperature field. Furthermore, the formation of dust is avoided, thus improving the operation feasibility.
The liquid heat carrier can be recycled. Products obtained by LPP are noncondensibles, pyrolysis oil, PO, and bio-char, PO being the target product. Typical process conditions and product distribution of LPP of spruce wood are summarized in Table 2.4.

Table 2.4.: Process conditions and product distribution of LPP[6]

Temperature	Pressure	Liquid yield	Bio-char	Gas
[°C]	[bar]	[wt%]	[wt%]	[wt%]
350	ambient	40-44	37-40	13-16

The yield, water content and elemental composition of PO (spruce wood) obtained by LPP are shown in Table 2.5.

Table 2.5.: Yield, water content and elemental composition of PO obtained by LPP[7]

Yield	Water	C	H
[wt%]	[wt%]	[wt%]	[wt%]
42	39	31.5	8.5

Due to the fact that LPP is a rather mild pyrolysis method, a major part of the lignin frame stays intact, thus constituting the bigger part of the bio-char, while cellulose and hemicellulose structures are more easily broken down and they are contained in all the reaction products.

Table 2.6 depicts the mass balances of cellulose, hemicellulose, lignin, and the overall mass balance of spruce wood. It shows how the different macromolecular substances are distributed among the different product categories, e.g. what percentage of cellulose is found in the liquid CHO-product, the solid, the gaseous product and in water, respectively[6,7].

Table 2.6.: Distribution of the macromolecular substances among liquid CHO-, solid and gaseous products and water[6]

	Cellulose	Hemicellulose	Lignin	Spruce wood
	[wt%]	[wt%]	[wt%]	[wt%]
Liquid CHO-products	34	16	6	26
Bio-char	29	44	79	40
Gas	16	21	9	17
Water formed by reaction	21	19	6	17

It was investigated whether various reaction parameters like reaction temperature have an influence on the product distribution and yield of spruce wood pyrolysis. It was found that the temperature has a major influence on the product distribution, see Table 2.7.

Table 2.7.: Influence of the reaction temperature on the product distribution[6]

Temperature	PO	Bio-char	Reaction water
[°C]	[wt%]	[wt%]	[wt%]
350	25	39	17
390	36	27	15

The higher the reaction temperature, the more liquid products are obtained. However, the degradation of the liquid heat carrier also increases with increasing temperature.

Furthermore, the influence of the particle size of the biomass was investigated. It was determined that for particle sizes within the range of 630 μm to 10 mm, no influence exists[8].

2.2. Hydrodeoxygenation

2.2.1. Comparison of Pyrolysis Oil to Crude Oil

Pyrolysis oil cannot be used in existing crude oil processing infrastructure nor in engines etc., as PO differs from conventional liquid energy carriers and fuels in many ways, see Table 2.8.

Table 2.8.: Comparison of PO and crude oil[9]

		PO	Crude oil
Water	[wt%]	15-30	0.1
pH value	[-]	2.8-3.8	-
Density	[g/cm^3]	1.05-1.25	0.86
Viscosity (50 °C)	[mPa s]	40-100	180
HHV	[MJ/kg]	16-19	44
C	[wt%]	55-65	83-86
O	[wt%]	28-40	<1
H	[wt%]	5-7	11-14
S	[wt%]	<0.05	<4
N	[wt%]	<0.4	<1
Ash	[wt%]	<0.2	0.1

As shown in Table 2.8, one of the major differences is the very high oxygen content. Whereas crude oil only contains minor amounts of oxygen and consists predominantly of hydrocarbons, PO contains many oxygenated species. Among the oxygenated species are various functional groups, like alcohols, ethers, esters, organic acids, aldehydes and ketones.

While some functionalities are not important or even advantageous (e.g. ethers like methyl-tert-butyl-ether in gasoline), others may pose serious problems, like organic acids. The organic acids are responsible for the high acidity and the very low pH-value of PO.

Major problems arise from the low pH-value, as the acids will attack construction material in existing infrastructure. Special alloys, linings etc. would be necessary for storage and handling of POs, resulting in high costs. In order to avoid the necessity of expensive infrastructure, the pH-value of PO should be increased by removing or transforming the organic acids fraction.

Furthermore, the higher heating value, HHV, of PO is considerably lower, mainly due to the high amount of oxygen-containing components and the high water con-

tent compared to crude oil. In order to increase the energy contained per weight unit, water should be removed. Advantages of PO compared to crude oil are the low content of sulfur and of nitrogen, making the hydrodesulphurization processes used in crude oil processing redundant for PO. Moreover, almost no nitrogen oxides will be emitted during combustion.[9]

2.2.2. Hydrodeoxygenation

In order to solve the aforementioned problems, a process called hydrodeoxygenation, HDO, is used. The goal of hydrodeoxygenation, as the name suggests, is the exclusion of oxygen by replacing it with hydrogen, in analogy to the hydrodesulphurization process, HDS, used in petrochemistry.

In general, a catalyst and high pressure are used to achieve this goal. Concerning process conditions, various types of HDO exist. In this work, it is distinguished between mild HDO and deep HDO, the respective process conditions are given in Table 2.9.

Table 2.9.: Process conditions of mild and deep HDO[10]

	Temperature	H_2 Pressure
	[°C]	[bar]
Mild HDO	250	100
Deep HDO	300	150

The efficiency of various catalysts was examined in our group, namely Ru/C, Pt/C, Pd/C and Raney-Nickel[10]. Depending on the catalyst and the process conditions, an aqueous phase, one or two organic phases and a gas phase are obtained. If only one organic phase is obtained, its density is usually higher than the density of water, if two organic phases are obtained, the density of water is between the density of the top organic phase and the bottom organic phase.

Various reactions occur during HDO, e.g. hydrodeoxygenation, decarbonylation, decarboxylation, hydrocracking, and hydrogenation, an overview is given in Figure 2.5.

Complete deoxygenation cannot be achieved because of various reactions taking place. For a specific HDO experiment with a given feed, a theoretical overall reaction equation, excluding the gas phase, was determined to be[9]

$$CH_{1.47}O_{0.56} + 0.39\ H_2 \longrightarrow 0.74\ CH_{1.47}O_{0.11} + 0.19\ CH_{3.02}O_{1.09} + 0.29\ H_2O \quad (2.1)$$

In Equation 2.1, $CH_{1.47}O_{0.11}$ is the organic product phase, and $CH_{3.02}O_{1.09}$ is the aqueous phase.

$$R\!-\!OH \quad + \quad H_2 \quad \longrightarrow \quad R\!-\!H \quad + \quad H_2O$$

(a) Hydrodeoxygenation

$$R\!-\!H \quad + \quad CO$$

(b) Decarbonylation

$$R\!-\!H \quad + \quad CO_2$$
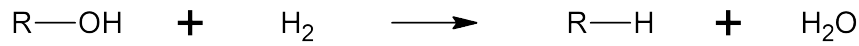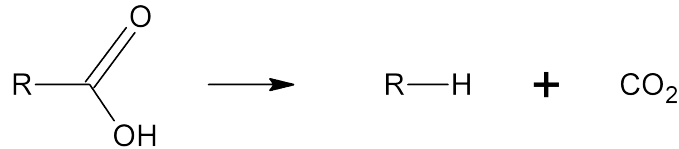
(c) Decarboxylation

$$R_1 \diagup R_2 \quad + \quad H_2 \quad \longrightarrow \quad R_1\!-\!CH_3 \quad + \quad H_3C\!-\!R_2$$

(d) Hydrocracking

$$+ \quad H_2 \quad \longrightarrow$$
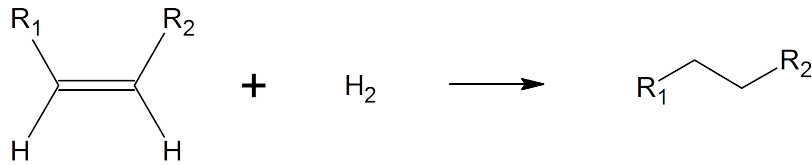
(e) Hydrogenation

Figure 2.5.: Overview of reactions during bio-oil upgrading[9]

Although some oxygen is still contained in the organic product phase, the O/C ratio is still significantly lower than in the PO feed, see Table 2.10.

Table 2.10.: O/C and H/C ratios of the PO feed, the organic phase and the aqueous phase[11]

Molar ratio	O/C	H/C
PO feed	0.56	1.47
Organic phase	0.11	1.47
Aqueous phase	1.09	3.02

Moreover, some organics are still contained in the water phase, for example alcohols like ethanol and propanediol, organic acids like formic acid and acetic acid (causing the low pH-value) and esters like methyl acetate and ethyl acetate[12].

Important parameters to evaluate the HDO process are the oil yield, Y_{oil}, given in Equation 2.2, and the degree of deoxygenation, DOD, given in Equation 2.3.

$$Y_{oil} = \left(\frac{m_{oil}}{m_{feed}} \right) \cdot 100 \tag{2.2}$$

$$DOD = \left(1 - \frac{wt\%_{O\ in\ product}}{wt\%_{O\ in\ feed}} \right) \cdot 100 \tag{2.3}$$

The Y_{oil} describes the selectivity towards an oil product, and the DOD describes how effectively the oxygen is removed from the organic product phase. These two values only make sense in combination, as an Y_{oil} of 100 % would only mean that there was no reaction. The DOD can be plotted versus Y_{oil} to visualize the results.
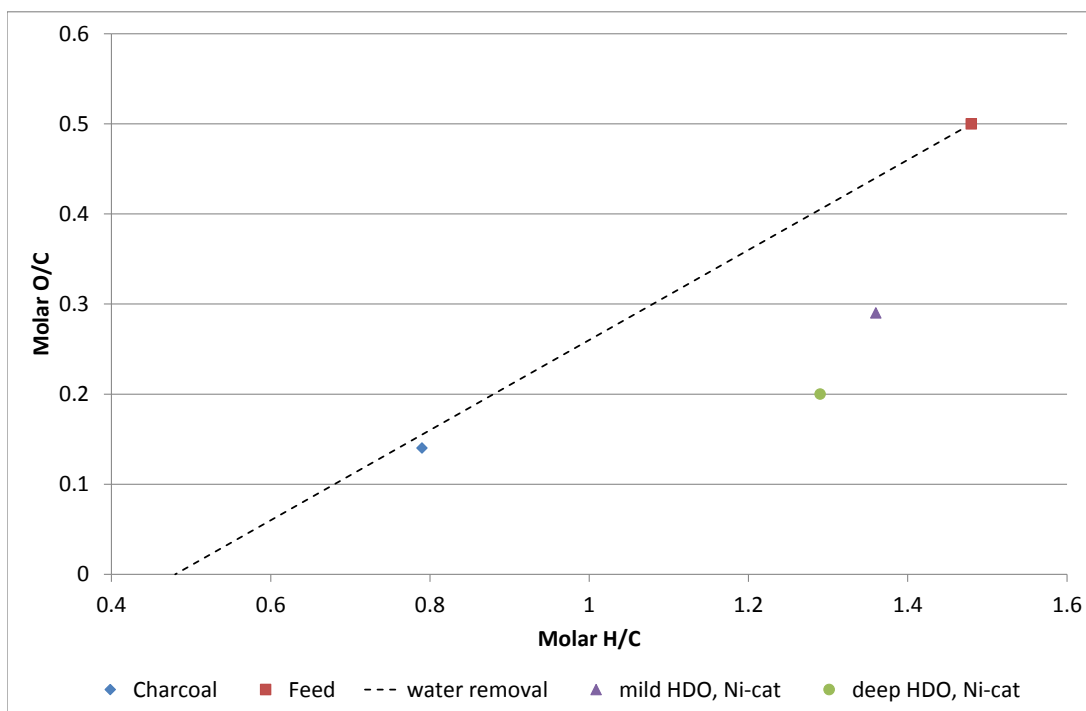
Figure 2.6.: Van Krevelen plot: feed, charcoal, a line for the abstraction of water, and the results of a mild and a deep HDO with a Raney nickel catalyst

Another option to visualize the results is the so-called van Krevelen plot. The molar O/C ratio is plotted versus the molar H/C ratio, giving information about the effect of HDO on the elemental composition. Figure 2.6 shows a van Krevelen

plot depicting the PO feed, charcoal, the results of HDO processes, and the line for the abstraction of water.

A major problem in HDO is the possibility of polymerization[13]. Polymerization reactions are the predominant reactions if not enough hydrogen is supplied. Polymerization should be avoided, as the viscosity of the organic product phase increases with increasing molecular masses of the hydrocarbons contained.

Moreover, more solid carbon residue is obtained if more polymerization reactions occur. In order to minimize polymerization, low temperatures and low heating rates should be applied. Furthermore, transport phenomena play an important role: a high stirring speed and an adequate catalyst particle size should be used[13].

2.3. Coal Liquefaction

2.3.1. Coal

Coal is an organic sedimentary rock of biochemical origin, it is combustible and brownish to black[14]. It is composed mainly of carbon and hydrogen, with varying amounts of oxygen, nitrogen and sulfur. Moreover, mineral matter, the so-called ash, moisture and gases may be contained in the coal matrix.

Coal developed out of biochemical material, became similar to peat and was then altered due to thermal and pressure effects. The longer thermal and pressure effects persist, the more chemical and physical changes occur in the coal. It is classified via the coal rank: the longer the maturation, the higher the rank of the coal.

The main types, in increasing rank, are lignite (brown coal), subbituminous, bituminous and anthracite, bituminous already being dark and hard. In general, the heating value increases with increasing rank, while the moisture content decreases. Furthermore, the oxygen and hydrogen content decrease with increased coal maturation, as shown in Table 2.11.

Table 2.11.: Change in elemental composition during the coalification process[14]

	C	H	O
	[wt%]	[wt%]	[wt%]
Wood	49	7	44
Peat	60	6	34
Lignite	70	5	25
Subbituminous	75	5	20
Bituminous	85	5	10
Anthracite	94	3	3

With increasing time, pressure and temperature, the aromatization increases while the oxygen content decreases[15].
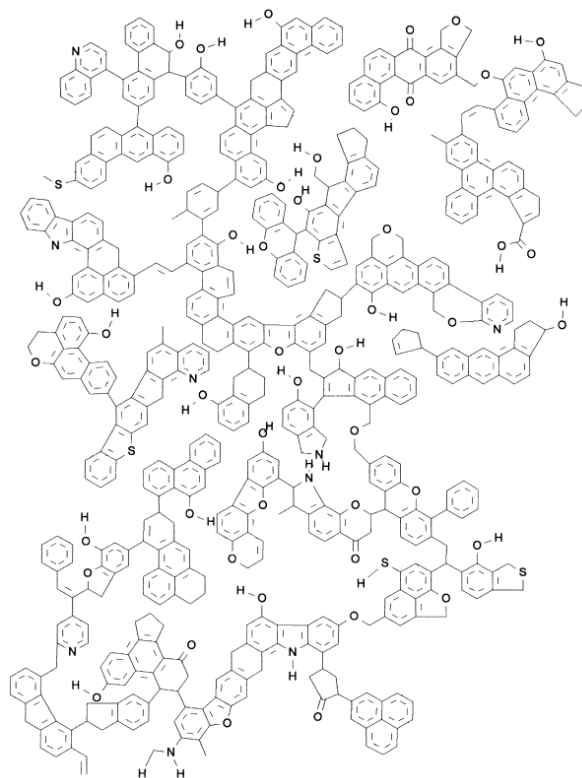
(a) An average molecular structure
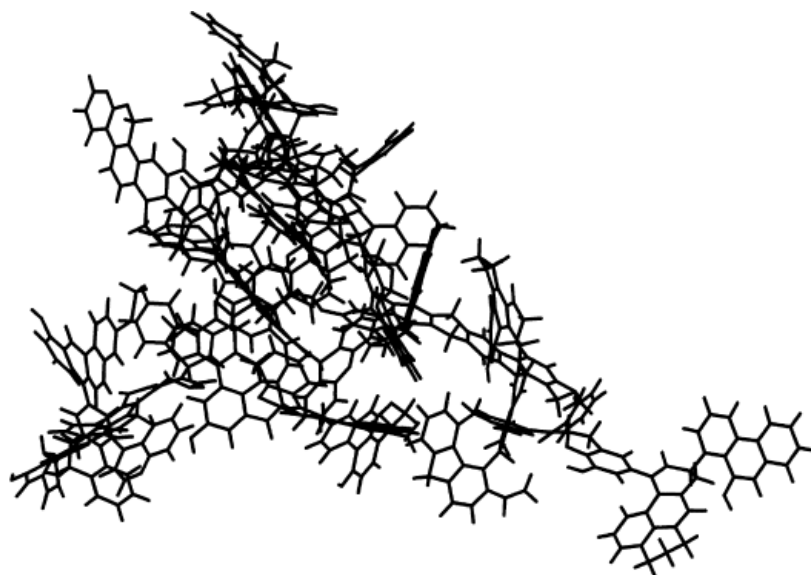
(b) Geometry optimized conformation of the average molecular structure

Figure 2.7.: A modeled average molecular structure of a bituminous coal[16]

Coal has an irregular structure and both the composition and the structure vary not only between coals of different ranks, but even between coals from the same deposit. It is only possible to simulate the average structure of a given coal sample on the basis of different data. Figure 2.7 is such a simulation and gives an idea about the complex structure of coal.

2.3.2. Coal Liquefaction

Coal liquefaction is a process with the goal of producing liquid fuels out of coal. Indirect and direct coal liquefaction processes exist, Figure 2.8 gives an overview.
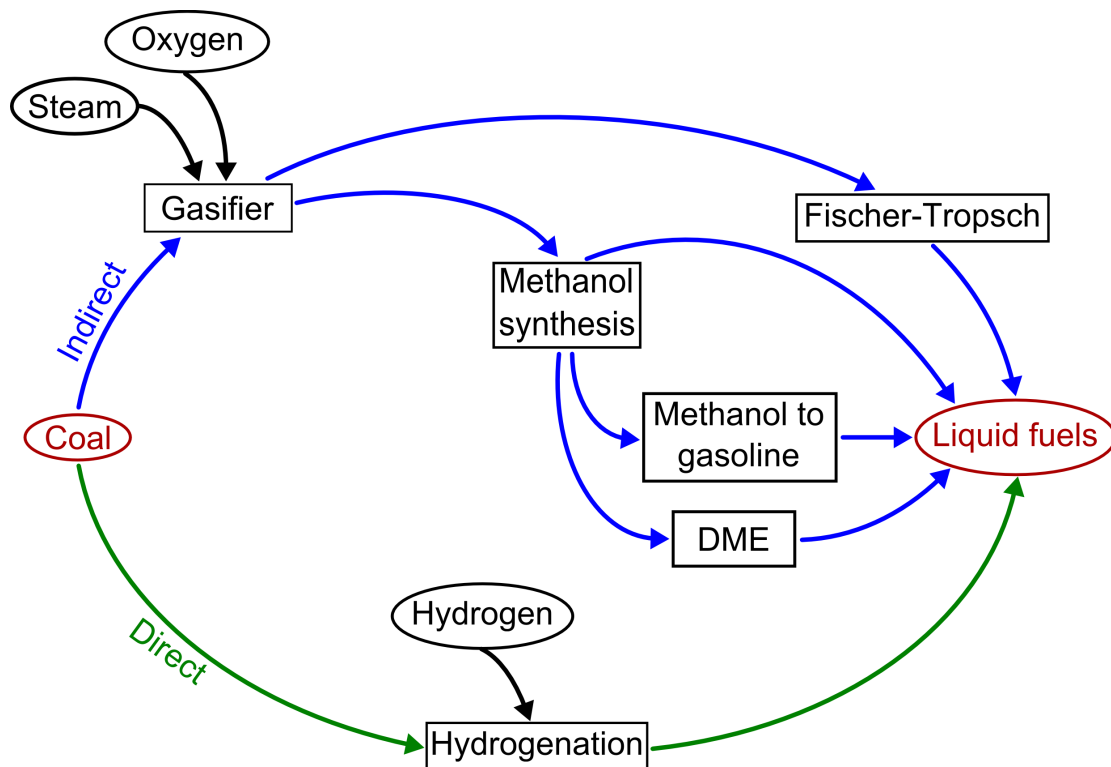
Figure 2.8.: Overview of the different coal liquefaction processes

Indirect coal liquefaction comprises the preparation of synthesis gas, followed by either the Fischer-Tropsch synthesis or methanol synthesis. Methanol can be directly used as fuel. A methanol to gasoline process or a dimethyl ether, DME, process can also follow the methanol synthesis in order to produce liquid fuels.
"*Direct coal liquefaction, DCL, converts solid coal (H/C ratio ≈ 0.8) to liquid fuels (H/C ratio ≈ 2) by adding hydrogen at high temperature and pressures in the presence or absence of catalyst.*"[17]

In more detail, the chemical changes that coal undergoes during liquefaction are:

- the reduction of weak interactions, like van-der-Waals bonds and hydrogen bonds, in order to separate larger units into smaller ones

- the decomposition of the main connecting bonds between aromatic-aliphatic, aromatic-aromatic and carbon-heteroatom structures to get smaller fragments

- the increase of the H/C ratio and the decrease of heteroatoms (heteroatoms being e.g. oxygen, nitrogen, sulfur).

As depicted in Table 2.12, the hydrogen content is significantly lower in coal. It has to be more than doubled to equal the H/C ratio of gasoline or crude oil.

Table 2.12.: Elemental composition and H/C ratio of gasoline, oils and coal[6,18]

	C	H	H/C
	[wt%]	[wt%]	[-]
Gasoline	86.0	14.0	1.95
Crude oil	85.8	13.0	1.82
Pyrolysis oil	31.5	8.5	3.22
Bituminous coal	77.7	4.9	0.76

Due to the very complex composition and structure of coal, no chemical reaction equations can be found for CL. Only very general suggestions exist as to what happens: As a first step, thermal rupture of the coal system may occur, followed by the addition of hydrogen.

Hydrogen can be supplied either by the hydrogen already present in the coal, resulting in a hydrogen-rich volatile fraction and a hydrogen-deficient solid residue or via a hydrogen-donor solvent or via high-pressure molecular hydrogen or a combination thereof.

The use of a catalyst is also possible, usually improving the liquid yield. The requirements for catalysts for DCL are[17]:

- a high hydrogen transfer activity

- a high activity for cracking and hydrocracking of carbon-carbon bonds

- contact maintenance with the solid coal

- low cost and/or possibility to be readily recovered and recycled

It is essential that the reactive coal species, coal radicals R•, the catalyst and the hydrogen are in close contact for the hydrogen addition reaction. Otherwise, the coal fragments may recombine in retrogressive reactions, resulting in undesired higher-molecular-mass units.

The hydrogen-donor solvent should fulfill the following requirements[19]:

- source of transferable hydrogen

- facilitation of heat transfer

- transport medium for the coal

- dispersion of the liquefaction products

The most effective hydrogen-donor solvents are solvents with a partially hydrated aromatic structure, e.g. Tetralin (1,2,3,4-Tetrahydronaphthalene), 9,10-Dihydro-phenanthrene or 4,5-Dihydropyrene, see Figure 2.9. Their activity is related to the number of rings and the extent of saturation.

(a) Tetralin   (b) 9,10-Dihydrophenanthrene   (c) 4,5-Dihydropyrene
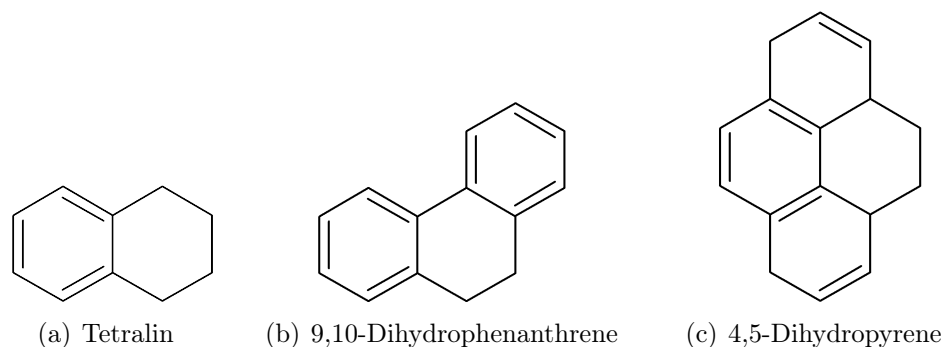
Figure 2.9.: Partially hydrogenated aromatic solvents

In general, polycyclic compounds are easily hydrogenated or dehydrogenated thermally or, more effectively, with the help of a catalyst. So during CL, the solvent can be re-hydrogenated in situ, in a hydrogenation-dehydrogenation cycle. The stabilization of coal radicals by hydrogen atoms derived from dehydrogenation of tetralin is shown in Figure 2.10.
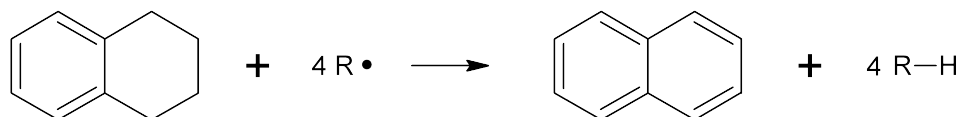
Figure 2.10.: Dehydrogenation of tetralin to naphthalene

The reaction of tetralin with coal is probably not as effective as the reaction of dihydrophenanthrene with coal. The re-hydrogenation of tetralin, hence the partial hydrogenation of naphthalene, is not as quantitative under CL conditions.[19] However, tetralin is cheaper and more easily commercially available.

2.4. Aging

Sufficient stability of bio-oils during storage, shipment and use is necessary and maintenance of chemical and physical properties is essential if bio-oils will be introduced into markets. Certain changes are observed, altering the storage and transportation behavior of the oils.

However, it is difficult to "quantify" aging processes, regarding what parameters to monitor, how to monitor them, and to classify with what change rate an oil "ages". Certain parameters are used to monitor aging, many of them adopted from the petroleum industry. Most often, the change of viscosity is investigated, but many more parameters are also used.

As already explained in previous chapters, the exact molecular composition of the bio-oils cannot be determined, as already the exact molecular compositions of the feedstock cannot be determined, and all the reactions occurring during pyrolysis, hydrodeoxygenation or coal liquefaction cannot be determined either.

So if the bio-oil is not completely known right after its production, it is not possible to know exactly what changes occur later on. However, it is known that certain chemical functional groups are present in bio-oils, and their reactions are known in organic chemistry.

2.4.1. Changes in Chemical Composition

Some of the compounds contained in bio-oils were evaluated concerning whether their reactions are possible under given storage conditions[20]. The thermodynamic equilibrium constants for reactions were calculated in order to evaluate whether reactions are possible during storage and in what time span they would occur. If the reaction time is very long, those reactions can be neglected. Furthermore, it was estimated to what yield or extent the reactions would take place.

Some of the most reactive compounds in bio-oils are organic acids, aldehydes, alcohols etc. Some of the reactions that may occur during storage of bio-oils are:

- polymerization: additions and condensations

- oxidation when stored under air

- acetalization

- hydration

- esterfication

Some of the reaction products can be in thermodynamic equilibrium with their educts, which means that changes in temperature or other storage conditions can influence these reactions and their extent. Some reactions can produce polymers, thus tar and they can be irreversible under storage conditions.

Polymerizations can be divided into addition polymerizations and condensation polymerizations, among others. Addition polymerizations include, for example, alkene or diene polymerizations. In condensation polymerizations, monomers are joined by the loss of a small molecule, usually water or methanol.

Alcohols can be oxidized to aldehydes or ketones when stored at air, see Figure 2.11.
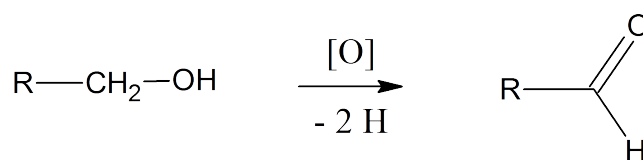
(a) Primary alcohol oxidation
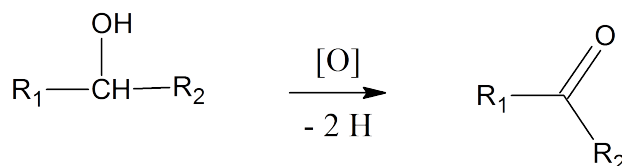
(b) Secondary alcohol oxidation

Figure 2.11.: Reaction schemes of the oxidation of a primary alcohol to an aldehyde and a secondary alcohol to a keton[20],[21]

Many more compounds can be oxidized when the bio-oils are stored under air, e.g. aldehydes to carboxylic acids, see Figure 2.12.
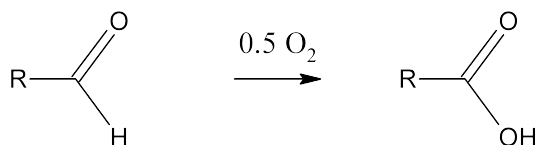
Figure 2.12.: Reaction scheme of the oxidation of an aldehyde[20],[21]

Furthermore, peroxides can be derived from alkenes, ethers, aldehydes and ketones and organic acids. These peroxides are a problem for the bio-oil stability, because they are not stable and decompose to free radicals. These free radicals can catalyze

the polymerization reactions of alkenes, which should be avoided.

Hemiacetals are derived from the reaction of an aldehyde with an alcohol, acetals from an aldehyde reacting with two alcohols, see Figure 2.13.

(a) Hemiacetalization
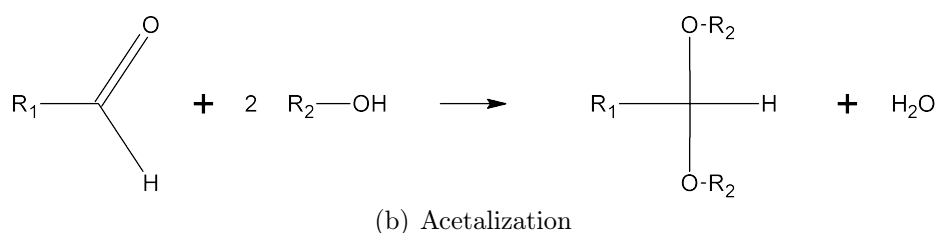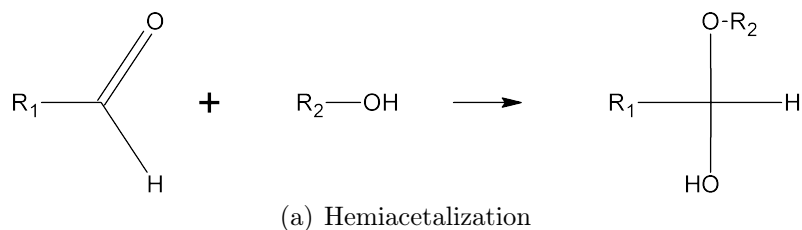
(b) Acetalization

Figure 2.13.: Reaction schemes of hemiacetalization and acetalization[20],[21]

Aldehydes or ketones react with water to hydrates, see Figure 2.14.
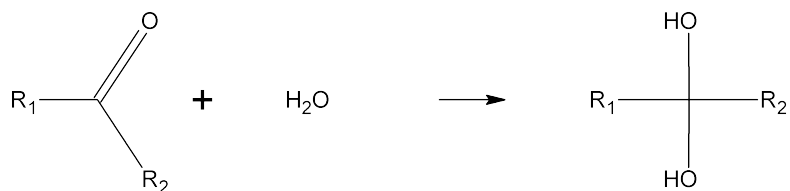
Figure 2.14.: Reaction scheme of the hydration of an aldehyde[20],[21]

Organic acids may react with alcohols to yield esters and water in esterfications. In transesterfications, two esters or an ester and an alcohol exchange their chains, see Figure 2.15.

Esterfications probably do not occur to a high extent. Esterfications are an equilibrium reaction yielding an ester and water. However, as there is already a high amount of water present in the pyrolysis oils, the equilibrium is pushed towards the educt side.

(a) Esterfication

(b) Transesterfication of two esters

(c) Transesterfication of an ester and an alcohol
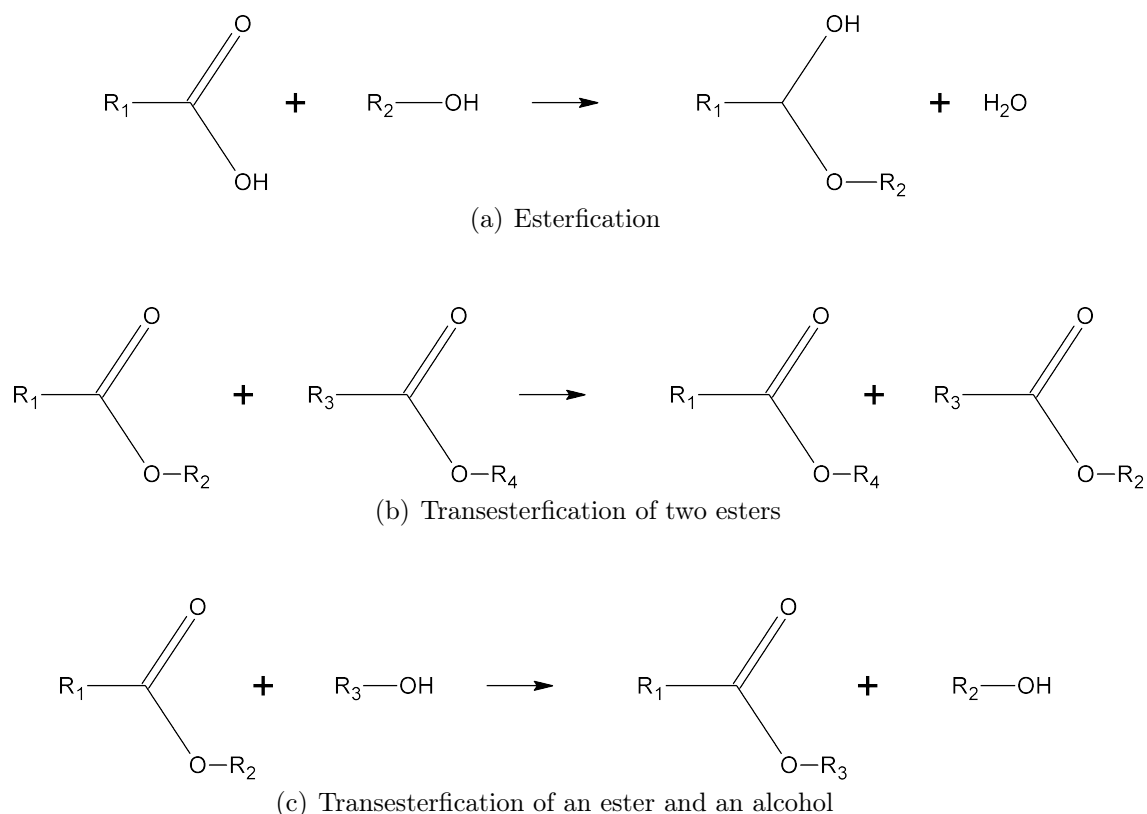
Figure 2.15.: Reaction schemes of esterfication and transesterfication[20],[21]

Some of these reactions occur fast, some very slowly, some only with catalysis. As there are many different compounds in bio-oils, it is possible that a compound acts as a catalyst for a certain reaction, so that the bio-oil already contains this catalyst. A functional group that can catalyze certain reactions and is already present in the bio-oils is the carboxyl-group, hence organic acids can act as catalysts.[20]

2.4.2. Changes in Physical Properties

The aforementioned chemical reactions can cause various changes in the physical properties: The most obvious effect is an increase of viscosity, which is unfavorable concerning the handling e.g. pumping, of the bio-oils.
Oasmaa and Kuoppala[22] and Oasmaa and Peacocke[23] have investigated the aging phenomenon. Their results are summarized in Table 2.13.
Usually along with an increase in viscosity, tar formation is observed. Certain components of the bio-oils can polymerize, thus increasing their molecular mass, forming tar that settles at the bottom of containers. Furthermore, tar can lead to clogging of pipes, and can destroy filters, injectors, valves etc.

Table 2.13.: Viscosity increase of PO - aging procedure [a]: room temperature, 6 months, aging procedure [b]: 80 °C, 24 hours

Temp. of measurement	Viscosity	Viscosity	Visc. Increase
[°C]	[mPa s]	[mPa s]	[%]
Oasmaa 2003[22]	**fresh**	**aged** [a]	
20	100	150	50
40	30	45	50
Oasmaa 2010[23]	**fresh**	**aged** [b]	
40	16.6	23.3	40
40	16.6	23.5	42
40	16.6	22.8	37
40	16.6	23.0	39

Another disadvantageous aging effect may be the increase of water content. Water can be released during certain reactions like condensation reactions. Up to a certain water content, bio-oils are homogenous, but a further increase in water content may result in phase separation and changes in solubility.

Moreover, a change of acid content and pH-value etc. may pose problems. If the pH-value decreases during storage, the bio-oil may attack the surface of the tanks, pipes, the linings etc.. These attacks may lead to leaking, which should be avoided.

2.4.3. Monitoring of Aging

Some of the changes during aging are visible, e.g. phase separation or the change of color, the oil may dim, or sediments may develop. But unfortunately, most of the aforementioned changes are not visible, so appropriate analytical techniques have to be developed and applied.

In order to investigate aging effects, different aging processes are used: Bio-oils can be aged at different temperatures, mostly room temperature, as it is most likely that oils will be stored at room temperature. The disadvantage is the very long time span necessary to obtain results.

To circumvent this problem, so-called accelerated aging processes are used, where the oils are kept at higher temperatures for a certain period of time. Furthermore, accelerated aging can be conducted in an atmosphere with high oxygen pressure in order to investigate the oxidation behavior of the sample.

It was found that an accelerated aging procedure of POs derived from pine wood and from forestry residues yielded the same results as the reference POs stored for one year at room temperature. The accelerated aging procedure used in these

experiments was heating the sample to 80 °C for 24 hours[22].

As already mentioned, the viscosity is usually monitored in aging experiments. Additionally to the monitoring of the viscosity, which helps to estimate thermal stability, the oxidative stability can be tested. Two methods are found in the literature:[24] the investigation of solids formation and the investigation of the oxidation onset temperature, OOT.
In order to determine the solids formation, the samples were acceleratedly aged: 90 °C, 8 bar oxygen pressure, 16 h. Subsequently the solids were filtered and weighed. A relation was established that oils with lower amounts of solids residue have a higher oxidative stability and hence a lower tendency to form solid residues in tanks during storage.
The OOT was determined via differential scanning calorimetry according to an ASTM (American Society for Testing and Materials) method that is usually used for edible oils and fats, lubricants, greases and polyolefins[25]. A small amount of the sample (approx. 3 mg) was heated from 25 to 350 °C at 10 °C/min in an oxygen atmosphere. The relation established in this test was that the higher the OOT, the more oxidatively stable the oil is[24].

Many other analytical techniques are used. The chemical composition and changes in chemical composition are usually monitored via GC-MS, the low-molecular mass compounds in the water phase can be analyzed via GC-FID. Changes concerning the functional groups are usually monitored via Fourier transform - infrared spectroscopy, FT-IR.
The average molecular mass and the molecular mass distribution can be determined with gel permeation chromatography, GPC, see section 2.5. The water content of the bio-oils can be examined with Karl-Fischer titration or via gas chromatography - thermal conductivity detector, GC-TCD (to circumvent problems with aldehydes and ketones).
Furthermore, the elemental composition is usually analyzed, as well as the lower or higher heating value with calorimetry. Along with the viscosity, the density is also determined in order to be able to calculate the dynamic viscosity from the kinematic one and vice versa.
Furthermore, different extraction methods can be used to divide the bio-oil into different compound groups, e.g. water-soluble and insoluble and soluble or insoluble in different solvents like e.g. diethylether or dichloromethane[23].

2.5. Gel Permeation Chromatography

2.5.1. Basics

Gel permeation chromatography (GPC) is an application of size exclusion chromatography (SEC), although the term size exclusion is misleading.

SEC is a type of liquid chromatography where the substance to be analyzed is separated in a column that is packed with a gel with a defined pore size. Depending on what system of stationary phase and mobile phase is used, SEC is called either gel filtration (hydrophilic packings, aqueous eluents) or gel permeation chromatography (hydrophobic packings, nonpolar organic solvents).

The separation process is based on the different molecule sizes, hence the name size exclusion chromatography, but more exactly on the hydrodynamic volume of the molecules. The hydrodynamic volume of a given molecule depends on the solvent, called eluent in GPC, as the molecule is convoluted and solvated in the eluent.

Moreover, shape, polarity and functional groups also play a role in the separation process. However, in the ideal separation process, no chemical interaction occurs. There are two extremes how the molecules can interact with the stationary phase:

- Molecules that are too large (more exactly: molecules whose hydrodynamic volume is too large) to diffuse into any of the pores cannot permeate the stationary phase at all and are eluted with the mobile phase. They are not retained at all but totally excluded.

- The other extreme are very small molecules that can diffuse into all the pores. This behavior is total permeation and the molecules are retained most strongly.

Molecules with medium size can diffuse into some of the pores and thus are retained only to a certain extent and elute between the largest and the smallest molecules. Commonly, detectors that give a signal proportional to concentration are used. Common detectors are refractive index detectors, UV absorption detectors, or flow viscosimeters.

The result obtained by a GPC measurement is a chromatogram with the retention volume in mL on the x-axis and a detector signal on the y-axis. In order to gain molecular masses and molecular mass distributions, a calibration with standards with a defined molecular weight is necessary[26].

2.5.2. Application for Analysis of Pyrolysis Oils

Originally, GPC was developed for the analysis of polymers. It was used to determine of how many monomer units a certain polymer was built up. All the polymers would have the same chemical properties, the same functional groups, would be in a chain and would have mass differences of at least one monomer unit.

However, pyrolysis oils consist of many different substances with very different chemical properties and functional groups, and the mass difference between two molecules might be as small as 1 g/mol.

Furthermore, the molecules are not all chains but may also be planar or any shape. All these facts pose challenges to the data processing and interpretation of GPC of pyrolysis oils.

2.5.2.1. Non-Ideal Interactions

Many non-ideal interactions may occur, including[27]:

- hydrogen bonding with the mobile phase

- adsorption to the column packing

- influence of the ratio of hydrodynamic volume to molecular mass

- influence of different functional groups

If the analyte does not show ideal interactions, two classifications are possible:

- underestimation

- overestimation

of the real molecular mass. These effects are further elucidated in subsection 3.5.2 and subsection 4.5.2.

3. Experimental

3.1. Pyrolysis

Two pyrolysis experiments are conducted in the reactor shown in Figure 3.1 and in the schematic in Figure 3.2.

Figure 3.1.: Photo of the pyrolysis reactor

The biomass is pyrolyzed in the liquid heat carrier at ambient pressure at 350 °C for 30 minutes altogether. The pyrolysis produces bio-char, a light and a heavy liquid phase and non-condensable products. The heavy phase is the desired product, the light phase is the entrained liquid heat carrier, see Table 3.1.

The feedstock for the pyrolysis is spruce wood shredded to small wood chips of approximately 0.5 cm size, dried overnight at 110 °C. The overall chemical formula of the dried spruce wood is $CH_{1.57}O_{0.67}$, the elemental composition, ash content and heat of combustion are given in Table 3.2.
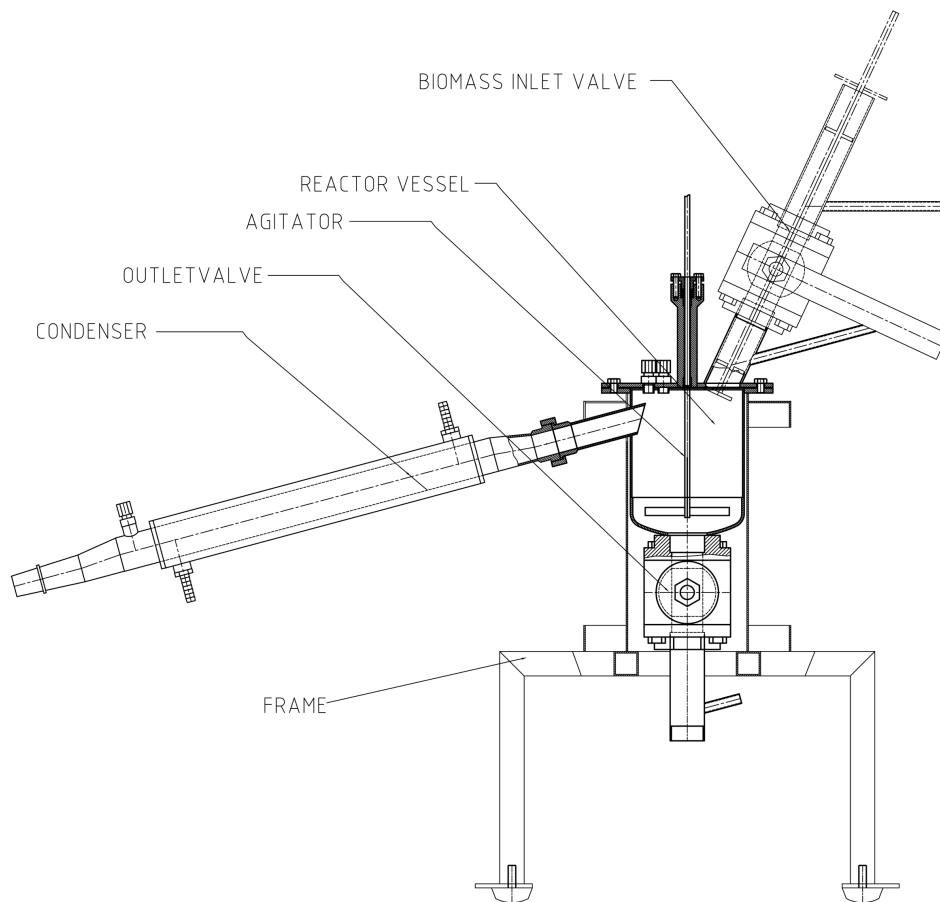
Figure 3.2.: Schematic of the pyrolysis reactor[8]

Table 3.1.: Overview of the pyrolysis experiments

	First experiment	Second experiment
Feed	spruce wood	spruce wood
	VGO	VGO
Catalyst	-	-
Reaction time	30 min	30 min
Reaction temperature	350 °C	350 °C
Reaction pressure	ambient	ambient
Product	pyrolysis oil PY1	pyrolysis oil PY2
By-products	bio-char	bio-char
	entrained heat carrier	entrained heat carrier
	non-condensibles	non-condensibles

Table 3.2.: Elemental composition, ash content and heat of combustion of the biomass[7,8]

C	H	O	Ash	Heat of combustion
[wt%]	[wt%]	[wt%]	[wt%]	[kJ/kg]
49.5	6.5	43.8	0.2	18.9

As a heat carrier, vacuum gas oil, VGO, a mixture of hydrocarbons is used. The elemental composition, thermal conductivity and heat capacity are shown in Table 3.3.

Table 3.3.: Elemental composition, thermal conductivity and heat capacity of the liquid heat carrier[7,8]

C	H	Thermal conductivity	Heat capacity
[wt%]	[wt%]	[W/m K]	[kJ/kg K]
86	14	≈ 0.1	≈ 2.4

The liquid heat carrier is loaded into the reactor (approx. 500 g). The reactor is purged with nitrogen to exclude oxygen and the condenser is cooled with water. The VGO is heated to 350 °C in 80 minutes while stirring at a speed of 150 rounds per minute, rpm. When the final temperature is reached, approx. 100 g of biomass are converted, a load of approx. 16,6 g is added every 5 minutes.

During the experiment, temperature and pressure in the reactor are recorded. Then the reactor is left to cool for around 90 minutes and the products are collected and further processed.

(a) First pyrolysis experiment   (b) Second pyrolysis experiment

Figure 3.3.: Phase separation with a separatory funnel of PY1 and phase separation in the round-bottom flask of PY2

All the weights are collected. The liquid products in the condenser and in the flask after the condenser are phase-separated in a separatory funnel, see Figure 3.3. The bio-char is filtrated, which allows to recycle the liquid heat carrier. A part of the solid residue from the filtration is extracted in a soxhlet extractor and the obtained ratio of coal to liquid heat carrier is then applied for the whole filter cake. The heavy phase from the flask after the condenser, called PY1 from the first experiment and PY2 from the second, respectively, is collected and used for the aging monitoring.

3.2. Hydrodeoxygenation

A deep hydrodeoxygenation reaction is carried out with twice the amount of pyrolysis oil, PO, as starting material as usual. The oil is hydrodeoxygenated for 120 minutes at 300 °C and 150 bar H_2 using a catalyst, see Table 3.4.

Table 3.4.: Overview of the hydrodeoxygenation experiment

Feed	pyrolysis oil
Catalyst	5 wt% Ra-Ni
Reaction time	120 min
Reaction temperature	300 °C
Reaction pressure	150 bar H_2
Product	dehydroxygenated pyrolysis oil DH1
By-products	aqueous phase
	non-condensibles

Figure 3.4.: Photo of the whole set-up of the HDO reactors, reactor II is the reactor on the right

The same reactor as for the coal liquefaction experiments is used, as shown in Figure 3.4 and Figure 3.5. The P&I diagram is depicted in Figure 3.6, reactor II is used.

Figure 3.5.: Photo of the HDO reactor
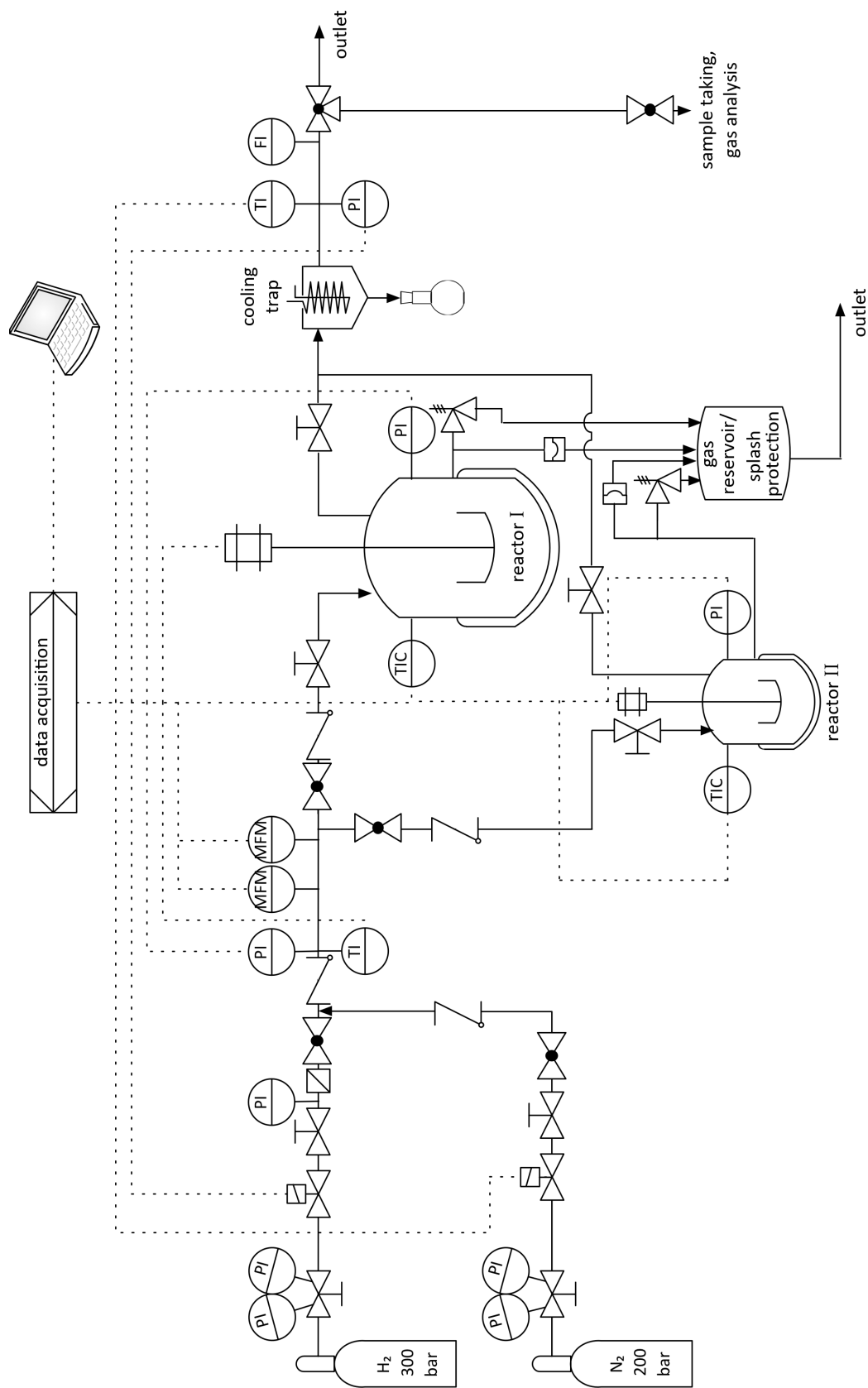
Figure 3.6.: P&I diagram of the HDO reactor set-up[28]

The overall chemical formula of the PO feed is $CH_{4.80}O_{2.12}$, the elemental composition and the water content of the PO is given in Table 3.5.

Table 3.5.: Elemental composition and water content of the PO used for HDO[10]

	C	H	O	Water
	[wt%]	[wt%]	[wt%]	[wt%]
	23.6	9.5	66.5	50

Raney-nickel is used as a catalyst. The pyrolysis oil and 5 wt% (of the PO feed) catalyst are loaded into the reactor. The reactor is shut and the reaction mixture is stirred with 500 rpm. A primary pressure of approx. 50 bar H_2 is set and the mixture is heated to 300 °C. Then the pressure is increased to 150 bar H_2. The pyrolysis oil is hydrodeoxygenated for 120 minutes at 300 °C, temperature and pressure in the reactor are recorded.

After cooling, a gas sample is taken. The liquid products are left overnight to settle in a separatory funnel. The following day, the phases are separated. The residual catalyst is filtered with a filter flask using a partial vacuum. As there are small dispersed droplets of water left in the organic phase, the sample is centrifuged (30 min with 4500 rpm and 30 min with 5500 rpm) and the water drops are decanted.

The products are shown in Figure 3.7. The organic phase is kept for aging and stability monitoring and is called DH1.

(a) Products in separatory funnel

(b) Aqueous phase

(c) Organic phase, DH1 after filtration and centrifugation
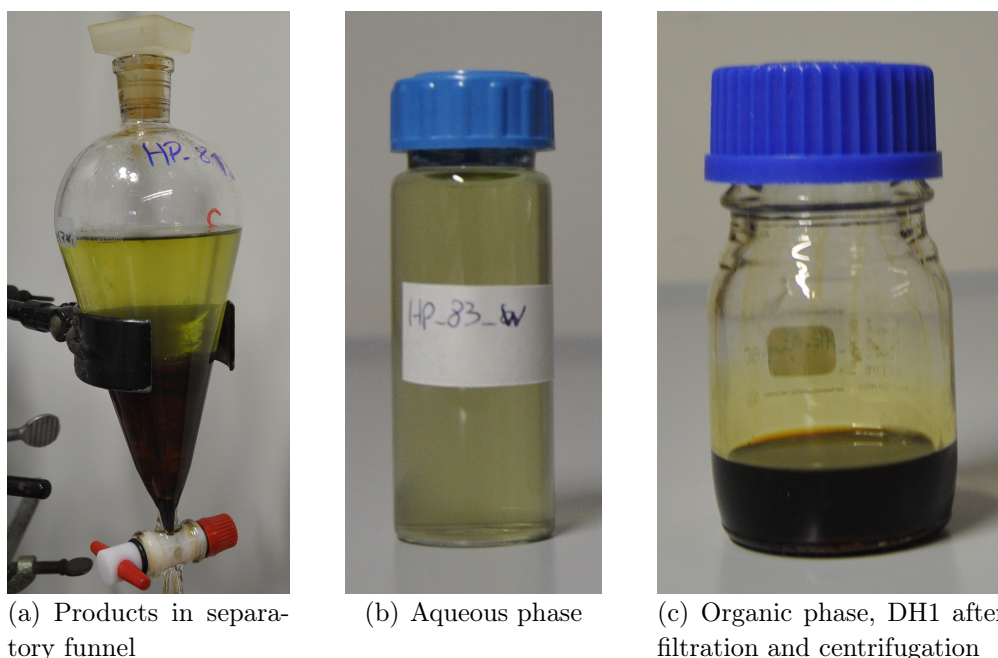
Figure 3.7.: Deep hydrodeoxygenation products

3.3. Coal Liquefaction

Two coal liquefaction experiments are conducted in the reactor already shown in section 3.2.

Two experiments are carried out: One part of ground bio-char is liquefied in three parts of hydrogen donor solvent with 1 or 5 wt% (of bio-char) catalyst, respectively. The reactions are conducted at 425 °C and 180 bar H_2 for 30 minutes, see Table 3.6. The products are separated into a solid and a liquid phase by filtration.

Table 3.6.: Overview of the coal liquefaction experiments

	First experiment	Second experiment
Feed	bio-char	bio-char
Solvent	tetralin	tetralin
Catalyst	1 wt% Ra-Ni	5 wt% Ra-Ni
Reaction time	30 min	30 min
Reaction temperature	425 °C	425 °C
Reaction pressure	180 bar H_2	180 bar H_2
Product	liquefied product CL1	liquefied product CL2
By-products	bio-char residue	bio-char residue
	tetralin	tetralin
	decalin	decalin
	non-condensibles	non-condensibles

The bio-char used for the liquefaction has a particle size of 200 μm and a residual moisture content of 0.68 wt%. The elemental composition is given in Table 3.7.

Table 3.7.: Elemental composition of the bio-char

C	H	O
[wt%]	[wt%]	[wt%]
80.1	5.3	14.4

The hydrogen donor solvent is tetralin, see Figure 3.8. In these two experiments, Raney-nickel is chosen as a catalyst.
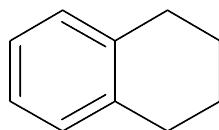
Figure 3.8.: Structural formula of tetralin

The bio-char and the solvent are loaded into the reactor, and 1 or 5 wt% (of bio-char) catalyst are added. The reactor is closed tightly and a primary pressure of 50 bar H_2 is set. The reaction mixture is stirred at 500 rpm and heated to 425 °C. At this temperature, the pressure is increased to 180 bar H_2 and the coal liquefaction is carried out for 30 minutes. Temperature and pressure in the reactor are recorded.

After cooling, the remaining coal is filtrated and then further extracted, while the liquid phase is bottled for the monitoring of the aging process. The liquid phase of the first experiment, with 1 wt% of catalyst, is called CL1, and the liquid phase of the second experiment with 5 wt% catalyst is called CL2.

The products are shown in Figure 3.9 and the filter cakes are shown in Figure 3.10.

(a) First liquefaction experiment

(b) Second liquefaction experiment
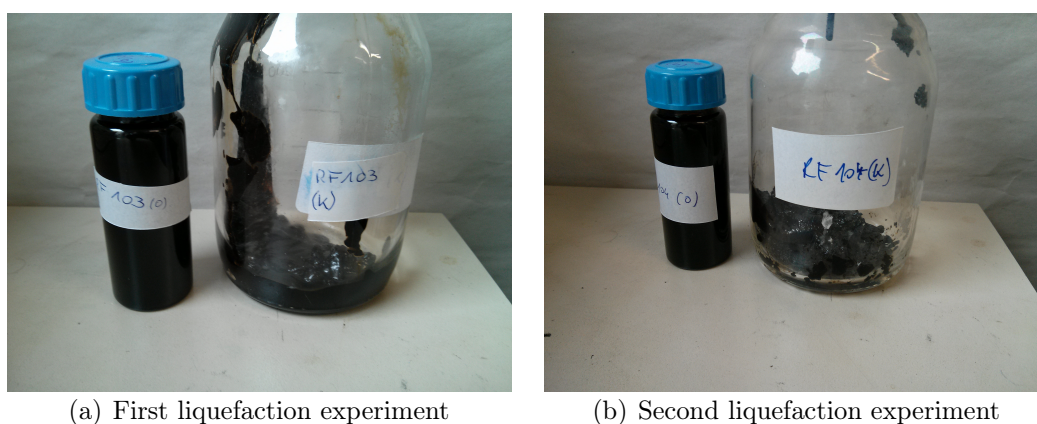
Figure 3.9.: Coal liquefaction products: The liquid phase, CL1 and CL2 is on the left, the solid phase (not washed and dried yet) on the right, respectively

(a) First liquefaction experiment

(b) Second liquefaction experiment
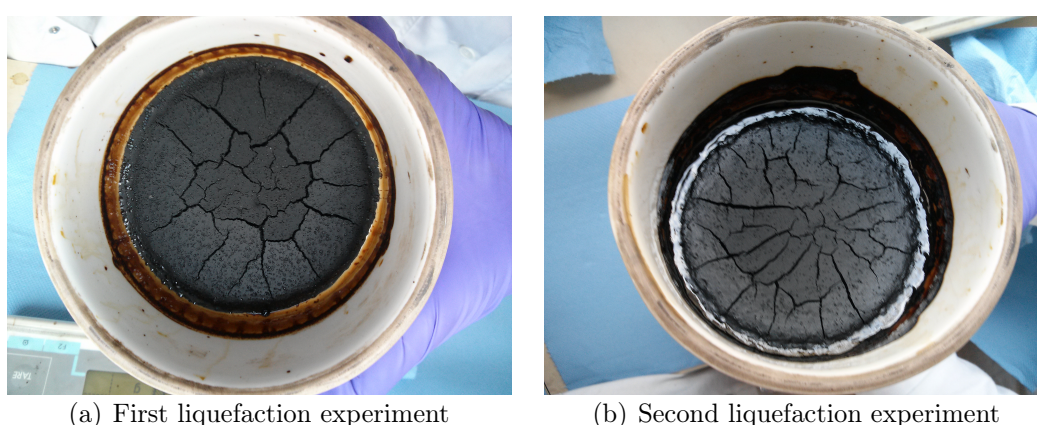
Figure 3.10.: Filter cakes of the residual coal

3.4. Aging

3.4.1. Storage of the Bio-Oils

The bio-oils are stored in tightly closed Schott glass bottles. The bottles are kept in a dark box at ambient temperature.

3.4.2. Monitoring of the Pyrolysis Products

For the monitoring of the bio-oils, the following analyses are carried out:

- GC-MS measurements

- GPC measurements

- viscosity measurements

- density measurements

- acid concentration measurements

- pH-value measurements

- water content measurements.

The schedule of the analyses is shown in Table 3.8.

Table 3.8.: Analyses schedule for the aging monitoring, PY includes samples PY1 and PY2, CL includes the samples CL1 and CL2

Week	PY	DH1	CL
1	daily	daily	daily
2	x	x	x
3	x	x	x
4	x	x	x
5	x		x
6	x	x	x
7	x		x
8	x	x	
9			x
10	x	x	
11			x

All of the aforementioned analyses are carried out according to the schedule at Graz University of Technology except for the analysis of the water content, which

is determined at BDI - BioEnergy International AG in Grambach. Deviations from this schedule are noted in the respective plots.

3.5. Analytics

In general, all sample preparations are done by mass for better accuracy. Tetrahydrofuran, THF, is always used as solvent, because all components of all the bio-oils can be dissolved in THF.

3.5.1. GC-MS

3.5.1.1. System

The GC-MS is shown in Figure 3.11, the system equipment of the GC-MS system is listed in Table 3.9, the GC-column is specified in Table 3.10.

Figure 3.11.: Photo of the GC-MS system

Table 3.9.: GC-MS system

Gas Chromatograph	Shimadzu	GC-2010
Gas Chromatograph Mass Spectrometer	Shimadzu	GCMS-QP2010 Plus
Autoinjector	Shimadzu	AOC-5000

Table 3.10.: Column specifications

Column	DB-1701
Length	60 m
Diameter	0.25 mm
Thickness	0.25 μm

3.5.1.2. Calibration

A calibration is carried out with the following molecules, their structural formulas are depicted in Figure 3.12:

- hydroxypropanone

- cyclopentanol

- 1,2-propanediol

- furfural

- γ-butyrolactone

- 2-hydroxy-3-methyl-2-cyclopenten-1-one

- phenol

- guaiacol

- 2,6-xylenol

- 2-methoxy-4-methylphenol

- 2-methoxy-4-propylphenol

- isoeugenol

- levoglucosan.

Cubic calibration curves are fitted using the Shimadzu LabSolutions GCMS software, see Equation 3.1, the respective coefficients are given in Table A.1.

$$y = a \cdot x^3 + b \cdot x^2 + c \cdot x + d \tag{3.1}$$

where x corresponds to the peak area and y corresponds to the concentration in mass-based parts per million, ppm, which is the same as mg/kg of diluted sample.

(a) Hydroxypropanone   (b) Cyclopentanol   (c) 1,2-Propanediol   (d) Furfural

(e) γ-Butyrolactone   (f) 2-Hydroxy-3-methyl-2-cyclopenten-1-one   (g) Phenol   (h) Guaiacol

(i) 2,6-Xylenol   (j) 2-Methoxy-4-methylphenol   (k) 2-Methoxy-4-propylphenol

(l) Isoeugenol   (m) Levoglucosan
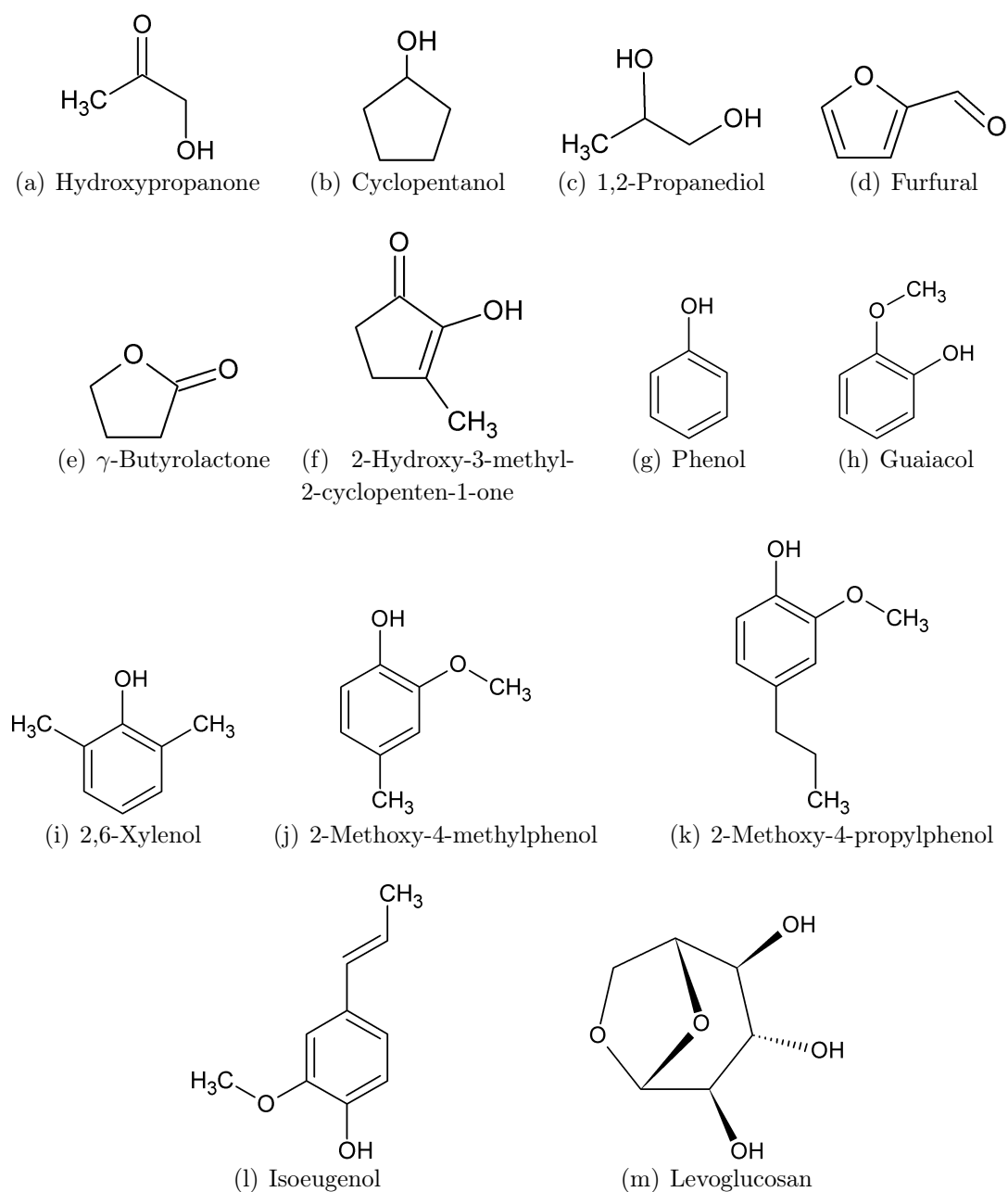
Figure 3.12.: Structural formulas of the calibrated molecules

3.5.1.3. Extended Calibration

It is not possible to calibrate all the substances detected by GC-MS in the bio-oils. For that reason, so-called "extended calibrations" are carried out. Molecules with a similar structural formula and similar functional groups are quantified with the calibration curve of a similar molecule.

If the structural formula and functional groups of a molecule are similar to a calibrated molecule, its behavior on the column should be comparable and it is expected to behave similar at evaporation, ionization and detection. In order to monitor compounds where no similar molecule is calibrated, the peak areas are compared. The dilution coefficients (by mass) of the samples are taken into account.

3.5.1.4. Measurements

The samples are diluted with THF, usually 1:15 or 1:20 by mass. The operation method is given in Table 3.11. A measurement takes 55 minutes, the temperature program is shown in Table 3.12. A temperature of 60 °C is held for a minute, then the oven is heated with a heating rate of 5 °C/min to a final temperature of 280 °C. Then, the temperature is held at 280 °C for 10 minutes.

Table 3.11.: Operation method of the GC-MS system

Injection		
Injection temperature	[°C]	270
Injection mode		split
Injection volume	[μl]	1
Split ratio		30 : 1
Gas		
Carrier gas		He
Column flow	[ml/min]	1.06
Interface		
Ion source temperature	[°C]	240
Interface temperature	[°C]	280
Detector		
Detector voltage absolute	[kV]	0.8
Start m/z	[g/mol]	35
End m/z	[g/mol]	500

Table 3.12.: Temperature program of the GC-MS system

Heating rate	Final temperature	Hold time
[°C/min]	[°C]	[min]
-	60	1
5	280	10

The data are collected with the Shimadzu LabSolutions GCMS software. Compounds are identified with included databases, e.g. databanks from Wiley and from NIST.

3.5.1.5. Statistics

The arithmetic mean $\bar{x}$ and the standard deviation s are calculated[29] for all calibrated substances with Equation 3.2 and Equation 3.3.

$$\bar{x} = \frac{1}{n} \cdot \sum x_i \tag{3.2}$$

$$s = \sqrt{\frac{\sum (x_i - \bar{x})^2}{n - 1}} \tag{3.3}$$

In order to characterize the sample preparation, six vials of the same sample are prepared and measured. The mean and the deviation of the GC-MS are determined by measuring the same sample six times. The results are presented in subsection 4.5.1.

3.5.2. GPC

3.5.2.1. System

The GPC system used in this work consists of a precolumn and two Polymer Standard Service (PSS) columns with a pore size of 1000 Å. At first, the eluent is degassed in a degassing unit, then it passes the pump, then the sample is added via a 6-way injection valve.
Then, the eluent and sample pass a precolumn, the separation takes place in the two columns. The sample is then detected first in a refractive index (RI) detector and subsequently in a UV detector. The GPC system is shown in Figure 3.13, the specifications of the equipment are given in Table 3.13.

Table 3.13.: GPC system

1	Degassing unit	Shimadzu	DGU-20A 3R prominence degassing unit
2	Pump	Merck Hitachi	L-6000A
3	Autosampler	Merck Hitachi	AS-2000A
4	Precolumn	PSS	SDV 5 μm 8x50 mm S/N 2090723
5	Column	PSS	SDV 1000 Å 5 μm 8x300 mm S/N 2090401
5	Column	PSS	SDV 1000 Å 5 μm 8x300 mm S/N 2090402
6	RI detector	Shimadzu	RID-10A refractive index detector
7	UV detector	Merck Hitachi	L-4250

Figure 3.13.: GPC system with precolumn and two separation columns

The column packing is a mixture of polystyrene and polydivinylbenzene, hence hydrophobic, the structural formulas are given in Figure 3.14. The eluent is a polar organic solvent, terahydrofuran (THF). Approx. 0.1 vol% of trifluoroacetic acid (TFA) are added to the eluent in order to protonate all molecules.

(a) Polystyrene   (b) Polydivinylbenzene
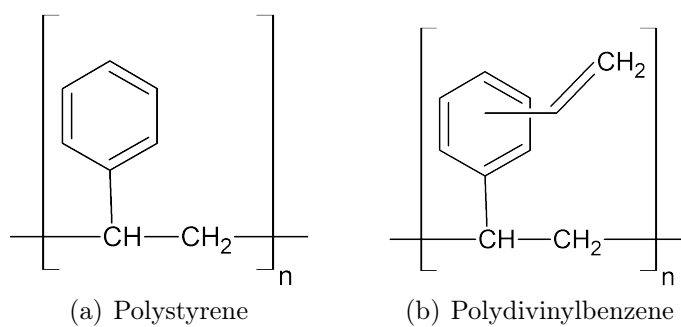
Figure 3.14.: Compounds of the polymer GPC column

3.5.2.2. Calibration

The GPC is calibrated frequently. Polystyrene standards from PSS with a defined molecular weight are used. The details are given in Table 3.14, M_w is the weight average molecular mass and M_n is the number average molecular mass.

Table 3.14.: Polystyrene standards for GPC calibration

	M_w	M_n
	[g/mol]	[g/mol]
Standard 1	162	162
Standard 2	360	306
Standard 3	570	492
Standard 4	972	869
Standard 5	1890	1790

3.5.2.3. Measurements

The samples have to be filtered before measuring with GPC, all catalyst particles or bio-char residue has to be removed carefully. Then the samples are diluted with THF, usually 1:2, 1:5 or 1:10 by mass. The flow of the eluent (THF with approx. 0.1 vol% TFA) is always set to 1 ml/min, resulting in a column pressure of approx. 63 - 65 bar.

The injection volume of sample injected onto the column is chosen between 1 and 60 μl. In general, the smallest possible injection volume is chosen, because the smaller the injection volume, the better the resolution. (The resolution is given in Equation 3.5.)

Due to the fact that the RID is a reference method, the reference cell of the detector is rinsed and filled with eluent before each series of measurements. The data are collected with the Shimadzu LCsolution LC Real Time Analysis software.

3.5.2.4. Aging of the Separation Columns

When comparing measurement results of different points of time, aging of the separation columns is observed. In order to quantify the aging process, a new calibration is carried out after a certain number of measurements and the changes in the calibration curves are compared. Moreover, the number of theoretical plates is calculated as explained below.

3.5.2.5. Theoretical Plates

The theory of theoretical plates is used to describe the efficiency of a separation column. In each theoretical plate, an equilibrium distribution of the analyte between the mobile and the stationary phase is achieved.

In order to monitor the column efficiency over time, the following substances are measured frequently and the number of theoretical plates are calculated:

- Guaiacol, Isoeugenol

- Pyrene, Naphthalene, Tetralin, Toluene

Equation 3.4 is used to calculate the number of plates N[26]:

$$N = 5.54 \cdot \left(\frac{t_r}{w_h} \right)^2 \tag{3.4}$$

t_r being the total retention time and w_h the width of the peak at half-maximum. Furthermore, the resolution, R_s, of two peaks A and B can be calculated via[26]

$$R_s = \frac{t_r^B - t_r^A}{\frac{w_A + w_B}{2}} \tag{3.5}$$

t_R^A and t_R^B being the retention times of the compound A and B, respectively, and w_A and w_B being their peak widths.

3.5.2.6. Non-Ideal Interactions

Non-ideal interactions, as already mentioned in section 2.5, are observed in the measurements. In order to describe these interactions, certain substances are measured and their actual molecular masses are compared to their measured molecular masses.

The substances are anthracene, decalin, eicosane, flouranthene, isoeugenol, naphthalene, phenanthrene, perylene, pyrene and tetralin, details are given in subsection 4.5.2.

3.5.3. Viscosity

3.5.3.1. System

The dynamic viscosity η is measured with a Stabinger Viscometer SVM 3000 from Anton Paar, see Figure 3.15. The Stabinger viscometer is a special type of rotational viscometer.

In a rotational viscometer, an object is rotated in a fluid at a defined speed, and

the torque required is measured. In a Couette-type rotational viscometer, to which subcategory the Stabinger viscometer belongs, there is an inner cylinder emerged in the fluid and an outer tube that rotates. The torque to rotate the outer tube is recorded.

In a Stabinger viscometer, the inner cylinder is hollow and thus floats freely in the fluid centered by centrifugal forces. Along with certain adaptions and the free-floating cylinder, both a good accuracy and a wide measuring range are possible with the Stabinger viscometer.

Figure 3.15.: Photo of the viscometer

The density ρ is also measured with this viscometer, based on the oscillating U-tube technique. A U-shaped glass tube is filled with the sample and then electronically excited into undamped oscillation. The volume of the U-tube is known, and the mass of the sample influences the oscillation, thus yielding the density of the sample.

With these two values, the kinematic viscosity ν can be calculated via Equation 3.6.

$$\nu = \frac{\eta}{\rho} \tag{3.6}$$

3.5.3.2. Measurements

The samples are measured at 20 °C. A measurement requires about 5 ml of sample, 4 ml of which can be recovered. In the literature[22,23], the viscosity is often measured at 40 °C to make the results comparable to oil measurements. However,

in the batch experiments presented in section 3.1, section 3.2 and section 3.3, only small amounts of organic products PY1 and PY2, DH1, CL1 and CL2 are produced.

In order to be able to monitor the aging processes over a long period of time before all the products are used up, the samples for viscosity measurements have to be recovered and reused. For that reason, the samples should not be put under extra thermal stress in order to not influence the aging process. Since the samples are stored at approx. 20 °C, the measurements are carried out at 20 °C.

3.5.4. Acid Concentration

3.5.4.1. System

The sample is titrated with the autotitrator shown in Figure 3.16. The titration workstation equipment is listed in Table 3.15.

Figure 3.16.: Photo of the autotitration system

Table 3.15.: Autotitrator system

Titration Manager	Radiometer analytical	Tim 900 TitraLab$^{\textregistered}$
Sample Station	Radiometer Copenhagen	SAM55 TitraLab TM
Burette	Radiometer analytical	ABU93 Triburette
Working electrode	pH glass electrode	PH G201-7
Reference electrode	saturated KCl electrode	Ref-201
Software	Labsoft	TimTalk 9

3.5.4.2. Measurements

0.1 M NaOH is used as titrant. The sample is titrated to the equivalence point and the amount of base required is used to calculate the acid value in g acetic acid per kg sample, w_{HOAc}, see Equation 3.7. The assumption is made that all the acid contained is acetic acid, which simplifies comparison of samples.

$$w_{\text{HOAc}} = \frac{n_{\text{NaOH}} \cdot M_{\text{HOAc}}}{m_{\text{sample}}} \tag{3.7}$$

The total acid number, TAN, can also be calculated. The TAN is defined as the mass of KOH required to neutralize a defined mass of sample, usually in mg KOH / g sample or g KOH / kg sample. The relation is given in Equation 3.8.

$$TAN = w_{\text{KOH}} = \frac{n_{\text{NaOH}} \cdot M_{\text{KOH}}}{m_{\text{sample}}} \tag{3.8}$$

Usually, approx. 0.3 g of sample are dissolved in approx. 100 ml water. For the DH1 sample preparation, approx. 0.3 g of sample are first dissolved in a few milliliters of isopropanol, then the water is added. Every sample is titrated twice to make sure the titration is reproducible, then the arithmetic mean is calculated. A typical titration curve is shown in Figure 3.17.
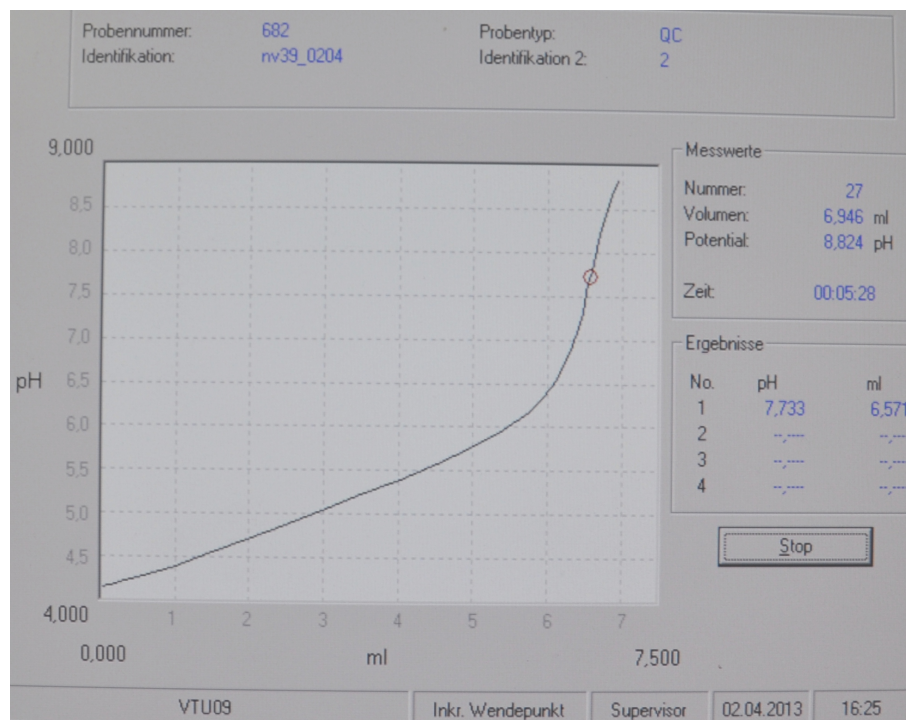
Figure 3.17.: Example of a titration curve, of the sample PY2

3.5.5. pH-Value

The pH-value measurement system is shown in Figure 3.18, the specifications are given in Table 3.16.

Figure 3.18.: Photo of the pH-value measurement system

Table 3.16.: pH Meter system

pH meter	WTW	inoLab pH Level 2
pH electrode	Hamilton	238000, glass electrode

3.5.6. Water Content

Figure 3.19.: Photo of GC-TCD system

The water content is measured at the BDI - BioEnergy International AG in Grambach. It is measured with the gas chromatography - thermal conductivity detector, GC-TCD, shown in Figure 3.19.

The common method of Karl-Fischer titration is not used in order to circumvent problems with aldehydes and ketones present in the sample. The measurement system is listed in Table 3.17.

Table 3.17.: GC-TCD system

	Agilent	GC 7890 A
Column	HP Innovax	30 m x 0.530 mm x 1 μm
Detectors		Thermal conductivity detector
		Flame ionization detector

4. Results and Discussion

4.1. Pyrolysis

Two pyrolysis experiments are conducted. The temperatures are set and recorded with a process control system, PCS. The records are shown in Figure 4.1 for the first pyrolysis experiment and in Figure 4.2 for the second.
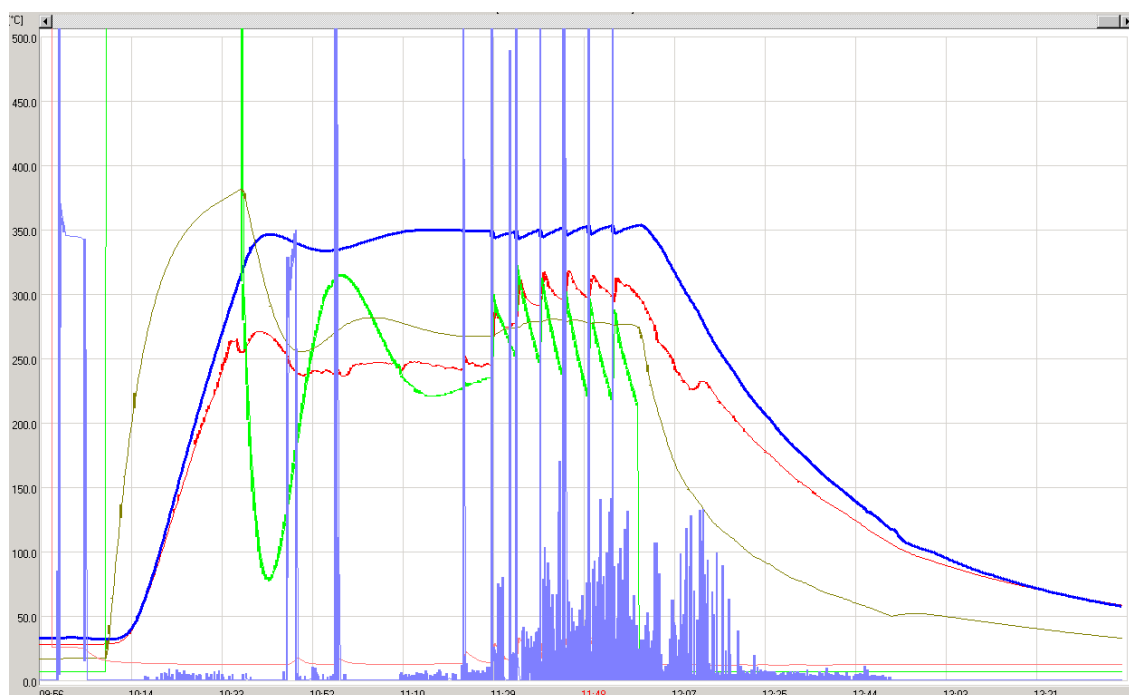
Figure 4.1.: PCS record of the first pyrolysis experiment - Time on the x-axis, temperature in °C on the y-axis. Red: temperature of the vapor space, blue: temperature in the reaction mixture, green: heating power, brownish: temperature of the heating jacket, pink: temperature after the condenser, light blue: gas volume

The mass balances are calculated with all the weights collected and listed in Table 4.1. They are closed with the value for the amount of gas produced. The balance error should be approx. 5 g, thus approx. 5 wt% based on biomass, or approx. 1 wt% based on the VGO, vacuum gas oil.
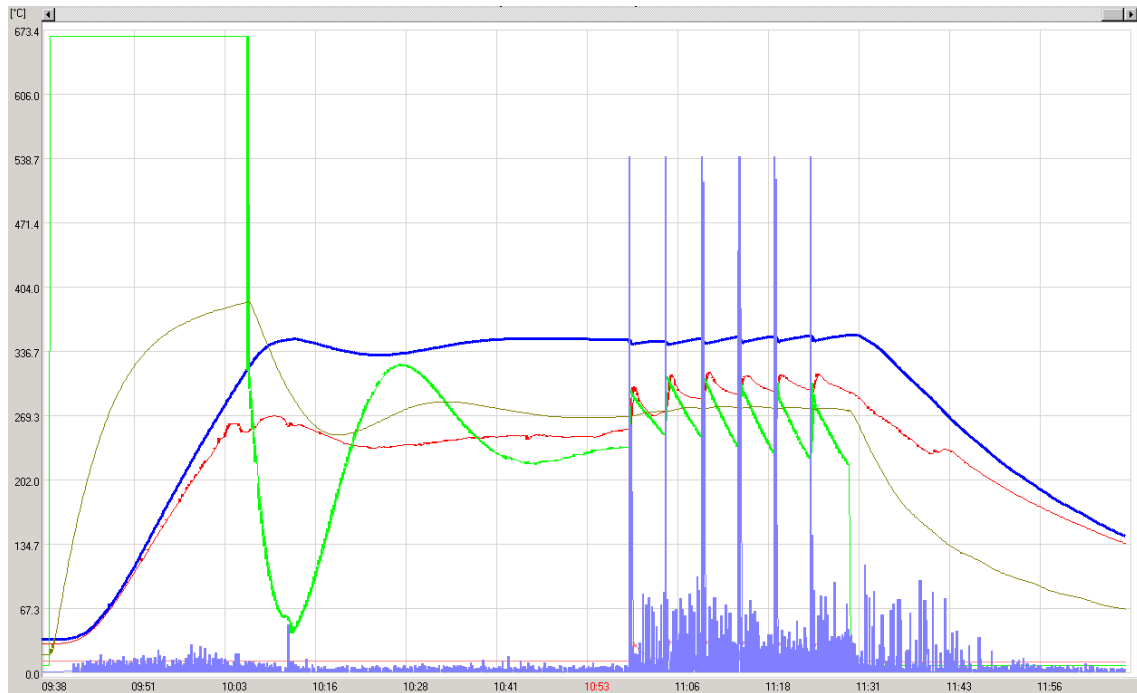
Figure 4.2.: PCS record of the second pyrolysis experiment - Time on the x-axis, temperature in °C on the y-axis. Red: temperature of the vapor space, blue: temperature in the reaction mixture, green: heating power, brownish: temperature of the heating jacket, pink: temperature after the condenser, light blue: gas volume

Table 4.1.: Mass balance of the pyrolysis experiments

		First experiment	Second experiment
In			
VGO	[g]	489.92	524.19
Biomass	[g]	95.41	98.24
Out			
Bio-char	[g]	35.32	34.86
VGO	[g]	349.82	389.92
Entrained VGO	[g]	140.27	140.03
Organic product phase	[g]	39.07	38.72
Non-condensibles	[g]	20.84	18.90

All the mass flows are shown in Figure 4.3, E-VGO is short for entrained VGO.
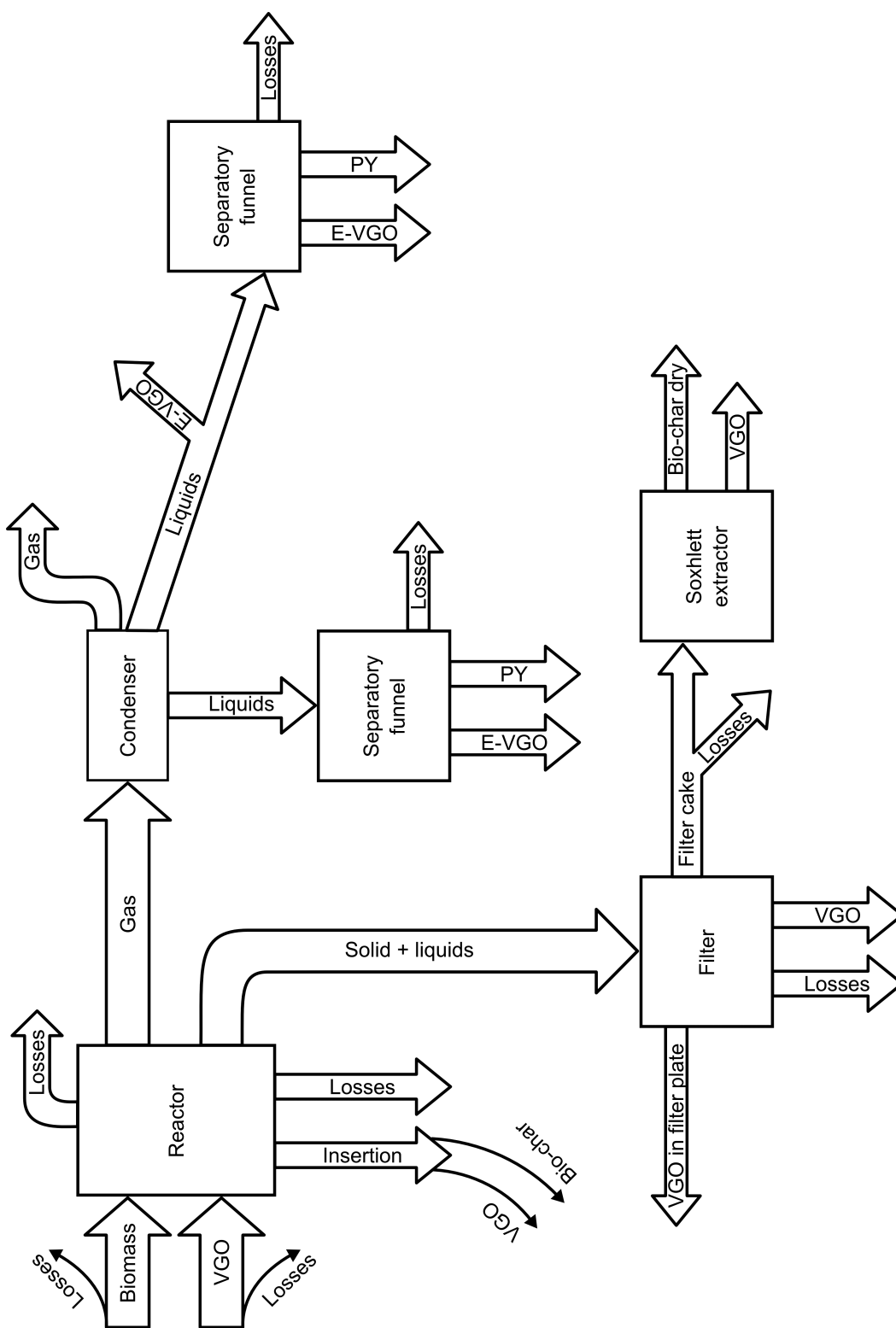
Figure 4.3.: Schematic of the mass flows in the pyrolysis experiments

The elemental composition of the biomass, of the VGO, of the products PY1 and PY2 and of the entrained VGO is listed in Table 4.2.

Table 4.2.: Elemental composition of reactants and products of the pyrolysis experiments

	C [wt%]	H [wt%]	O [wt%]	N [wt%]
First experiment				
Biomass	49.9	6.4	43.4	0.3
Bio-char	75.1	5.5	19.3	0.1
PY1	31.7	8.4	59.6	0.3
VGO	87.1	13.0	-	0.4
Entrained VGO	86.3	12.7	0.7	0.4
Second experiment				
Biomass	49.9	6.4	43.4	0.3
Bio-char	74.6	5.3	19.9	0.2
PY2	32.4	8.4	58.8	0.4
VGO	87.3	12.6	-	0.4
Entrained VGO	86.8	12.8	-	0.4

The elemental composition of the gas formed during reaction is given in Table 4.3. The values are not measured, but calculated from the balance. The hypothetical chemical formula is $CH_{1.7}O_{0.8}$ for the first and $CH_{0.3}O_{1.6}$ for the second experiment.

Table 4.3.: Elemental composition of the gas formed during pyrolysis experiments

	C [wt%]	H [wt%]	O [wt%]
First experiment	46	7	47
Second experiment	32	1	67

The formation of gases is recorded during the experiments, the records are depicted in Figure 4.4 and Figure 4.5.

Conversion factors have to be applied to quantify other gases than nitrogen. The gas compositions are calculated via the mass and elemental balances, and Figure 4.4 and Figure 4.5 show the qualitative volume per volume composition. The amount of gas is calculated to close the mass balances.

54
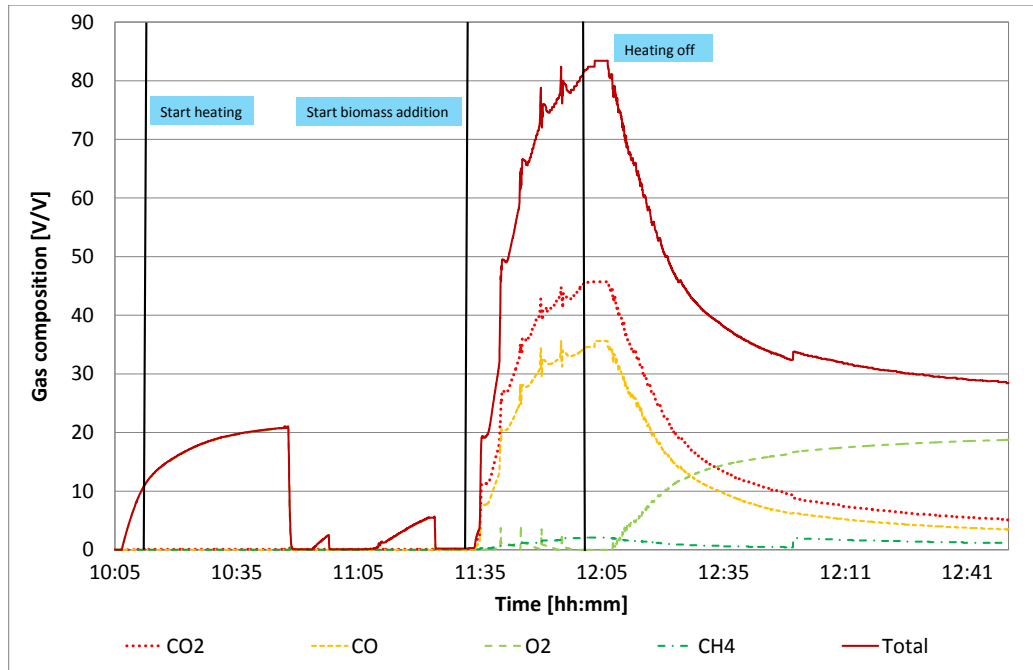
Figure 4.4.: Gas formation during the first pyrolysis experiment

In the first experiment, the inlet pipes are not tight at first, so the reactor is purged with nitrogen while heating. These purges can be seen in Figure 4.4.
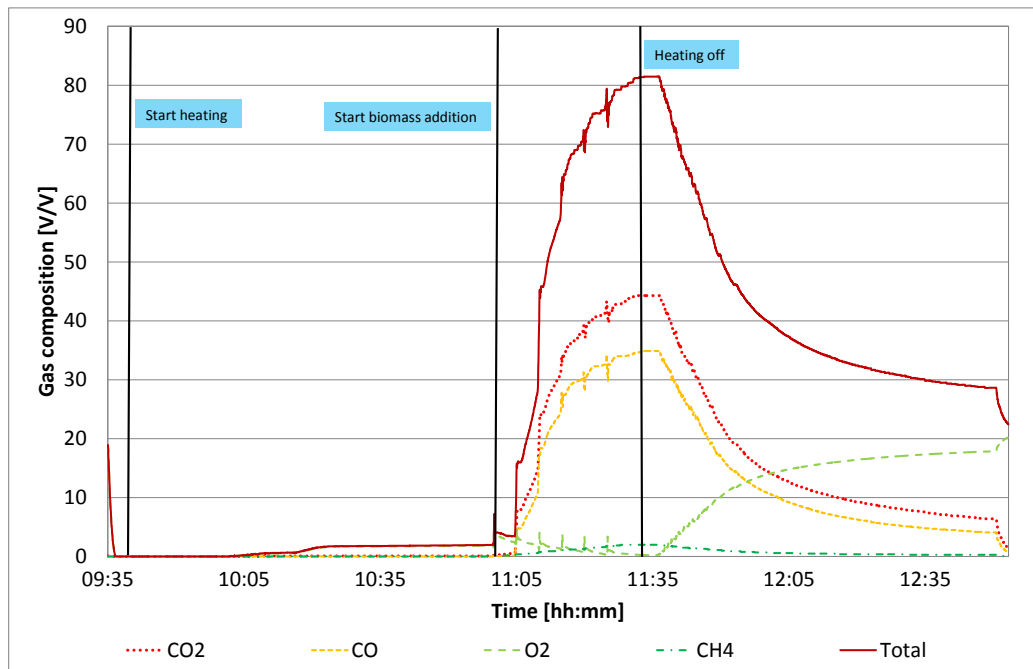
Figure 4.5.: Gas formation during the second pyrolysis experiment

4.2. Hydrodeoxygenation

The temperature and pressure profiles of the deep HDO experiment are shown in Figure 4.6.
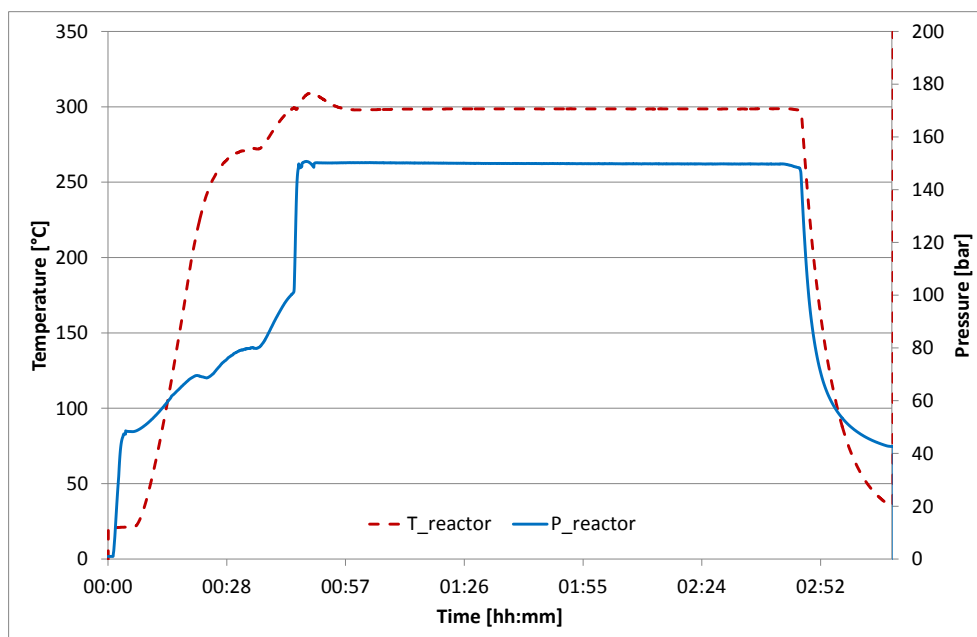
Figure 4.6.: Temperature (on the left axis) and pressure (on the right axis) profile of the deep HDO experiment

The input and output weights are listed in Table 4.4. Altogether, at least 7.4 g H_2 is consumed during the reaction. However, the pressure does not rise as much as usually during HDO experiments, and it is found that the reactor outlet valve is not completely tight, so the exact amount of H_2 consumed cannot be determined.

Table 4.4.: Input and output weights of the hydrodeoxygenation experiment

	[g]	[wt%]	
PO feed	222.99		
Ra-Ni	11.09	5	of PO feed
H_2 consumed	> 7.4		
Product	229.2		
Organic phase	56.15	24.5	of product
Aqueous phase	173.05	75.5	of product

A gas sample is collected in a gas sack and analyzed with Micro-GC by the Fuel Cell Systems Department of the Institute of Chemical Engineering and Environmental Technology, Graz University of Technology. The results are given in Table 4.5.

Table 4.5.: Composition of the gas formed during the HDO experiment

H_2	CO_2	CH_4
[vol%]	[vol%]	[vol%]
73.1	24.4	2.6

The results of the elemental analysis are presented in Table 4.6.

Table 4.6.: Elemental composition of the organic and the aqueous phase

	C	H	O	N
	[wt%]	[wt%]	[wt%]	[wt%]
Organic phase	65.7	8.7	25.1	0.5
Aqueous phase	10.7	10.5	78.5	0.3
	[mol%]	[mol%]	[mol%]	[mol%]
Organic phase	5.5	8.6	1.6	0.0
Aqueous phase	0.9	10.4	4.9	0.0

The van Krevelen plot, Figure 4.7, compares the molar O/C to H/C ratio of the PO feed, the aqueous product phase and the organic product phase, DH1 and gasoline for comparison.

Figure 4.7 shows that the molar O/C ratio of DH1 is lower than that of the feed, which means that some oxygen has successfully been removed. However, the molar H/C ratio is also smaller than in the feed, which is mainly attributed to the removal and loss of water.

For comparison, the molar H/C ratio of gasoline is 1.95[18], whereas the ratio of DH1 is 1.57. So depending on the application of hydrodeoxygenated bio-oils, the oxygen content should be further decreased and the hydrogen content should be further increased.

Furthermore, the oil yield, Y_{oil}, is plotted over the degree of deoxygenation, DOD, in Figure 4.8. For comparison, data from Wildschut et. al.[12] are shown, they are called MH-W and DH-W.

MH-W is the organic product phase from a mild HDO experiment, DH-W of a deep HDO experiment, both from a fast pyrolysis oil prepared from beech wood. The mild HDO experiment was conducted at 250 °C, 100 bar, the deep HDO experiment was conducted at 350 °C, 200 bar, and both for 4 h, over a NiMo/Al$_2$O$_3$ catalyst.

In general, more oxygen can be removed under harsher conditions, but at the expense of the oil yield.
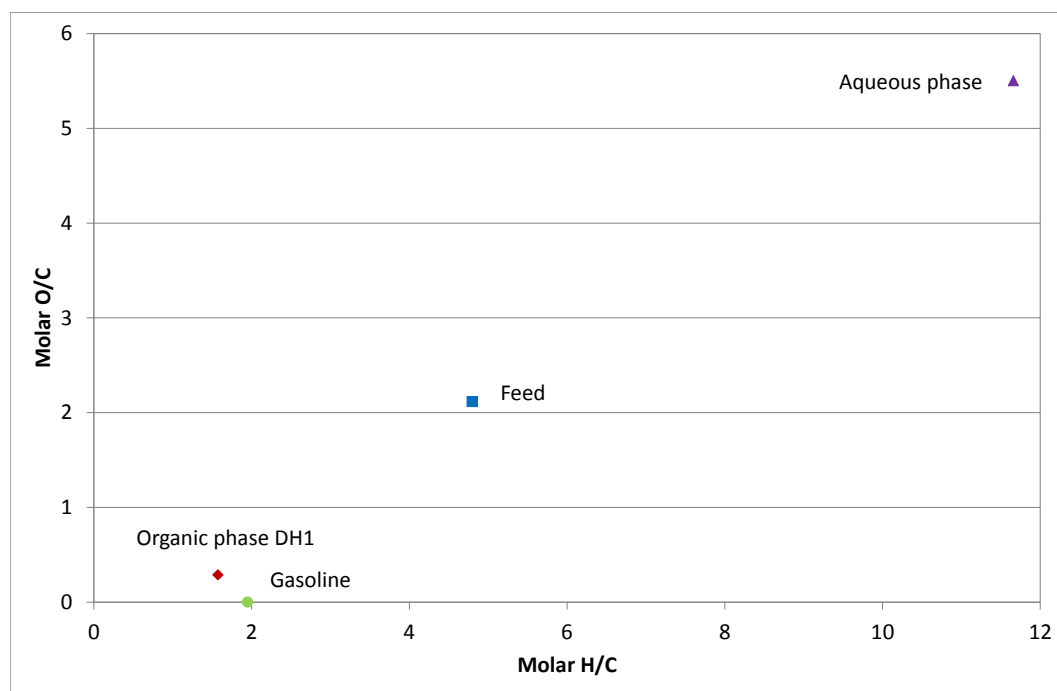
Figure 4.7.: Van Krevelen plot depicting the PO feed, the aqueous product phase and the organic product phase, DH1 and gasoline
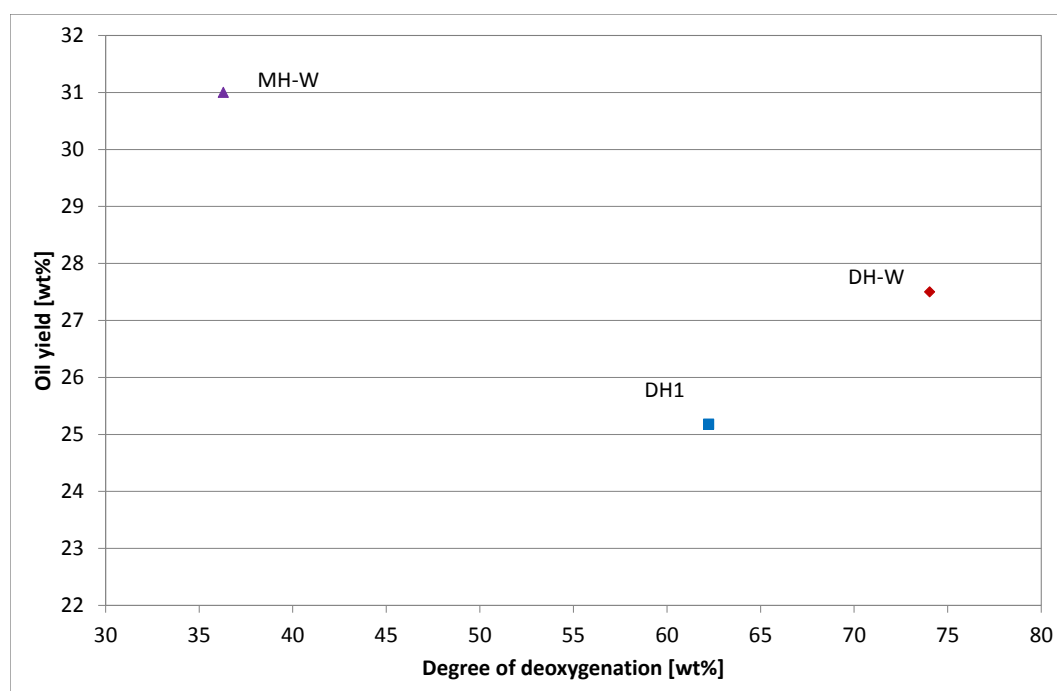
Figure 4.8.: Oil yield, Y_{oil}, over degree of deoxygenation, DOD, of DH1 and MH-W and DH-W from Wildschut et. al.[12]

4.3. Coal Liquefaction

The first coal liquefaction yields 22.97 wt% solid and 77.03 wt% liquid phase, the second liquefaction 23.70 wt% and 76.30 wt%, respectively.

Moreover, 25.6 l and 24.0 l gas is formed during the reaction. According to the hydrogen balances, 2.19 and 2.11 g H_2 is consumed, respectively.

The temperature and pressure profiles are shown in Figure 4.9 and Figure 4.10.
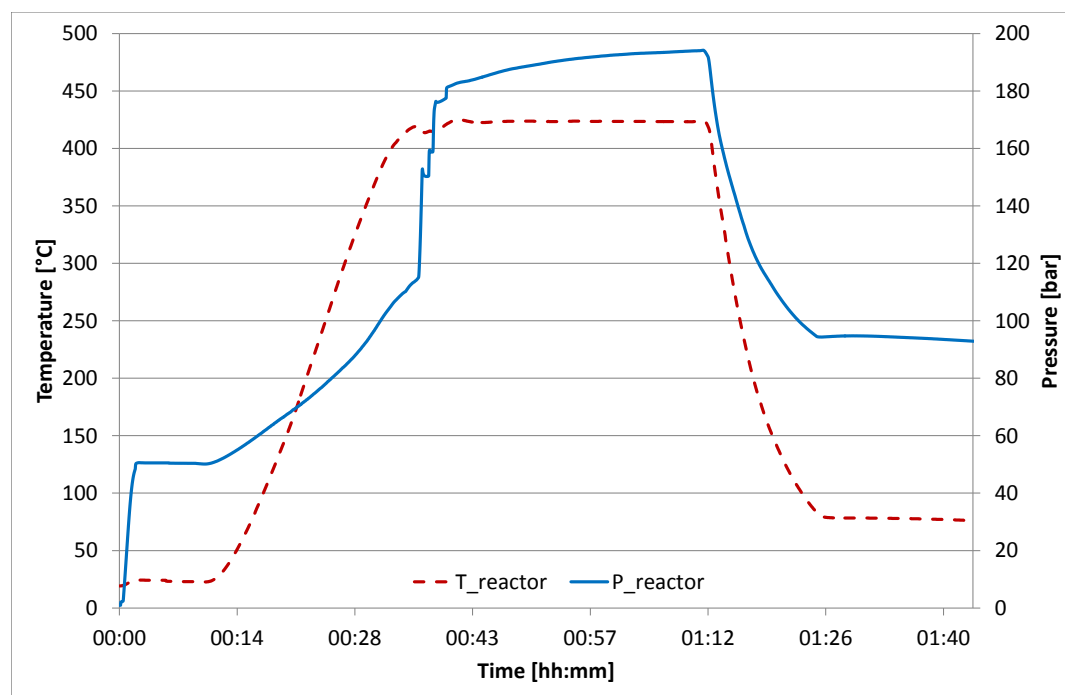
Figure 4.9.: Temperature (on the left axis) and pressure (on the right axis) profile of the first CL experiment

The pressure in the reactor does not increase strongly but stays rather constant during the liquefaction, especially for the second experiment with 5 wt% Raney-Nickel catalyst. Usually, the pressure increases because volatile compounds are formed and hydrogen is still supplied.

The findings of rather constant pressure for these two experiments suggest that some of the supplied hydrogen is used up. The solvent, tetralin, supplies some of its hydrogen during CL, turning into naphthalene. So maybe naphthalene is in situ re-hydrogenated to tetralin and decalin with the help of the catalyst, see section 2.3.

The elemental compositions of the liquid products are presented in Table 4.7. Samples of the gas formed during the reaction are collected in a gas sack analyzed via Micro-GC. The gas compositions are shown in Table 4.8.
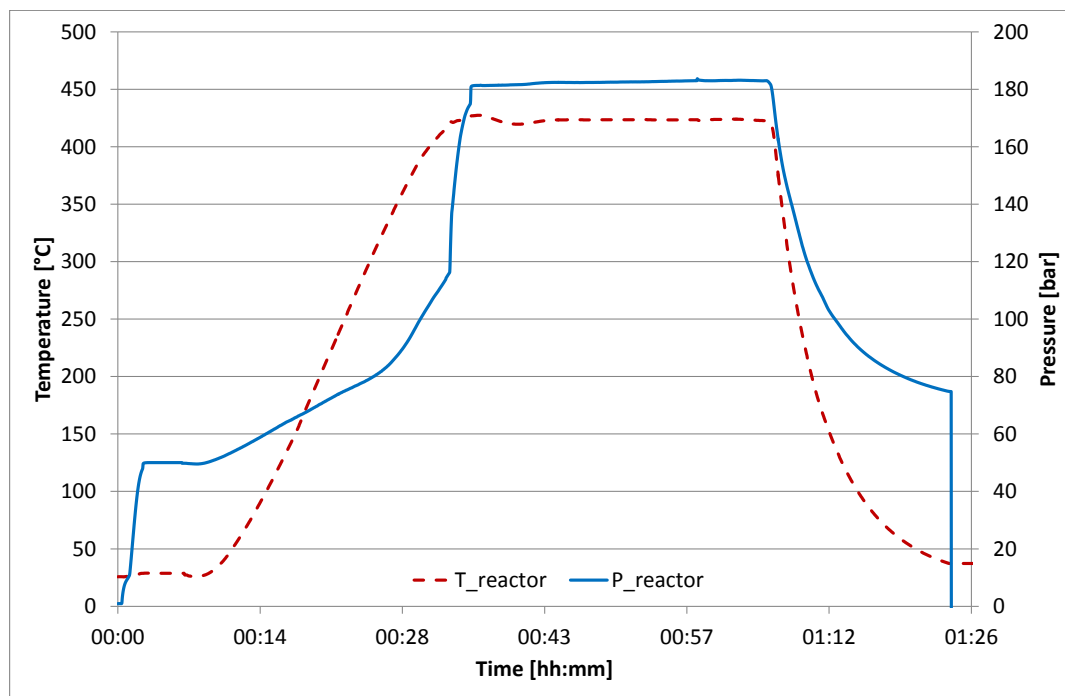
Figure 4.10.: Temperature (on the left axis) and pressure (on the right axis) profile of the second CL experiment

Table 4.7.: Elemental composition of CL1 and CL2

	C	H	O
	[wt%]	[wt%]	[wt%]
CL1	90.6	8.4	0.7
CL2	90.7	8.6	0.4

Table 4.8.: Composition of the gas formed during coal liquefaction

	H_2	CO_2	CH_4	C_2H_4
	[%]	[%]	[%]	[%]
CL1	95.6	1.1	3.2	0.1
CL2	94.0	0.4	5.4	0.1

4.4. Aging

4.4.1. Pyrolysis

The behavior and changes in the pyrolysis oils PY1 and PY2 during elongated storage are monitored. All analyses are carried out according to the schedule and according to the descriptions in section 3.5.

In general, the same behavior is observed in both PY samples, suggesting that the aging in two different pyrolysis oils is comparable. Furthermore, all the obtained data show that the pyrolysis experiments are reproducible.

4.4.1.1. GC-MS

Figure 4.11 and Figure 4.12 show the results of the GC-MS measurements of the pyrolysis oils.
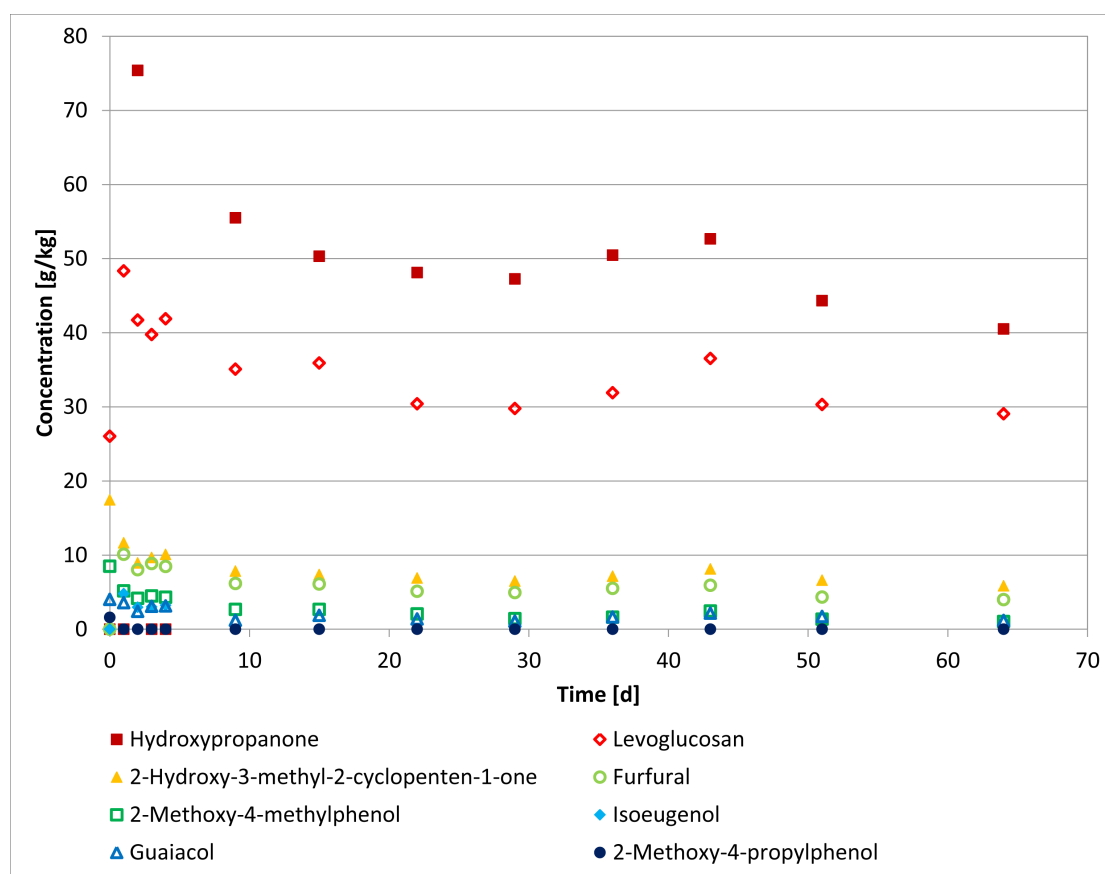
Figure 4.11.: GC-MS of PY1 versus storage time

Various substances are identified and are shown in Figure 4.11 and Figure 4.12.

Levoglucosan and furfural are degradation products of the polysaccharides, cellulose and hemicellulose. 2-Methoxy-4-methylphenol, 2-methoxy-4-propyphenol, guaiacol and isoeugenol are derived from lignin.
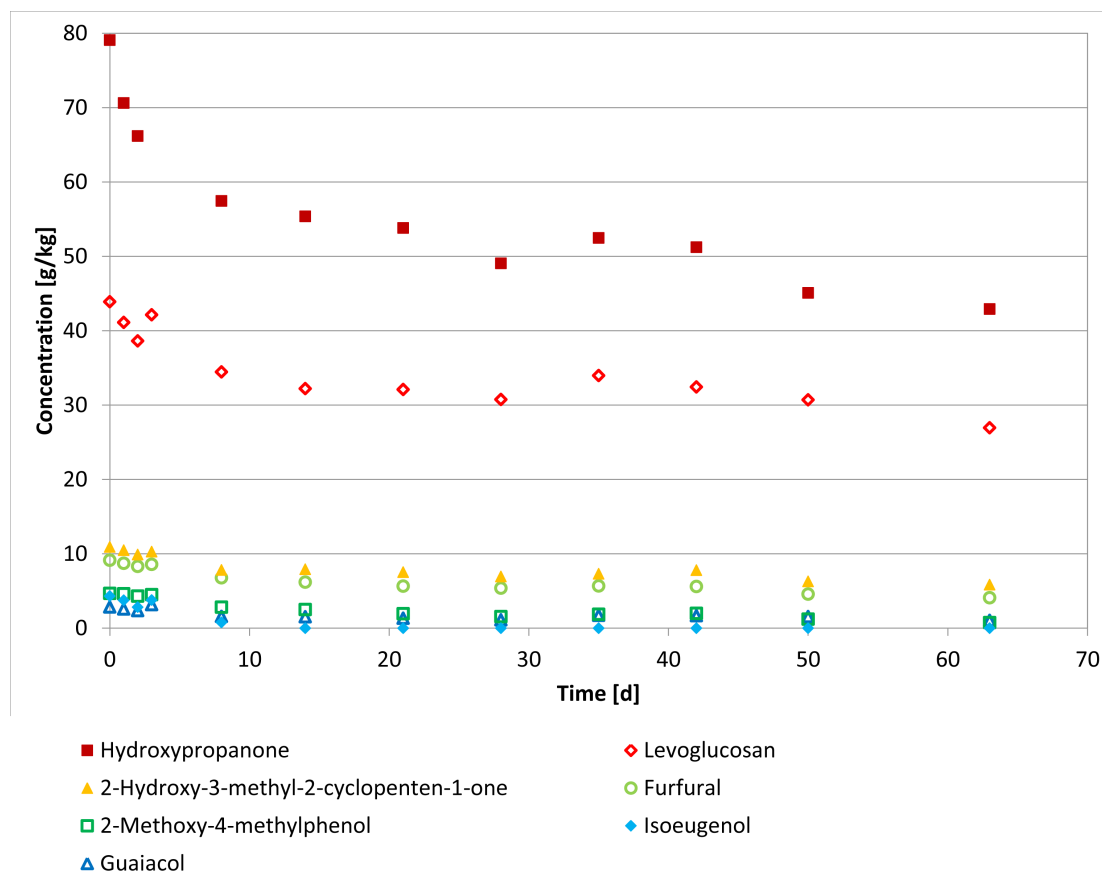
Figure 4.12.: GC-MS of PY2 versus storage time

Hydroxypropanone is contained in the highest amount, between approx. 40 to 80 g/kg sample. It is a secondary degradation product of the sugar fraction. γ-butyrolactone is a degradation product from the solvent THF. Unstabilized THF is used, and when the sealed bottle is openend and the THF is subsequently stored under air, oxidation reactions may occur. For that reason, γ-butyrolactone is not quantified. Artifacts from THF can also be found in the GPC chromatograms, see subsubsection 4.5.2.9.

Moreover, it can be observed that the lignin-derived molecules are in lower concentrations in the pyrolysis oils than the polysaccharides-derived molecules. This observation is explained by the fact that the polysaccharides make up approx. 60 wt% of spruce wood, while lignin only comprises approx. 30 wt%.

Furthermore, it has been proved by Schwaiger et al.[8] that under the given pyrol-

ysis conditions, most of the lignin frame of the wood stays intact and mainly the polysaccharides are decomposed. For these reasons, the amounts of polysaccharides-derived molecules are up to 80 times larger than the lignin-derived molecules detected via GC-MS.

4.4.1.2. GPC

Figure 4.13 and Figure 4.14 show the GPC-chromatograms of PY1 and PY2.
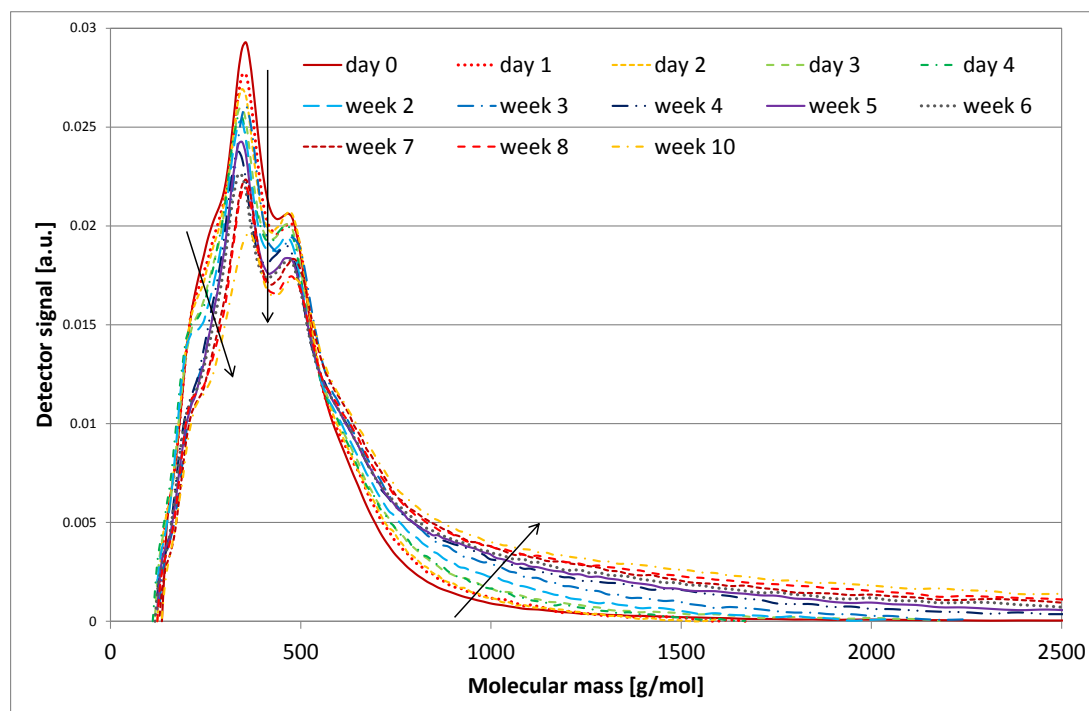
Figure 4.13.: Chromatograms of PY1, recorded for different storage times, the arrows highlight the main trends

The arrows mark the changes with advancing time. The trends are the same in both pyrolysis oils. It can be seen that the peaks at smaller molecular masses, at approx. 250 and 400 g/mol, decrease, which probably indicates that the amount of molecules with smaller molecular masses decreases.

Furthermore, there is a shift to higher molecular masses at approx. 1000 g/mol. The amount of molecules within the range of approx. 600 to 6000 g/mol increases with increasing storage time. Within the first week of aging, no molecules with molecular masses higher than approx. 1600 g/mol can be detected.

However, the highest molecular mass increases to 2000 g/mol within 3 weeks and to approx. 3200 g/mol within 5 weeks. After 10 weeks of storage, even molecules

with masses as high as approx. 10000 g/mol can be detected, although only in very small amounts.
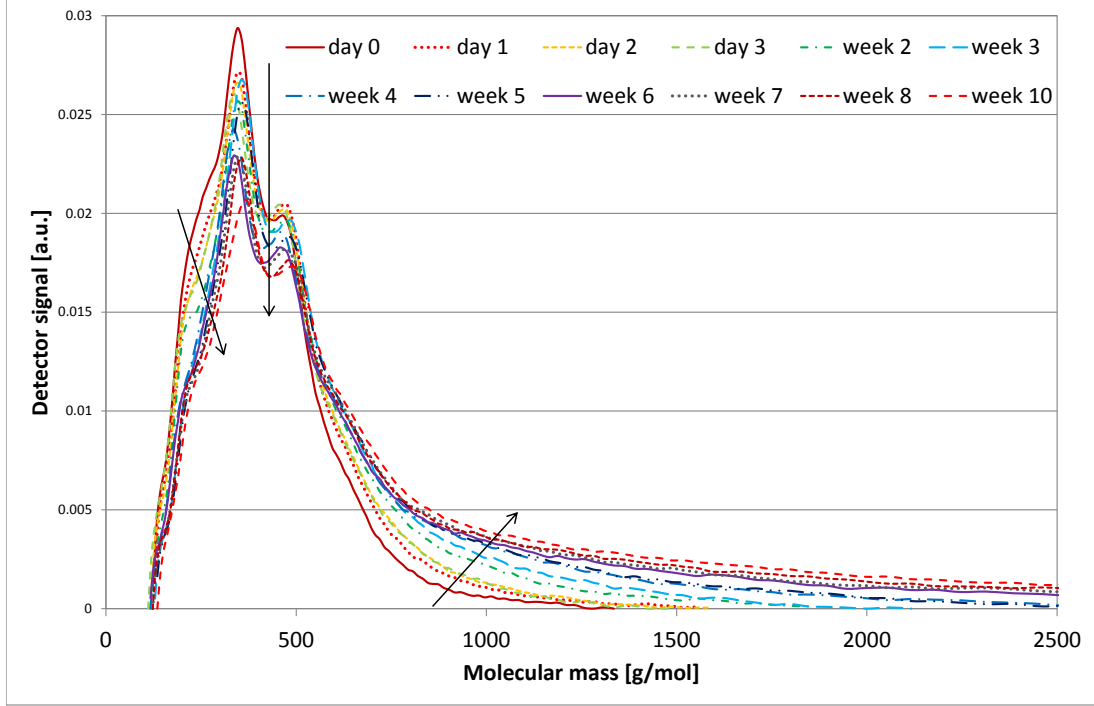
Figure 4.14.: Chromatograms of PY2, recorded for different storage times, the arrows highlight the main trends

This shift to higher molecular masses can also be observed in the number average molecular mass, M_n, and the weight average molecular mass, M_w. These values are depicted over storage time in Figure 4.15.

M_n and M_w can be calculated with Equation 4.1 and Equation 4.2, where N_i is the number and M_i the molecular mass of the ith molecule. The values are automatically calculated by the Shimadzu LabSolutions GCMS software.

$$M_n = \frac{\sum N_i \cdot M_i}{\sum N_i} \tag{4.1}$$

$$M_w = \frac{\sum N_i \cdot M_i^2}{\sum N_i \cdot M_i} \tag{4.2}$$

The M_n lies at approx. 340 g/mol in the fresh samples, but then increases linearly with a slope of approx. 1.4 g/(mol d). The same trend is observed for the M_w: in the fresh samples, the M_w is calculated to be approx. 400 g/mol, and then increases with approx. 3.8 g/(mol d).
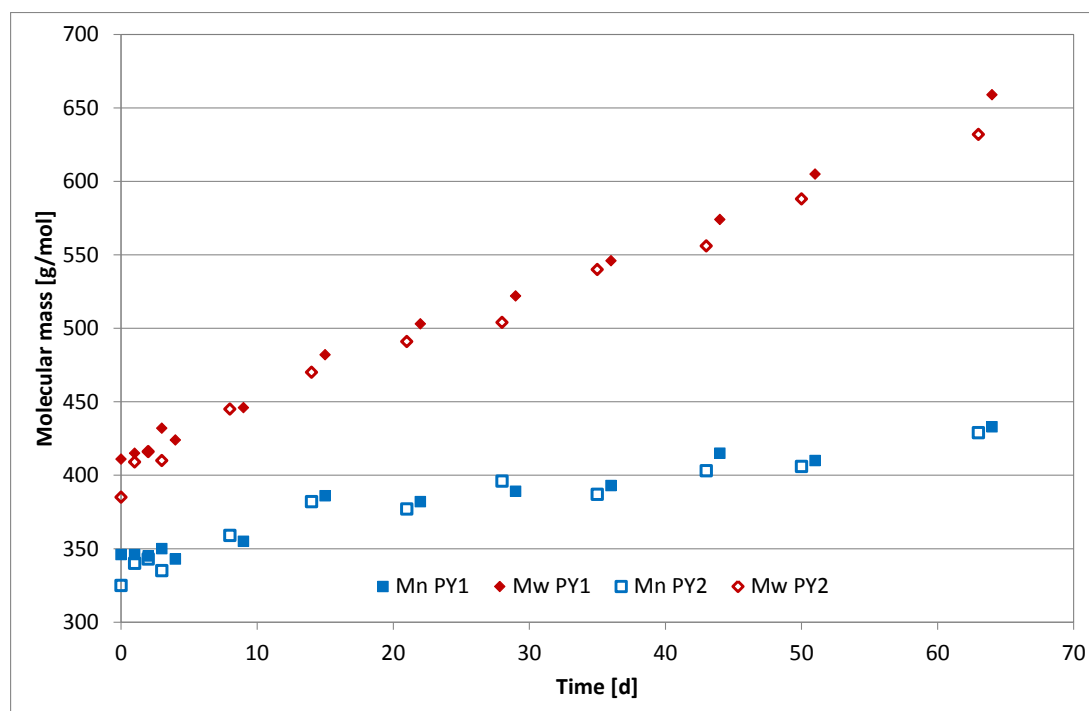
Figure 4.15.: Number average molecular mass, M_n, and weight average molecular mass, M_w, of PY1 and PY2, plotted over the storage time

To sum up, the GPC analyses prove that polymerization reactions occur in the samples. The amount of molecules with smaller molecular masses decreases over time, which comes along with chain length increase.

4.4.1.3. Viscosity

Figure 4.16 depicts the results of the viscosity measurements. The measurements are carried out at 20 °C, as explained in subsection 3.5.3.

The dynamic viscosity of both oils is very low, at about 7 mPa s. Figure 4.16 shows an overall increase in the viscosity. However, two regimes can be distinguished. Within the first week of storage, the viscosity increase rate is high, with approx. 0.2 mPa s/d. After the first week, the viscosity increase rate becomes constant with a value of only approx. 0.03 mPa s/d.

Thus, the viscosity increase rate decreases by one order of magnitude after the first week of storage. So the increase in viscosity is negligible, especially as the pyrolysis oils obtained by liquid phase pyrolysis have a very low viscosity compared to literature values, as shown in subsection 2.4.2.
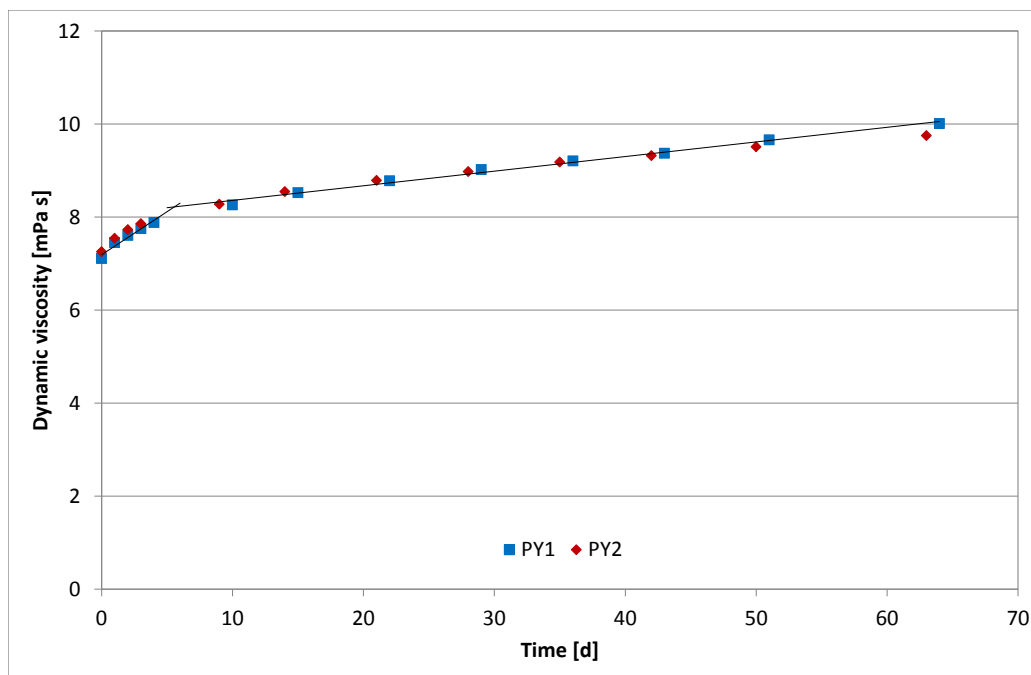
Figure 4.16.: Viscosity of PY1 and PY2 plotted against storage time

4.4.1.4. Acid Concentration

Figure 4.17 shows the results of the acid concentration measurements calculated according to subsection 3.5.4.
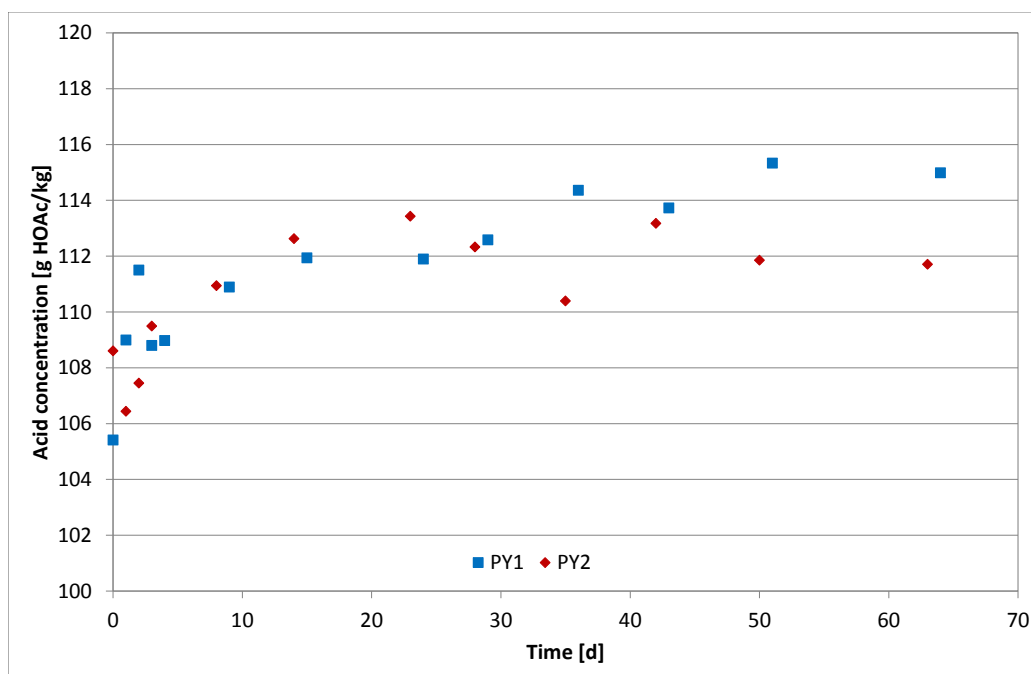
Figure 4.17.: Acid concentration of PY1 and PY2 versus aging time

In general, the amount of acids in PY1 and PY2 is high, with approx. 110 g acetic acid in 1 kg of sample. This high acid content causes the low pH-value elucidated below.

No specific trends can be observed concerning the acid content over storage time. The values vary within the standard deviation and fluctuate too much to draw conclusions. It is not possible to find a linear trend over time.

4.4.1.5. pH-Value

The pH-values of PY1 and PY2 are depicted in Figure 4.18.
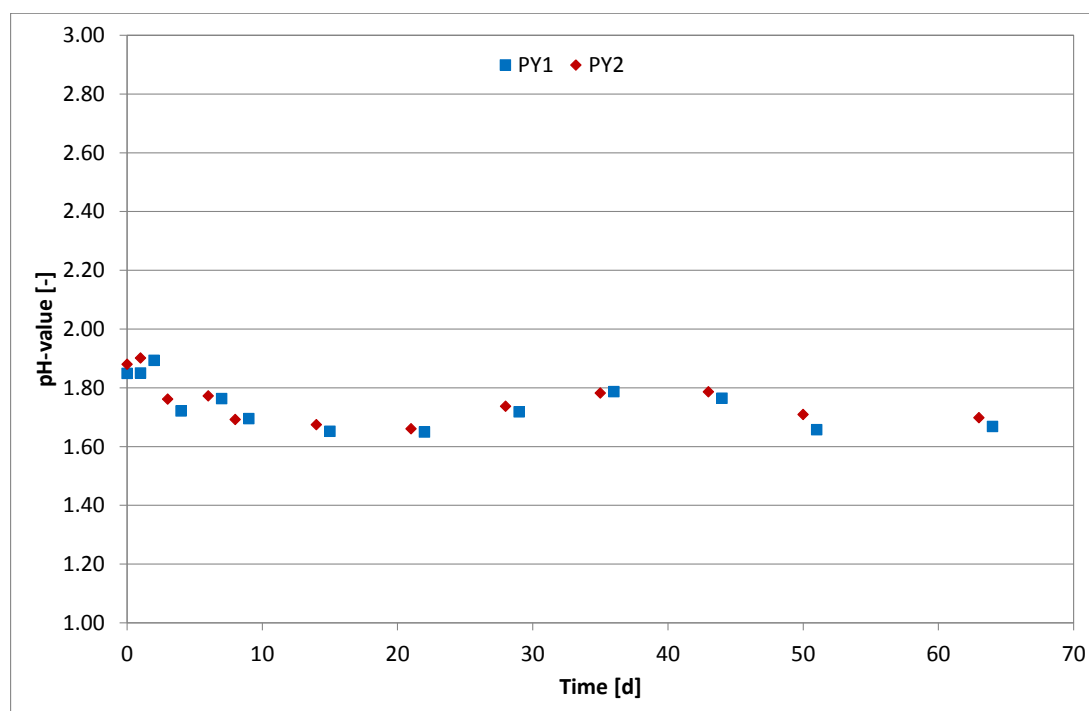
Figure 4.18.: pH-value of PY1 and PY2 plotted against storage time

The pH-values are very low, causing problems concerning materials for storage and processing. However, as with the acid concentration, no specific trends over time can be found.

4.4.1.6. Water Content

Figure 4.19 shows that the water content of PY1 and PY2 is constant over time. Thus, no condensation reactions occur. However, as the molecular masses increase according to the GPC results, addition reactions probably take place.

In these addition reactions, oxygen-rich compounds combine without the elimination of water. Due to the constant water content, neither possible equilibrium reactions influenced by the water content are likely, nor phase separation caused by an increase of the water content. In general, the water content is high, at approx. 35 to 40 wt%, leading to a low higher heating value, HHV, but also to an advantageous low viscosity.
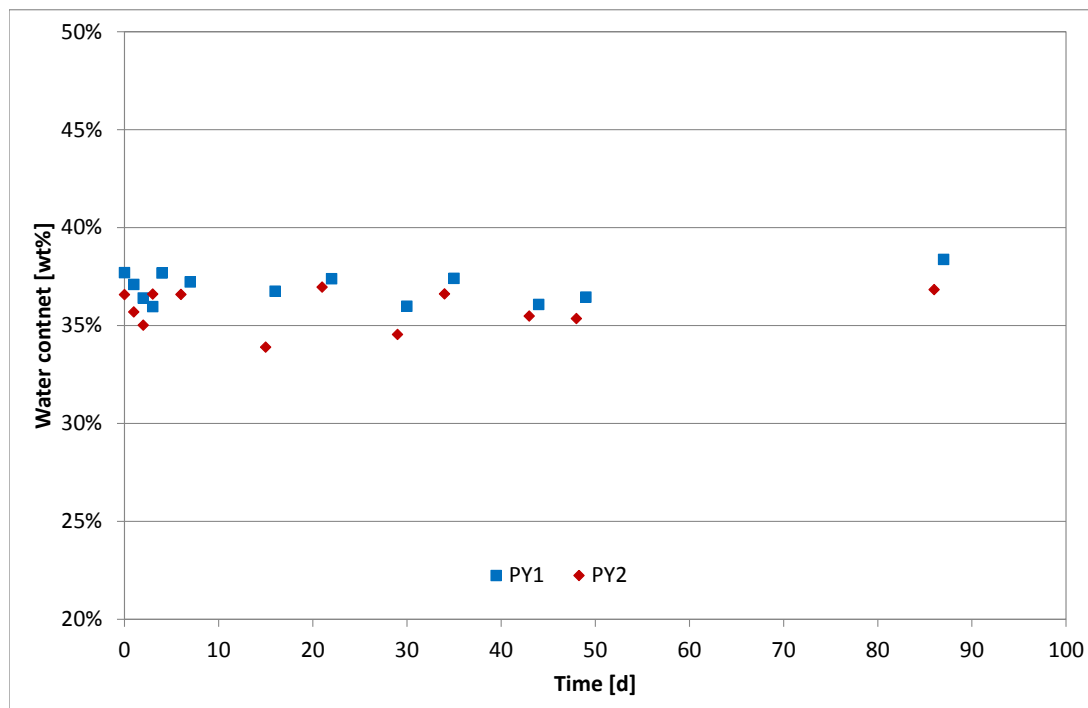
Figure 4.19.: Water content of PY1 and PY2 over storage time

4.4.2. Hydrodeoxygenation

4.4.2.1. GC-MS

Figure 4.20 and Figure 4.21 show the results of the GC-MS measurements of the hydrodeoxygenated pyrolysis oils. As already explained in section 3.5, it is not possible to calibrate all molecules found with GC-MS. Some of the calibrated molecules are found in the hydrodeoxygenated pyrolysis oil, they are shown in Figure 4.20.

However, most of the molecules are not calibrated, so they cannot be quantified. So in order to monitor the changes during aging of these molecules, the peak areas are compared over time, as depicted in Figure 4.21.
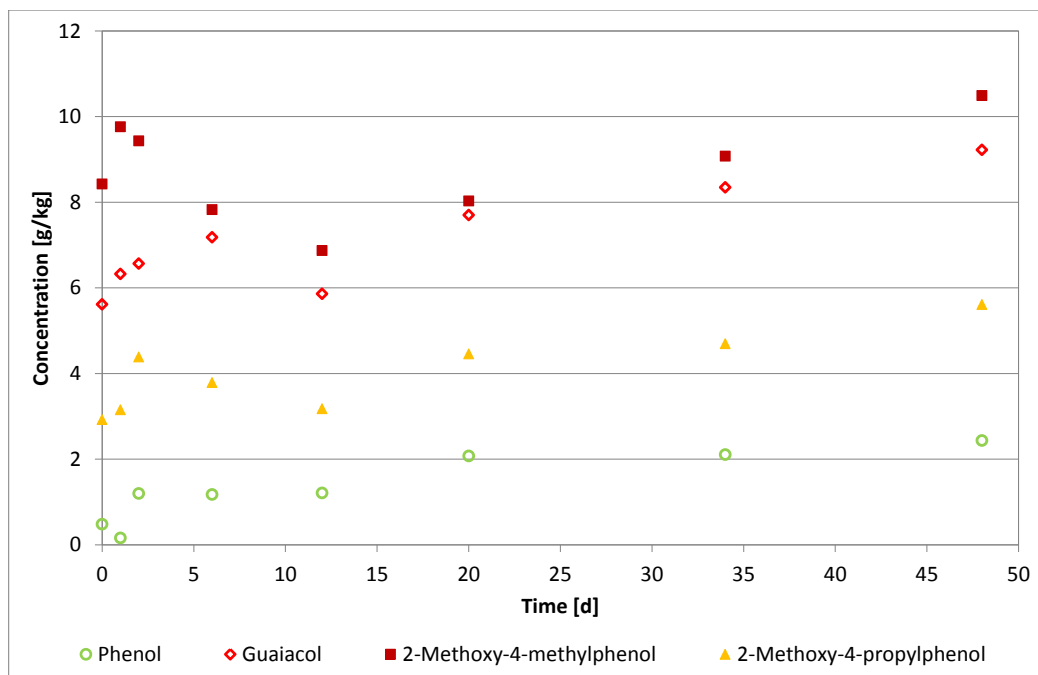
Figure 4.20.: GC-MS of DH1, quantified molecules, plotted versus time
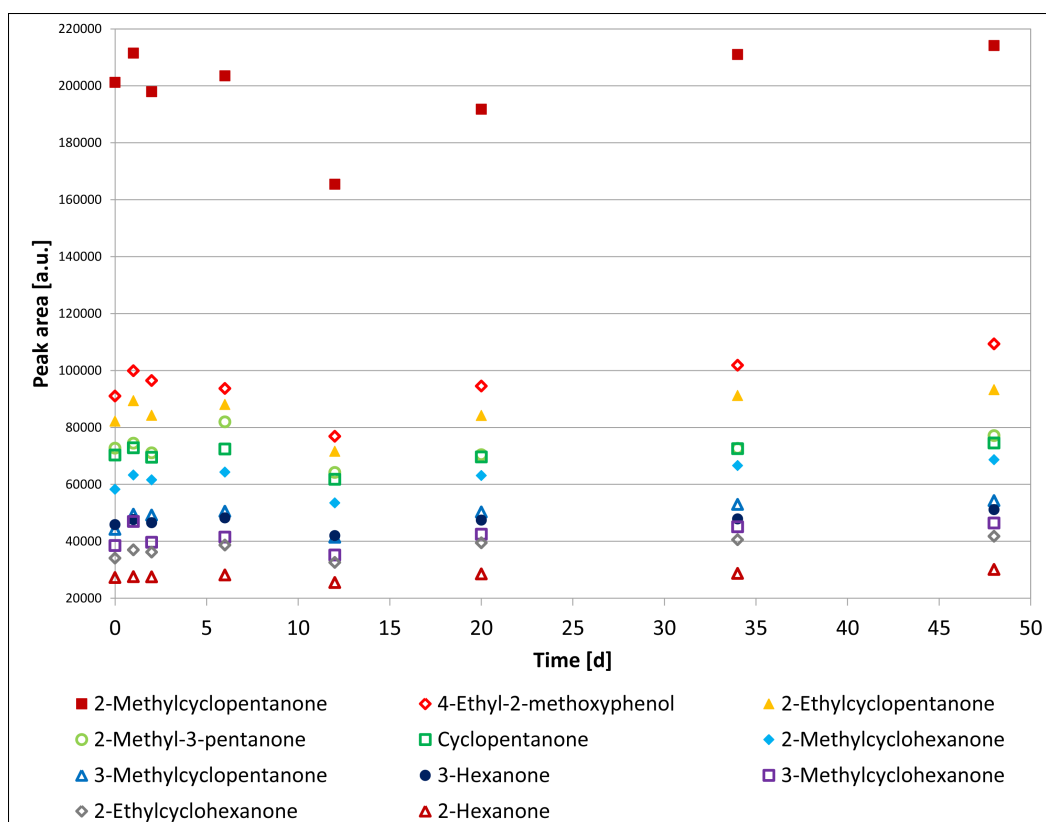
Figure 4.21.: GC-MS of DH1, plotted versus time

A small concentration increase is found for phenol, guaiacol and 2-methoxy-4-propylphenol. The concentration of 2-methoxy-4-methylphenol is higher at first, then decreases, and starts to increase after two weeks. It is not clear if there is a trend or if the concentration of 2-methoxy-4-methylphenol only fluctuates.

In general, many of the oxygenated species found in the pyrolysis oils cannot be found in the hydrodeoxygenated oil, clearly demonstrating the effectiveness of the hydrodeoxygenation step.

Instead, considerable amounts of methylated and ethylated pentanones and hexanones as well as cyclopentanones and cyclohexanones can be detected. These molecules are also chosen for monitoring because they have high enough peaks with a good chromatographic resolution and do not overlap with other molecules, so the attribution of the peak area is feasible.

As already observed for 2-methoxy-4-methylphenol, the concentration first decreases and after two weeks of storage, a small concentration increase is observed over time.

4.4.2.2. GPC

Figure 4.22 depicts the GPC results of DH1.
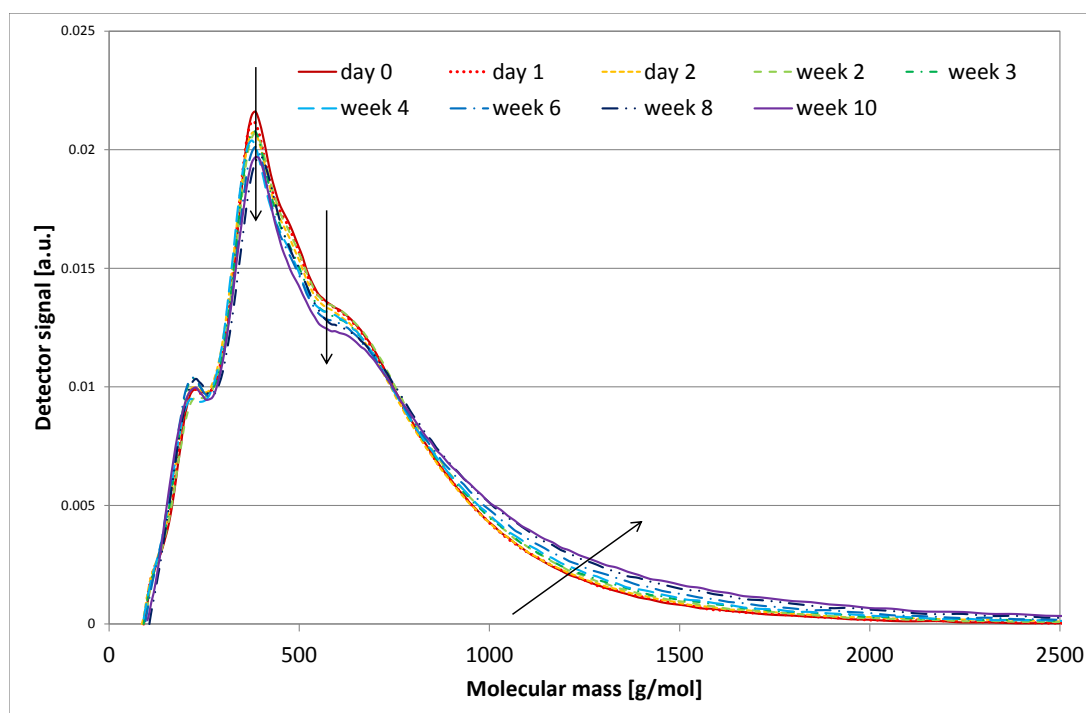
Figure 4.22.: GPC of DH1, recorded for different storage times, the arrows highlight the main trends

70

The same trends over time as for the pyrolysis oils are observed: The amount of molecules at the peak maximum, at approx. 380 g/mol decreases, as well as the amount of molecules at approx. 500 g/mol. The amount of molecules with molecular masses higher than 600 g/mol increases. These changes are marked by the arrows.

However, these changes are very small compared to the changes in the pyrolysis oils. This means that polymerization reactions do occur, but less frequently than in the pyrolysis oils. So concerning molecular masses, the hydrodeoxygenation step does make the oil more stable.

These findings are confirmed in Figure 4.23. M_n and M_w do increase over time, but only in so small quantities that these changes are negligible.
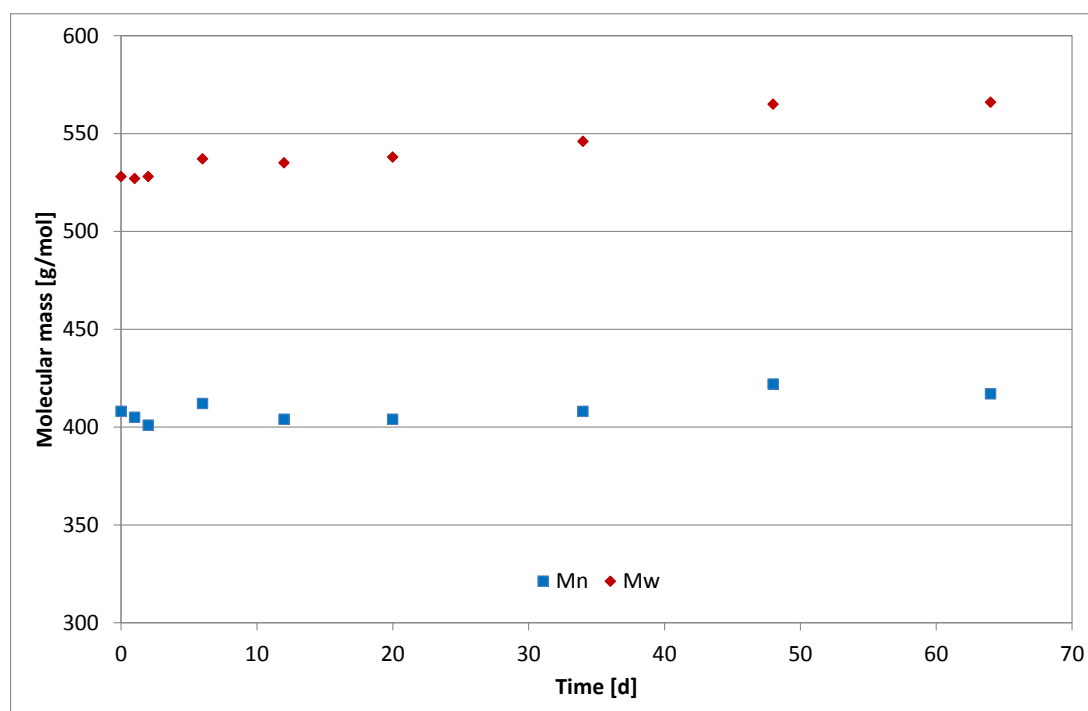
Figure 4.23.: Number average molecular mass, M_n, and weight average molecular mass, M_w, of DH1, plotted over the storage time

4.4.2.3. Viscosity

The changes of the dynamic viscosity over time of DH1 are shown inFigure 4.24. Compared to the pyroylsis oils PY1 and PY2, the viscosity of DH1 is approx. an order of magnitude higher for the fresh oil.

The hydrodeoxygenation step yields two phases: an aqueous phase and an organic

product phase. Because of the immiscibility of the two phases, the organic product phase, DH1, has a lower water content than the pyroylsis oils PY1 and PY2. So the high water content in pyrolysis oils 'dilutes' the oils, thus lowering their viscosity.

Furthermore, when there is a high water content, the probability that two oxygenated molecules meet and combine in a polymerization reaction is lower. This may be a possible explanation for the observation that the viscosity does not increase as much over time in pyrolysis oils PY1 and PY2 (that have a higher water content) as in the hydrodeoxygenated pyrolysis oil DH1.
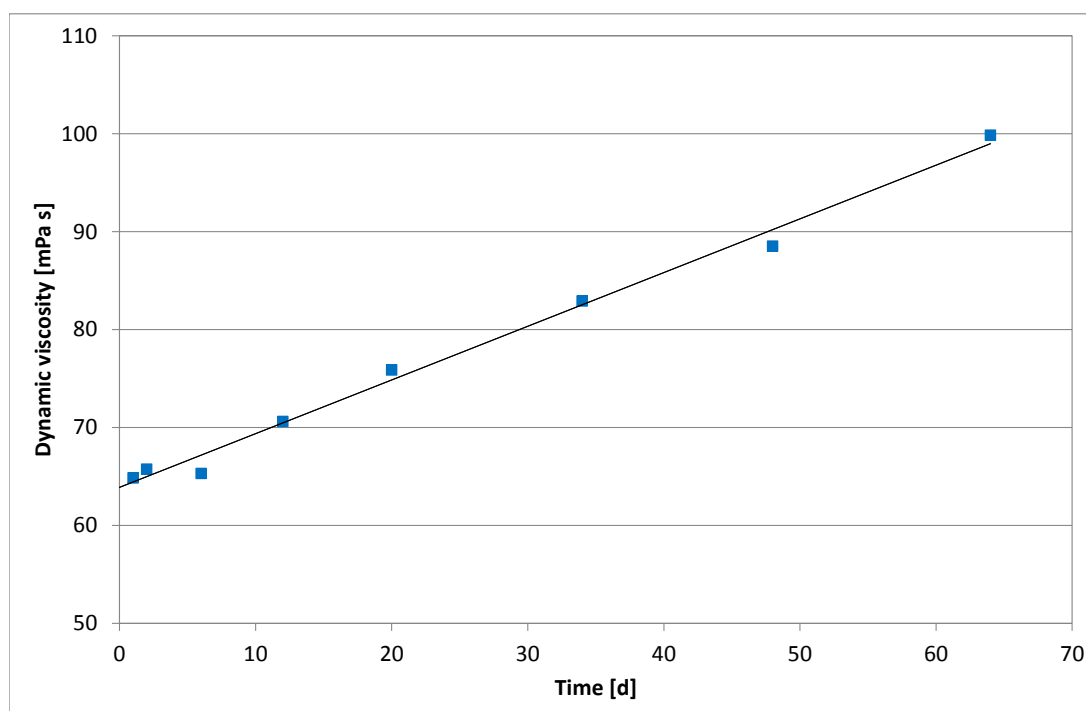
Figure 4.24.: Change of viscosity of DH1 over time

The trend that the viscosity increase rate becomes constant at a lower value after the first week of storage, as observed for the pyrolysis oils, cannot be observed for DH1. The viscosity increase rate stays constant during the whole storage time, at approx. 0.5 mPa s/d. This high increase in viscosity definitely poses a problem concerning storage stability. This aspect should be improved concerning hydrodeoxygenation.

In the literature[20,24] it is found that pyrolysis oils are diluted, for example with methanol. Maybe this is also a viable possibility in this case, as the methanol would lower the viscosity and the probability of polymerization reactions.

4.4.2.4. Acid Concentration

Figure 4.25 depicts the acid concentration over time. As already observed for the pyrolysis oils, no specific trends can be observed regarding the change in acid concentration during storage.
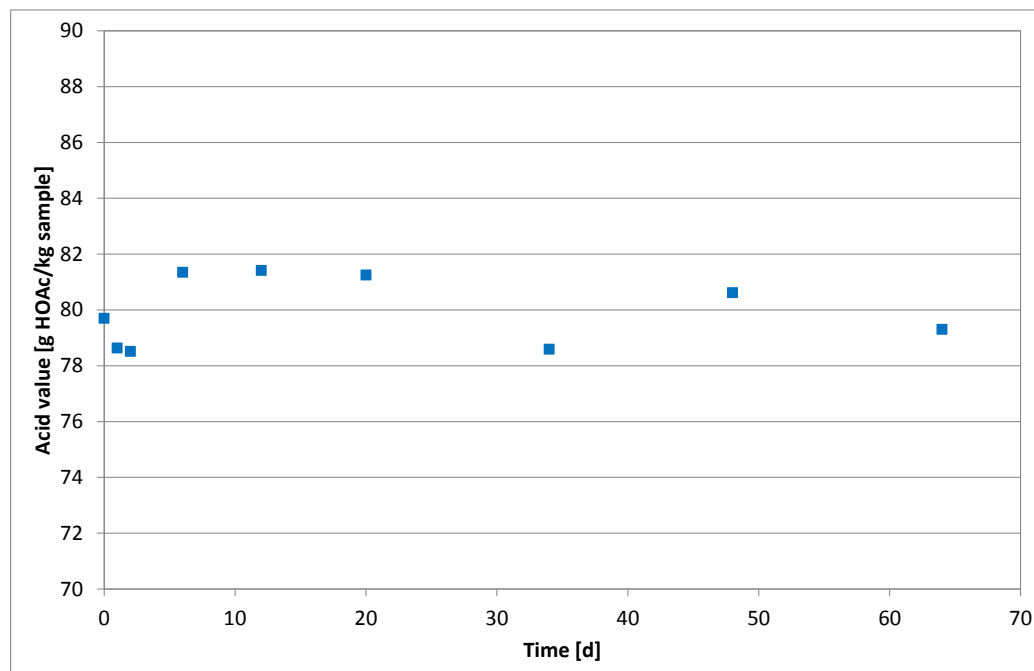
Figure 4.25.: Acid concentration of DH1, monitored over storage time

In general, the acid content is lower in the hydrodeoxygenated pyrolysis oil than in the pyrolysis oils. This means that in the hydrodeoxygenation step, a part of the organic acids can be converted to aldehydes and possibly alcohols.
Another possibility is that most of the acids are dissolved in the aqueous phase. This theory is supported by the higher acid number of the aqueous phase, which lies at 98.42 g HOAc/kg sample, compared to a value of approx. 80 g HOAc/kg sample of the organic phase.

4.4.2.5. pH-Value

The pH-values are shown in Figure 4.26. Again, no specific trends over time can be found. The pH-value is higher in the hydrodeoxygenated oil, confirming the conversion of some of the organic acids or the transfer of acids into the aqueous phase.
Again, the pH-value of the aqueous phase is lower, 2.646, so probably some of the acids contained in the pyrolysis oil feed are dissolved into the aqueous phase, resulting in the aqueous phase having a lower pH-value than the organic phase.
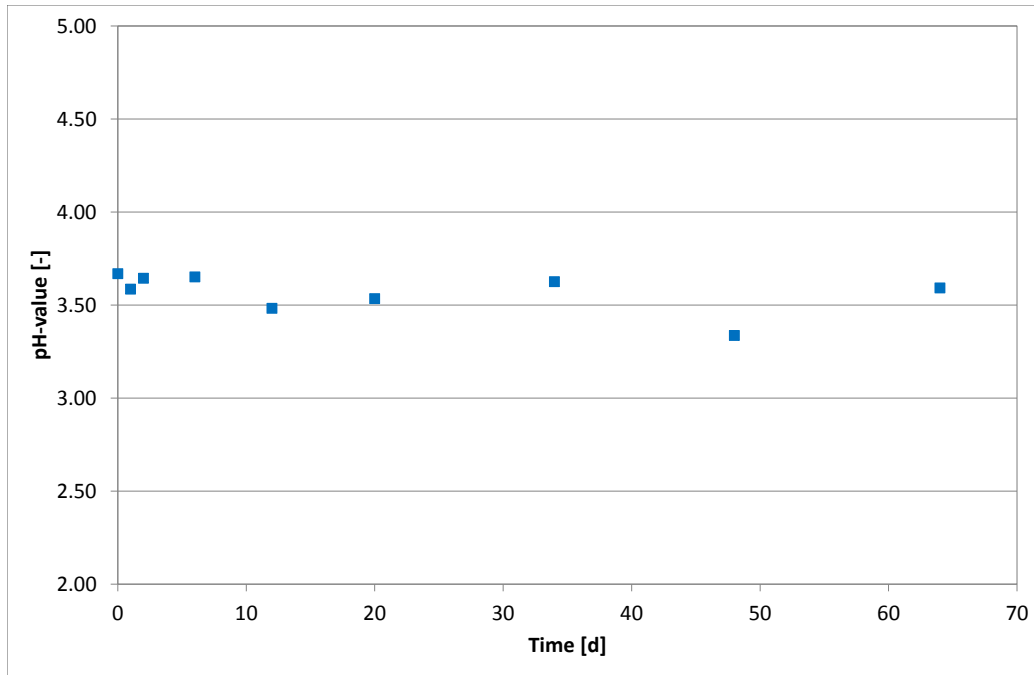
Figure 4.26.: pH-value of DH1 versus aging time

4.4.2.6. Water Content

Figure 4.27 shows the water content over time.
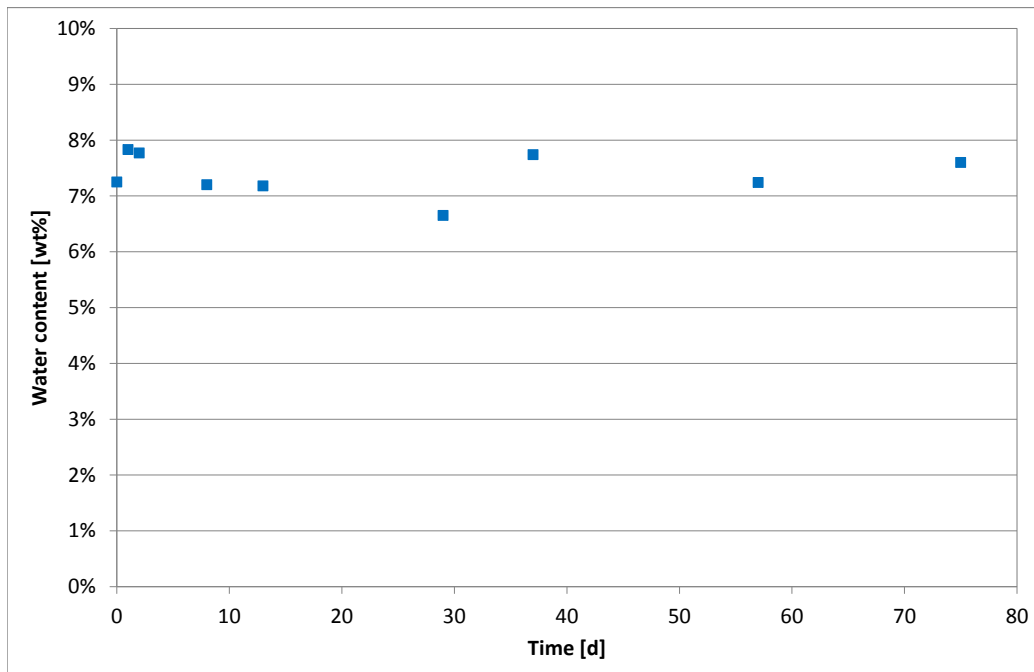
Figure 4.27.: Water content of DH1 plotted versus time

The water content of DH1 stays constant. This is advantageous for storage stability. Many of the possible reactions that could occur over time are equilibrium reactions, that may be influenced e.g. by the water content. So if the water content stays constant, these reactions can be avoided.

Furthermore, the solubilities of the components are influenced by the water content. Thus if the water content is constant, changes in solubilities which may lead to phase separation will not occur. Hence the phase separation into an organic and an aqueous phase is not likely, and it is also not observed during the storage time.

So no increase in the water content is observed but a small increase of the molecular masses. These observations mean that not condensation reactions lead to higher molecular masses, as a water molecule would be liberated. Thus, the molecular masses are increased by addition reactions of compounds with a high oxygen content.

In general, the water content is lower in the hydrodeoxygenated POs than in the POs. A lower water content causes an increased higher heating value, HHV. On the downside, the viscosity is higher with a lower water content.

4.4.3. Coal Liquefaction

4.4.3.1. Observations during Storage

All the liquid products are stored in tightly closed Schott glass bottles in a dark environment. For CL1 and CL2 the following observations are made: The inner walls of the glass bottle are covered in a thin black particulate film. The film only starts above the liquid level, but it is possible to dissolve some of the film into the liquid phase again.

The film probably developed when the liquid product covered all the inner walls of the bottle at first. Then, the solvents ran down the walls into the liquid pool, but some of the hydrocarbon products stayed on the walls, possibly preasphaltenes and asphaltenes.

4.4.3.2. GPC

In Figure 4.28 and Figure 4.29, the GPC chromatograms of the coal liquefaction products CL1 and CL2 are shown. It is not possible to attribute molecular masses to the elution volumes of the CL products, see subsubsection 4.5.2.11 for details. For that reason, the chromatograms show the detector signal over the elution volume.
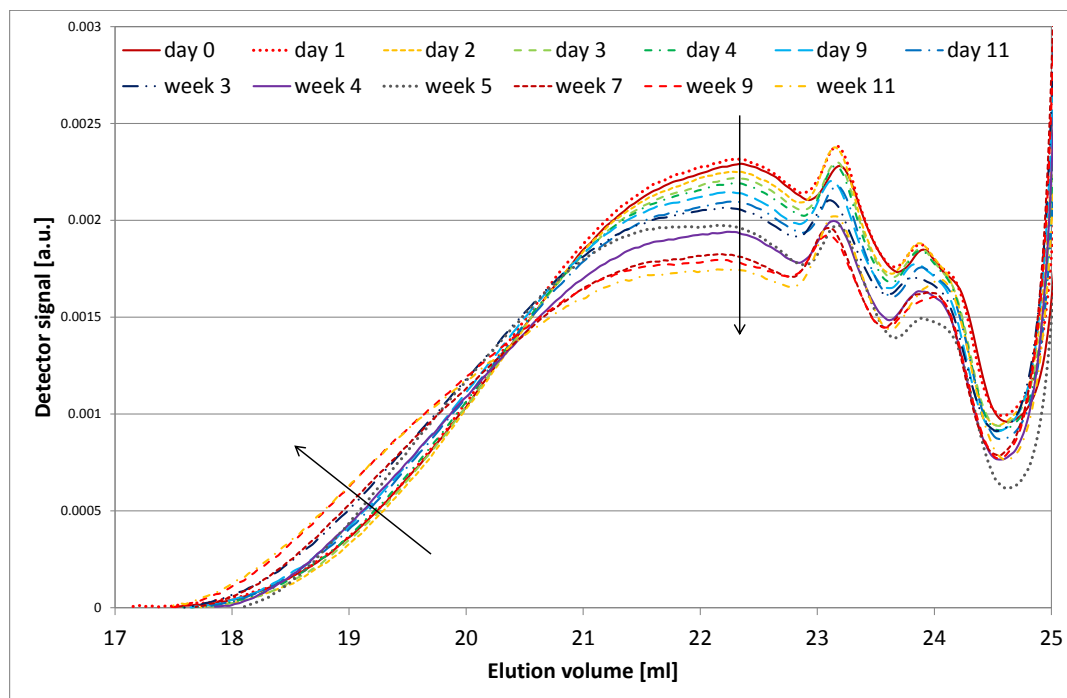
Figure 4.28.: GPC of CL1, recorded for different storage times, the arrows highlight the main trends
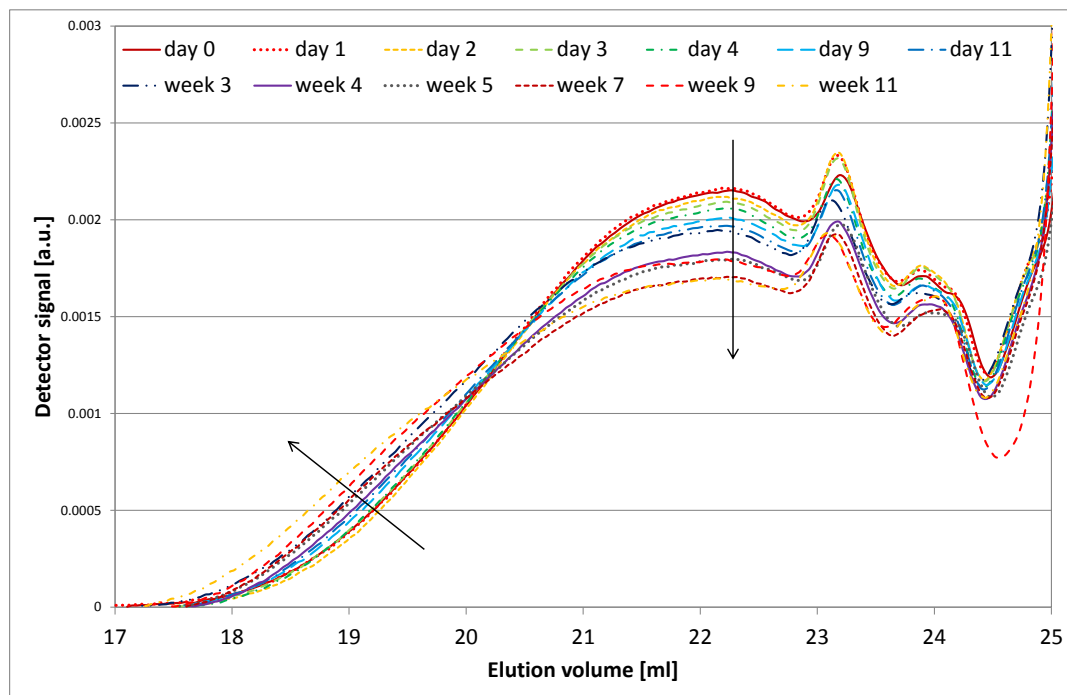
Figure 4.29.: GPC of CL2, recorded for different storage times, the arrows highlight the main trends

The chromatograms are also limited to 25 ml elution volume although they would extend to 30 ml. However, the solvent tetralin elutes at approx. 25.5 ml, and its peak is so high, as it is contained in so high amounts, that it overlaps all other substances eluting at this time.

Naphthalene, to which some of the tetralin is converted during the reaction, elutes at approx. 26 ml, which is visible in a bump in the tail of the tetralin peak. As no other substances can be found beneath the solvent peak, the x-axis is always limited to 25 ml.

As already elucidated in section 2.5, a smaller elution volume generally corresponds to higher molecular masses and vice versa. The amount of substances eluting between 20.5 to 24.5 ml decreases over storage time while the slope at elution volumes smaller than 20.5 ml shifts to smaller elution volumes, as marked by the arrows.

This means that the amount of molecules with lower molecular masses decreases while the higher-mass fraction increases, and an overall shift from lower to higher molecular masses is observed over storage time.

4.5. Analytics

4.5.1. GC-MS

Altogether, more substances are calibrated than can be identified in the measurements. The main problem is that too many different molecules are contained in the pyrolysis oils, so that some cannot be separated properly in the GC column. Some of the peaks in the spectra overlap partially or totally, hence it is not possible to quantify these molecules. It is only possible to quantify molecules with a sufficient chromatographic resolution.

Moreover, concentration is also an issue. The GC-column should not be overloaded, marking the upper concentration limit. Substances should not be contained in concentrations lower than in the most diluted standard of the calibration, as the calibration curve is never extrapolated. This limitation marks the lower concentration limit.

4.5.1.1. Data Processing

The GC-MS software automatically calculates the concentrations of the calibrated substances in ppm by mass of injected sample. Additionally, the dilutions have to be taken into account. The injection volume is always the same, so this factor can be neglected.

The obtained results in ppm in diluted sample are converted into g substance per kg of sample by Equation 4.3,

$$w = \frac{x}{1000} \cdot \frac{(m_{sample} + m_{solvent})}{m_{sample}} \tag{4.3}$$

x being the concentration of the substance in the diluted sample in ppm and w being the mass fraction of the substance in the sample in g/kg.

The cubic calibration curves are automatically calculated by the Shimadzu LabSolutions GCMS software and are given in Table A.1.

When substances should be quantified via a so-called extended calibration, the peak area is converted into the concentration x in ppm of diluted sample via the calibration curve of a similar calibrated molecule, see Equation 4.4. The actual mass fraction w can then be calculated with Equation 4.3 as explained above.

$$x = \frac{-b + \sqrt{b^2 - 4 \cdot a \cdot (c - A)}}{2 \cdot a} \tag{4.4}$$

where a, b and c are the coefficients of the cubic calibration curve (Table A.1) and A is the peak area.

4.5.1.2. Statistics

The arithmetic mean $\bar{x}$ and the standard deviation s are calculated according to Equation 3.2 and Equation 3.3.

The results for the sample preparation are listed in Table 4.9. The same sample is measured six times in order to determine the mean and deviation of the actual GC-MS measurements, the results are listed in Table 4.10.

Table 4.9.: Arithmetic mean and standard deviation of the sample preparation

Substance	$\bar{x}$	s	s
	[g/kg]	[g/kg]	[%]
Hydroxypropanone	51.9	2.4	4.6
Furfural	5.9	0.2	4.0
2-Hydroxy-3-methyl-2-cyclopenten-1-one	7.4	0.2	2.5
Guaiacol	1.7	0.1	6.7
2-Methoxy-4-methylphenol	2.5	0.2	6.7
Levoglucosan	33.9	1.4	4.2

Table 4.10.: Arithmetic mean and standard deviation of the GC-MS, the same sample is measured six times

Substance	$\bar{x}$	s	s
	[g/kg]	[g/kg]	[%]
Hydroxypropanone	52.7	3.4	6.4
Furfural	6.0	0.1	2.3
2-Hydroxy-3-methyl-2-cyclopenten-1-one	7.3	0.2	3.1
Guaiacol	1.8	0.1	5.5
2-Methoxy-4-methylphenol	2.5	0.2	6.7
Levoglucosan	32.7	1.6	4.9

4.5.2. GPC

4.5.2.1. Data Processing

The collected data are processed with the Shimadzu LCsolution GPC Postrun Analysis software. As a result, a diagram with the elution time on the x-axis and the detector intensity on the y-axis is obtained. Depending on the type of sample, the data are further processed. The procedure for samples of pyrolysis and hydrodeoxygenation is as follows:

- A calibration is used to relate the elution volume to the molecular mass.

- Integration boundaries are chosen, see subsubsection 4.5.2.7 and subsubsection 4.5.2.8.

- A horizontal baseline is drawn.

- The detector signal is standardized to compensate for different sample concentrations.

The result is a diagram with the standardized intensity on the y-axis and the molecular mass on the x-axis. The procedure for samples of coal liquefaction is the same, with the difference that the elution volume is not related to the molecular mass. It is not possible to attribute molecular masses to the elution volume of coal liquefaction samples because the samples mainly contain PAHs, see subsubsection 4.5.2.11.

4.5.2.2. Calibration

The calibration is carried out with polystyrene standards. Figure 4.30 shows the chromatograms of the standards. The main peaks used for the calibration are marked with a black line. The rightmost peaks are caused by solvent impurities. The elution volumes for the respective molecular masses are fitted with a cubic function, see Equation 4.5 and Table 4.11.

$$y = a \cdot x^3 + b \cdot x^2 + c \cdot x + d \tag{4.5}$$

Table 4.11.: Coefficients of the cubic calibration curve

a	-0.01220153
b	0.7860195
c	-17.04526
d	127.3162
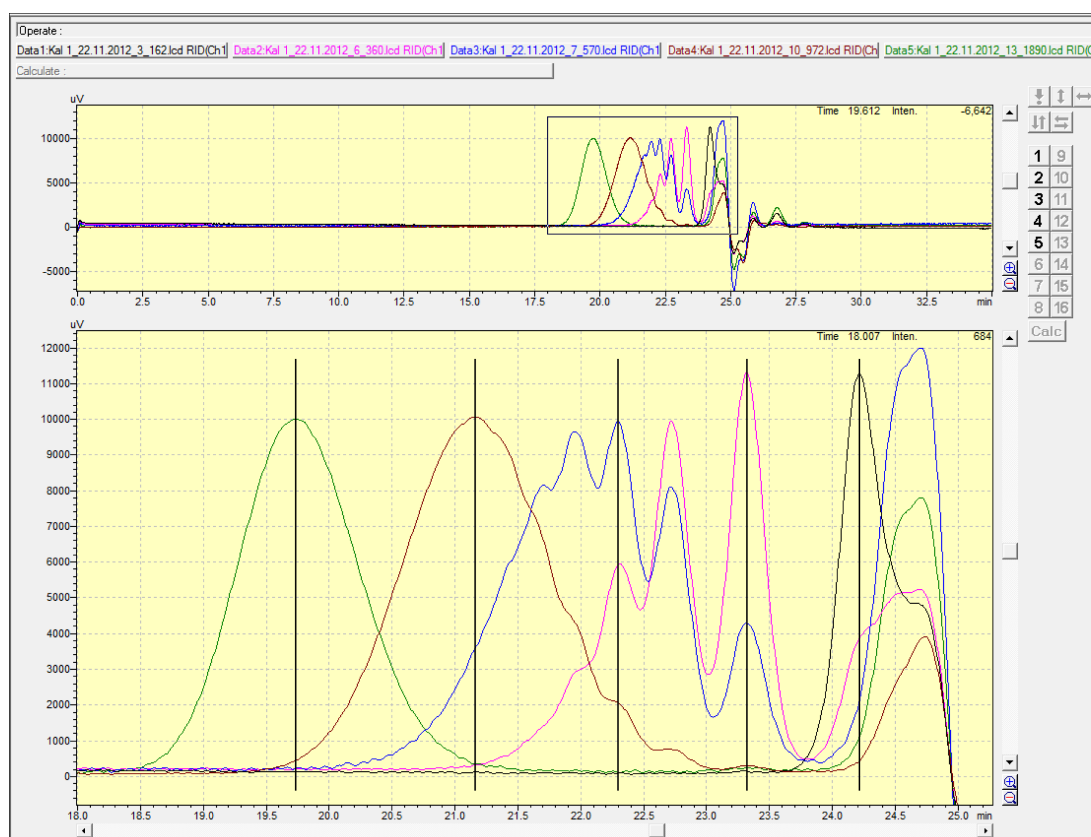
Figure 4.30.: Chromatograms of the GPC calibration standards - green line: 1890 g/mol standard, brown: 972 g/mol, blue: 570 g/mol, pink: 360 g/mol, black: 162 g/mol

4.5.2.3. Aging of the Separation Columns

Aging of the separation columns is observed. In order to compensate for the aging effect, a new calibration is carried out frequently. With these calibrations, a shift towards smaller molecular masses is observed, as depicted in Figure 4.31.

The first calibration, Cal1, is carried out on the new column, the second calibration, Cal2, is carried out a month later, and the third calibration, Cal3, three months later.

The polystyrene standards elute earlier the longer the columns are in use. So when the third calibration is used on sample data, smaller molecular masses are attributed to molecules eluting at a given elution volume. For example, if a molecule eluted at 22 ml, using the first calibration, a molecular mass of approx. 680 g/mol would be obtained, while a mass of approx. 540 g/mol would be obtained using the third calibration.

So a new calibration should compensate for the effects of column aging. However, it is found that the polystyrene standards elution volumes shift more over the

months than the elution volumes of the actual samples.
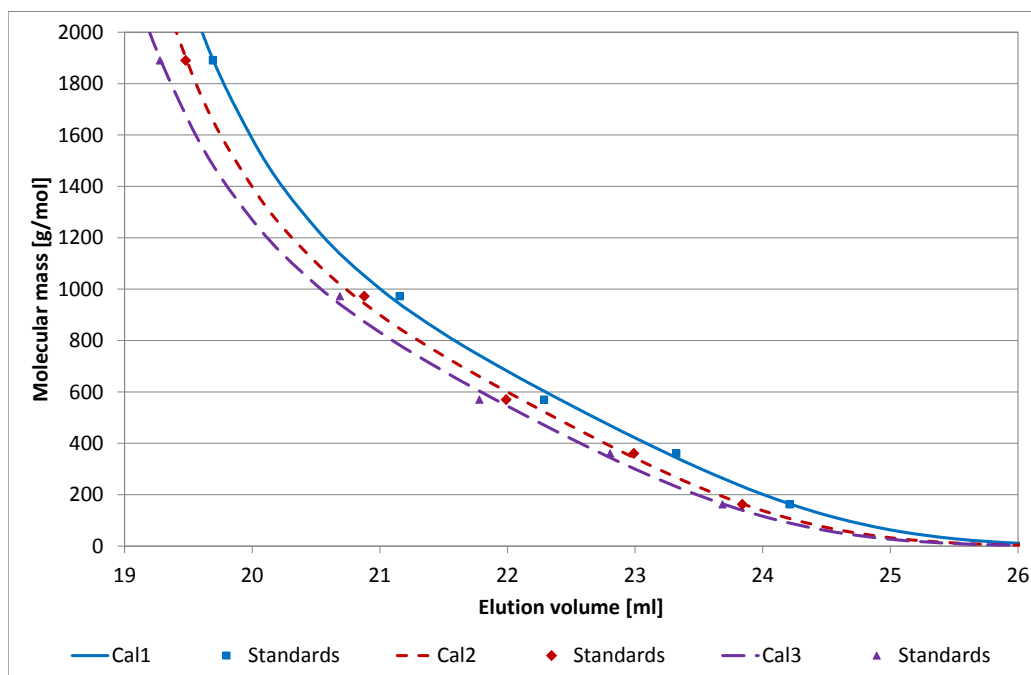
Figure 4.31.: Shift of the polystyrene standards to smaller elution volumes with aging of the separation columns
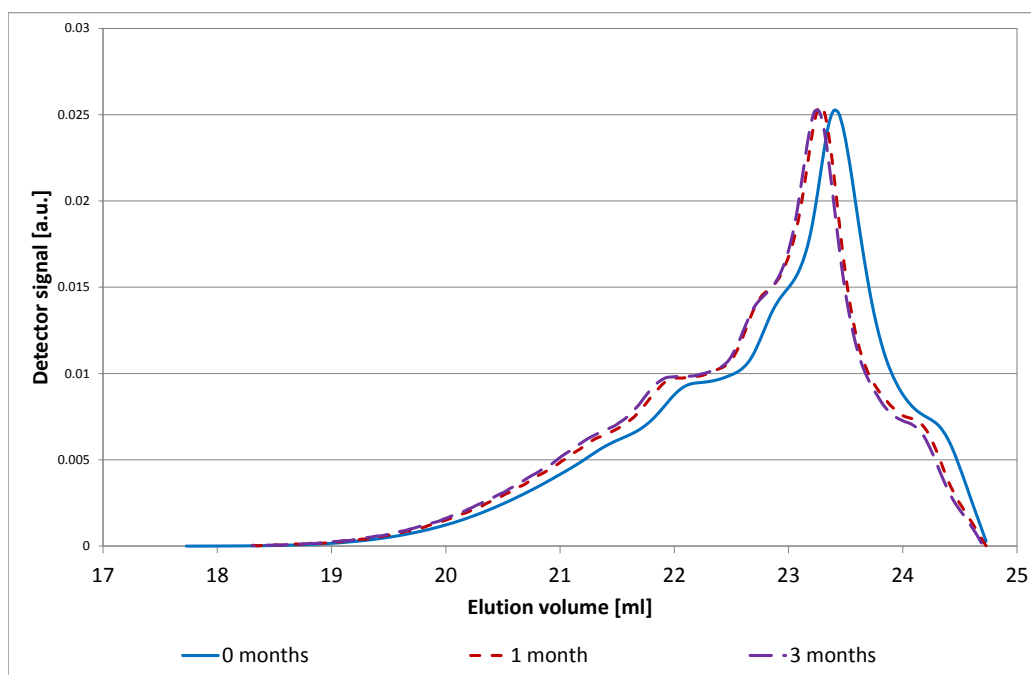
Figure 4.32.: Chromatograms of POww, measured after 0, 1 and 3 months of columns utilization

Figure 4.32 shows the chromatograms of water-reduced pyrolysis oil, POww. The columns are new at the first measurement (blue line), they are in use for one month in the second measurement (red line) and for 3 months in the third measurement (purple line).

As depicted in Figure 4.32, there is a small shift towards shorter elution volumes between the first measurement on the new column and the subsequent measurements, while there is no shift observed between the measurements after one or three months. The maximum of the first measurement lies at 23.40 ml, the maximum of the second at 23.27 ml and the maximum of the third measurement at 23.23 ml, so the shift between one and three months is negligible.

However, the application of the respective calibrations to convert the elution volumes to molecular masses leads to non-negligible shifts, see Figure 4.33.
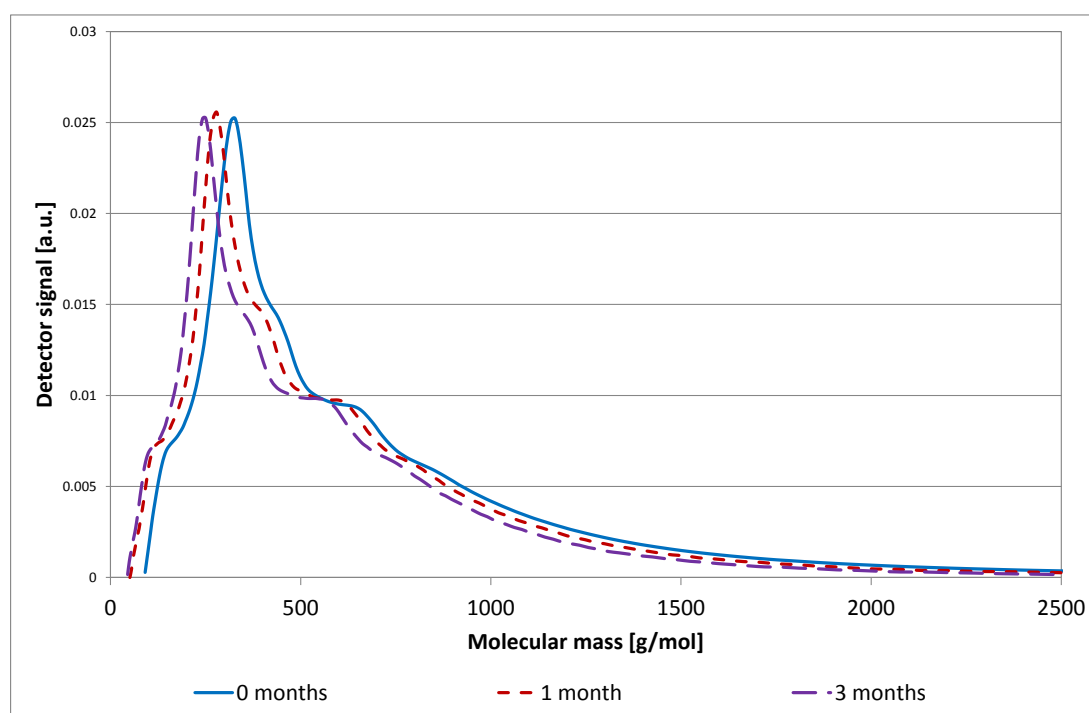
Figure 4.33.: Chromatograms of POww, measured after 0, 1 and 3 months of columns utilization, the respective calibration is used to convert the elution volumes to molecular masses

The first calibration is used to convert the first measurement, the second calibration is used for the second measurement and the third for the third. To the maximum of the first measurement, a molecular mass of 327 g/mol is attributed, 279 g/mol for the maximum of the second measurement, and 250 g/mol for the third.

The differences in elution volumes were about 0.6 % and 0.7 %, but when converted with the respective calibrations, the differences in the molecular masses rise to values as high as 14.7 % and 23.5 %.

For that reason, the first calibration is used on all the samples. Figure 4.34 shows the chromatograms of the POww, where Cal1 is used on all the measurements to attribute molecular masses to the elution volumes. There is still a small difference between the peak maxima of the measurement on the new column and the later measurements.

However, there is only a very small shift between the second and the third measurement: the peak maximum of the second measurement is found at 356 g/mol, while the maximum of the third measurement is found at 365 g/mol. For comparison, the maximum of the measurement on the new column is found at 327 g/mol.
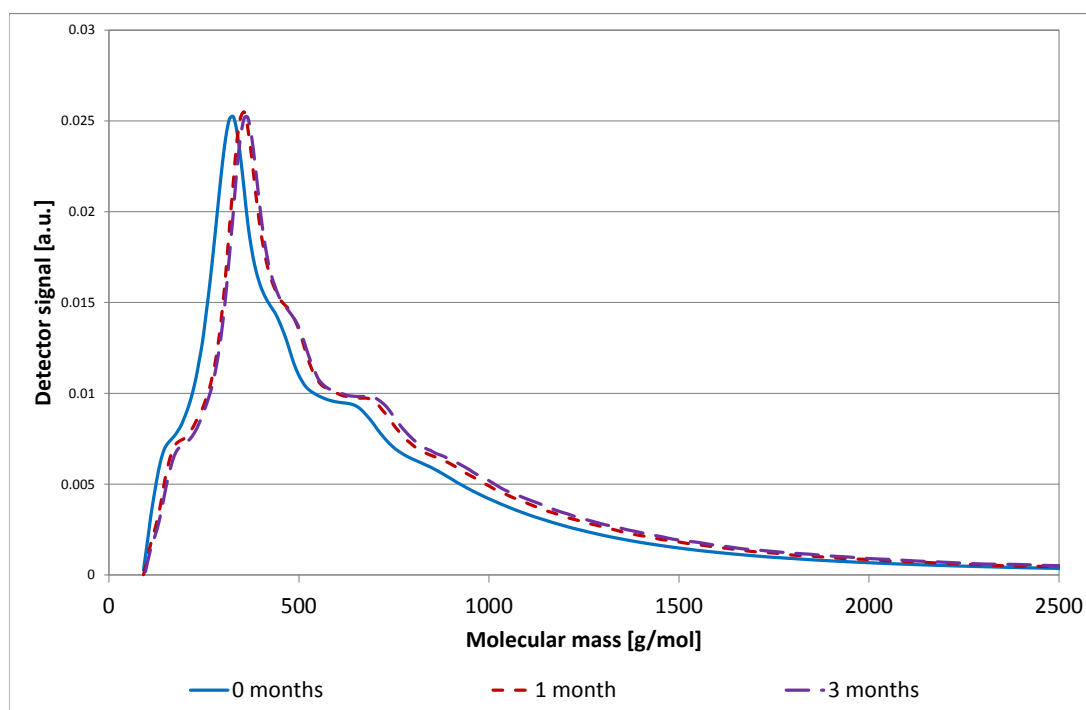
Figure 4.34.: Chromatograms of POww, measured after 0, 1 and 3 months of columns utilization, the first calibration is used to convert the elution volumes to molecular masses

4.5.2.4. Theoretical Plates

The numbers of theoretical plates of different molecules are calculated in order to monitor column efficiency over time. Equation 4.6 is used to calculate the number

of plates N,

$$N = 5.54 \cdot \left(\frac{t_r}{w_h}\right)^2 \tag{4.6}$$

t_r being the total retention time and w_h the width of the peak at half-maximum. Figure 4.35 depicts the number of theoretical plates for guaiacol, isoeugenol, naphthalene, pyrene, tetralin and toluene.

In Figure 4.35, it can be seen that the number of theoretical plates of all molecules decreases the longer the GPC system is used. The decrease in the number of theoretical plates is compound-dependent and seems to be slightly higher for the oxygenated compounds, guaiacol and isoeugenol.
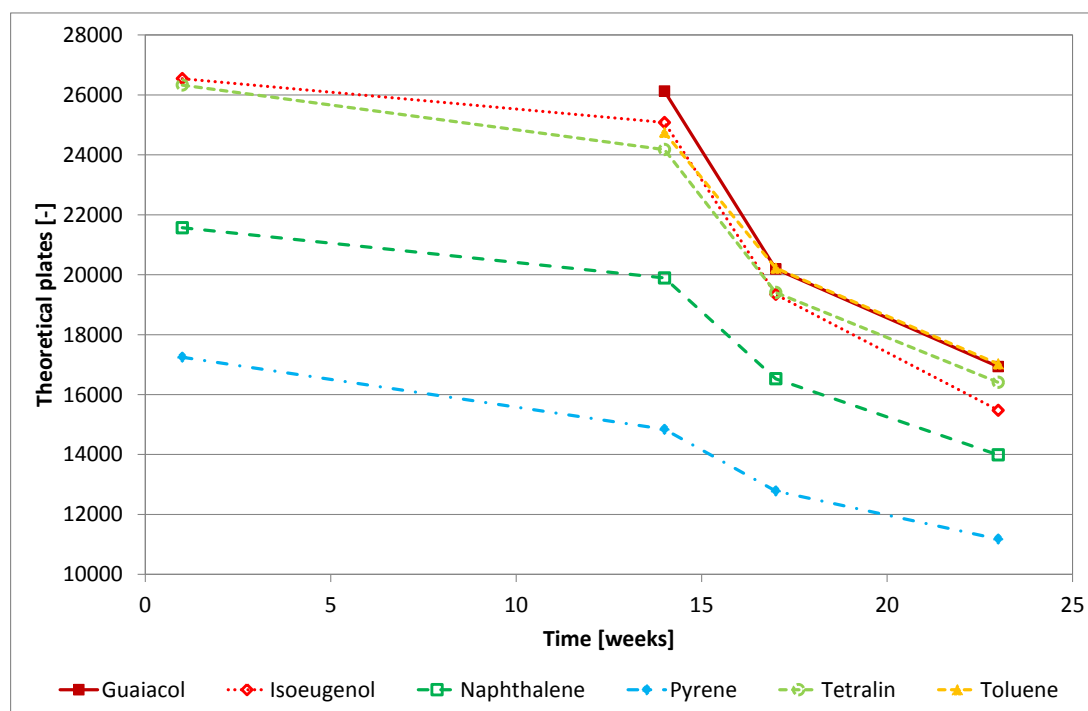
Figure 4.35.: GPC number of theoretical plates for various molecules over time

Altogether, the separation efficiency of the columns clearly decreases over time. This deterioration is probably caused by substances that adsorb on the columns and cannot be eluted with the eluent used.

Furthermore, certain amounts of water and acids are usually present in the samples. The column company advises to avoid measuring these substances as they may be harmful to the column packing.

However, water and acids cannot be excluded when measuring pyrolysis oils. Frequent calibrations cannot compensate for the column fouling, as the fouling influences the behavior of different compounds with different functionalities to a

different extent. So the number of theoretical plates of different compounds contained in the samples should be monitored, and when they decrease too much, the columns have to be replaced.

4.5.2.5. Quantification

Unfortunately, quantification of molecular mass fractions and compounds is not possible for pyrolysis oils, which will be explained subsequently.
The detection is carried out with a refractive index detector, RID. Every substance has a response factor α. With α, the injected mass can be related to the obtained area in the chromatogram, as shown in Equation 4.7.

$$\int_{v_1}^{v_2} f\left(v\right) dv = \alpha \cdot m \tag{4.7}$$

Every substance may have a different response factor α, which may have a different dependence on concentration as well. Thus α is neither defined as compound-independent nor as concentration-independent.
Response factors for different molecules contained in pyrolysis oils were investigated by Hoekstra et al.[27] and are given in Table 4.12.

Table 4.12.: Response factor α for substances contained in pyrolysis oils[27]

	α
	$[m^3/\text{g}]$
Eicosane	41
Anthracene	307
Fluoranthene	292

The area of a peak depends on the refractive index and the response factor α. For a given peak, it is not possible to say whether the compound causing the peak is a major compound that has a refractive index similar to the RI of the eluent, or if it is a minor compound with a large RI.
Furthermore, for the investigation of pyrolysis oils, Hoekstra et al.[27] found that α is indeed not dependent on the concentration of the compound within the range investigated. However, they found that the response factor is not compound independent.
In general, the response factor as well as the RI are higher for aromatic compounds, roughly increasing with increasing number of aromatic rings. Especially the lignin-derived fraction in the PO products and the coal liquefaction products

contain high amounts of aromatic compounds. In a given sample, the aromatics fraction gives a higher signal, leading to an overestimation of the amount of aromatics contained.

So for example, if an aromatic compound and a non-aromatic compound have the same peak area, the non-aromatic compound is contained in a higher amount in the sample, because the aromatic compound has a higher response factor and thus yields a higher signal. Or, from another point of view: If an aromatic compound and a non-aromatic compound are measured in the same concentration, the peak of the aromatic compound is higher.

To sum up, within one sample, the peak area cannot be used to derive information concerning the relative concentrations of different mass fractions and component groups. The areas are not quantitative as some compounds cause higher detector signals while others cause lower detector signals if contained at the same concentration.

Altogether, the assumption of α being compound independent is true for a small investigated range, but the assumption of α being compound-independent is wrong for pyrolysis oil samples. So mass fractions cannot be quantified. In order to avoid making these wrong assumptions, the detector signal is plotted on the y-axis instead of any concentration value. This detector signal is only divided by the whole peak area in order to circumvent differences in sample concentration, it is standardized for every measurement.

4.5.2.6. Column Overload

If too much sample is injected, the columns will be overloaded. Too many molecules are in the columns and most of the pores are occupied. Thus these pores are not available for smaller molecules and they will directly pass through the columns, eluting earlier than they would if pores were available.

So the peaks of overloaded substances shift towards smaller elution volumes and hence higher molecular masses. The substances tetralin and naphtahlene are chosen to elucidate the overload effect, as they are both contained in high amounts in the coal liquefaction products.

Figure 4.36 shows the GPC chromatogram of tetralin and naphthalene, each substance is measured separately. The plot clearly shows that the peaks of the two substances would overlap when measured together, as their retention times are very similar.

In Figure 4.37, two GPC chromatograms of a coal liquefaction product are depicted.
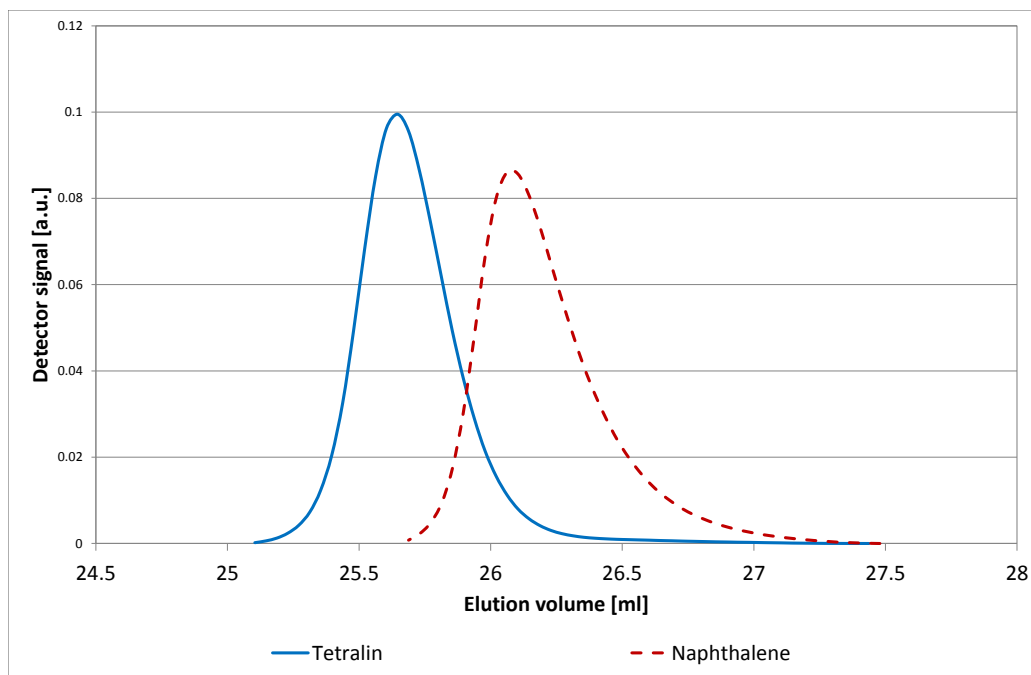
Figure 4.36.: Chromatograms of tetralin and naphthalene, measured separately
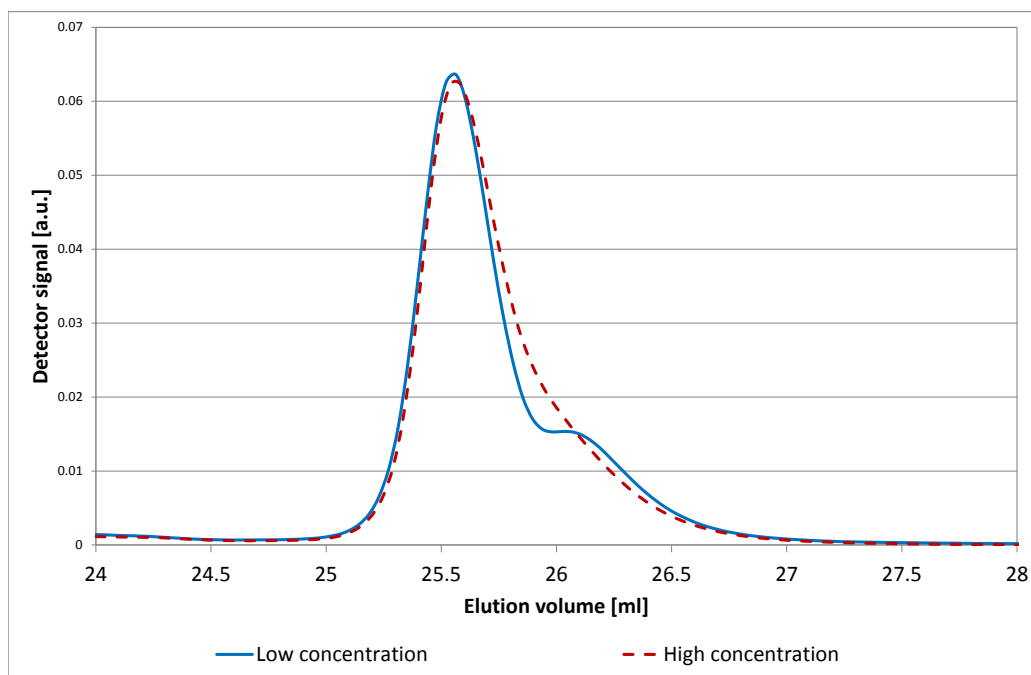
Figure 4.37.: Chromatograms of a CL product, measured at two different concentrations

Figure 4.37 only shows the part of the chromatogram where tetralin and naphthalene elute. The same CL product is measured at two different concentrations

on the columns. Both samples are diluted 1:2 by mass, for the sample with low concentration, 1 μl is injected onto the columns, for the sample with the high concentration, 5 μl are injected. In general, tetralin is contained in higher amounts, as it is used as a hydrogen donor solvent for the coal liquefaction. Naphthalene is obtained when tetralin is dehydrogenated, and thus contained only in smaller amounts in the CL product.

As depicted in Figure 4.37, in the measurement with the low concentration, a bump is visible where the naphthalene starts to elute. However, in the measurement with the high concentration, this bump is not visible. Too much tetralin is in the columns, it occupies all the pores. So the naphthalene molecules cannot find any pores to diffuse into, and thus elute earlier, together with the teralin.
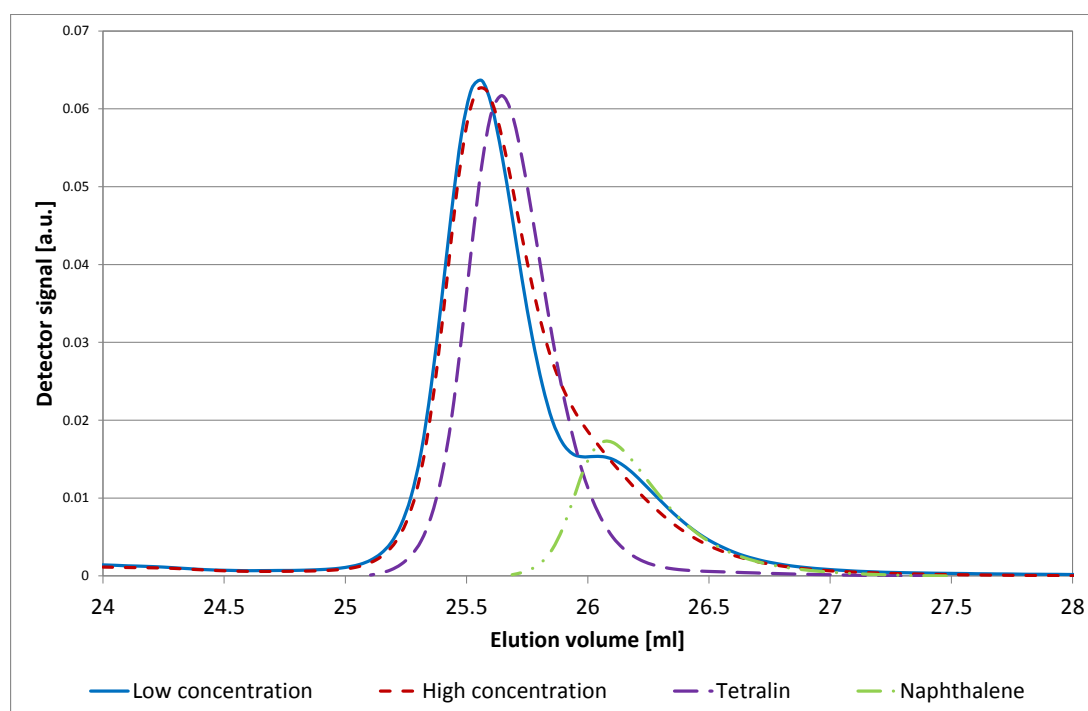
Figure 4.38.: Chromatograms of a CL product measured at two different concentrations, and the chromatograms of tetralin and naphthalene for comparison

All chromatograms are shown together in Figure 4.38. As already mentioned, when a column is overloaded, the molecules elute earlier. This effect is clearly visible in Figure 4.38.

The peak maxima of the CL product, corresponding to the maximum of tetralin, are found at earlier elution times than when tetralin is measured alone. The same effect is found for naphthalene. The maximum of the naphthalene bump elutes at an earlier time than the naphthalene measured separately.

However, the columns overload when analyzing CL products is not a problem. The part of interest is the part in the chromatograms where the coal liquefaction products are found. They elute earlier, in the range of approx. 18 to 24 ml elution volume.

The amounts of tetralin and naphthalene can be determined via GC-FID, gas chromatography-flame ionization detector. It is not possible to say if there are substances contained in the CL products eluting at the same time as tetralin and naphthalene, since their high peaks would overlap everything else eluting at the same time.

4.5.2.7. Limits of Analysis

As a molecular weight limit for the analysis by GPC, the molecular weight of isoeugenol could be used. It is possible to analyze molecules with low molecular masses up to approximately the mass of isoeugenol via GC-MS. Hence, it is not necessary to analyze them via GPC.

The behavior of isoeugenol on the GPC column is not ideal but acceptable. As depicted in Figure 4.39, it consists of a benzene ring, which is apolar, but it has one apolar and two polar functional groups that prevent that it exhibits non-ideal eluting behavior.
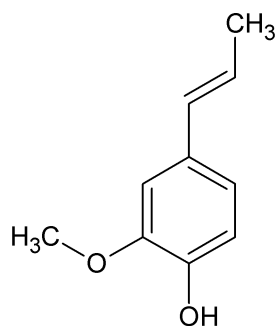
Figure 4.39.: Structure of isoeugenol

The retention time of isoeugenol is approximately 24 minutes, so all the peaks obtained later than 24 minutes of retention time do not have to be included in the analysis.

To the retention time of approx. 24 minutes, a molecular mass of approx. 160 g/mol is attributed, as shown in Figure 4.40. However, a different lower limit of analysis is used, see below.
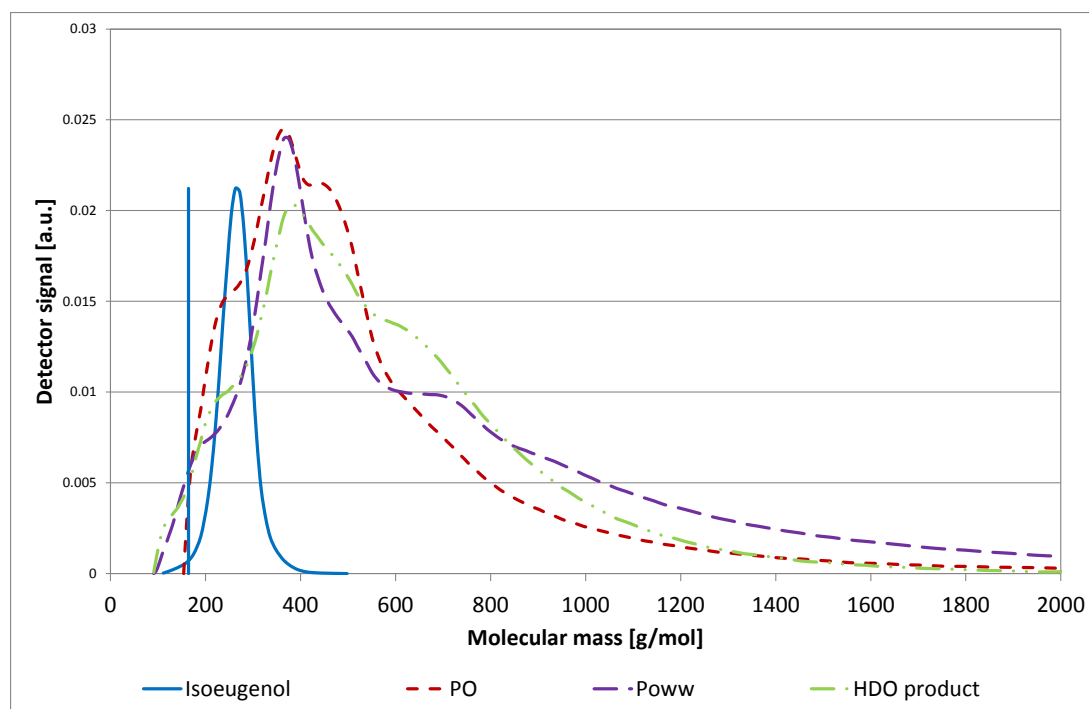
Figure 4.40.: Molecular weight distribution of several samples, of isoeugenol, and the calculated retention time t_R of isoeugenol as a possible limit of analysis for GPC

4.5.2.8. Refractive Index Detector

The detector that is used to monitor the eluting substances is a refractive index detector, RID. The RID is a reference detector, for that reason, the reference cell is rinsed and filled with new eluent before every series of measurements. Being a reference method further means that in reference to the eluent, the refractive index of a certain substance may be negative.

As a reference refractive index, the eluent, THF with 0.1 vol% TFA, is used. Compared to the refractive index of the eluent, the refractive index of water and of acetic acid is negative. Usually, the negative regions are not integrated when processing analysis data. In Figure 4.41, the data are not processed, so not integrated but the mere detector signal is shown over the elution volume.

The blue line in Figure 4.41 is the chromatogram of water. Compared to the eluent, water has two negative peaks, one peak at approx. 23.3 ml, and the major negative peak at approx. 24.9 ml elution volume. Acetic acid, which is also contained in the pyrolysis oils, has a negative peak at approx. 24.3 ml elution volume.
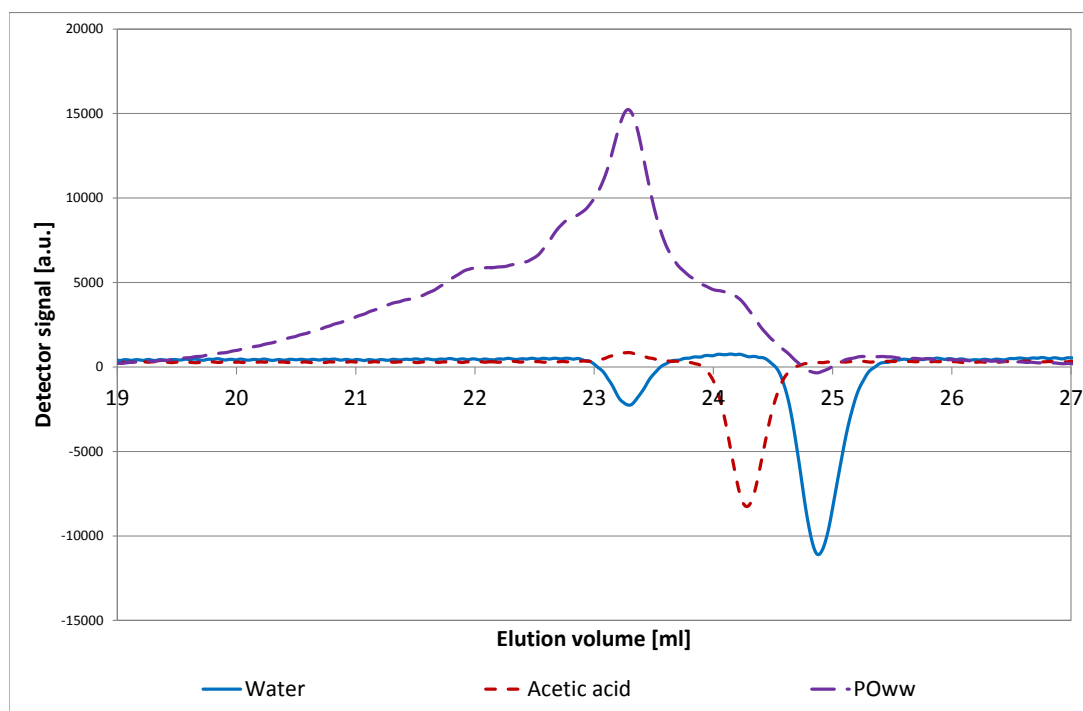
Figure 4.41.: Chromatograms of water, acetic acid and POww, the chromatograms are not integrated and no baseline is drawn, the data are shown unprocessed

When a substance with a negative peak compared to the eluent and a substance with a positive peak elute at the same time, their peaks overlap in the resulting GPC chromatogram. So it may be the case that two substances elute at the same time but no peak at all is detected when the two peaks exactly compensate each other.

More likely, the peaks do not have the same height. So for example, if the positive peak is higher than the negative peak, the resulting peak is positive, but smaller as it would be if the substance eluted alone, as the negative peak is subtracted from the positive one.

Hence it is possible that in the GPC-chromatograms, more negative peaks exist, but they cannot be found if substances with higher positive peaks elute at the same time.

In most of the samples, water is contained in high enough amounts so that the second negative water peak is visible in the chromatograms, as shown in Figure 4.42. Figure 4.42 shows the chromatograms of water, of a pyrolysis oil, PO, and of a water-reduced pyrolysis oil, POww.

In both the PO chromatogram and the POww diagram, the second negative water peak is visible. In the PO chromatogram it is obviously much larger, but it is also

visible in the POww, as there is still some water contained.
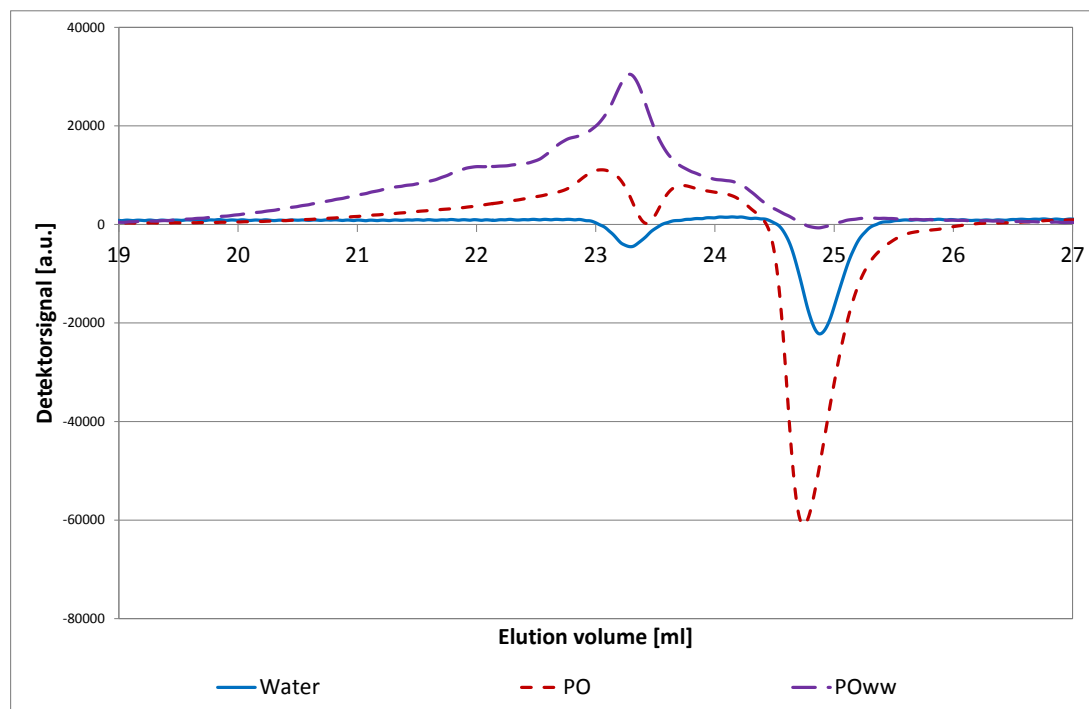
Figure 4.42.: Chromatograms of water, PO and POww, the chromatograms are not integrated and no baseline is drawn, the data are shown unprocessed

So instead of using the molecular mass of isoeugenol as the lower limit for analysis, the negative peak of water is used. This limit is more obvious when processing GPC analysis data. This limit corresponds to approx. 90 g/mol.

4.5.2.9. THF Artifacts

Degradation products of the THF eluent are not only found in the GC-MS spectra, but also in the GPC chromatograms. Artifacts that are caused by the THF degradation products are shown in Figure 4.43.

However, compared to the peak heights of the samples, the THF peak heights are very small. So the THF peaks are usually overlapped by the sample peaks, as the samples are injected in a much higher concentration. Thus the THF degradation problem can be neglected in the GPC analyses.
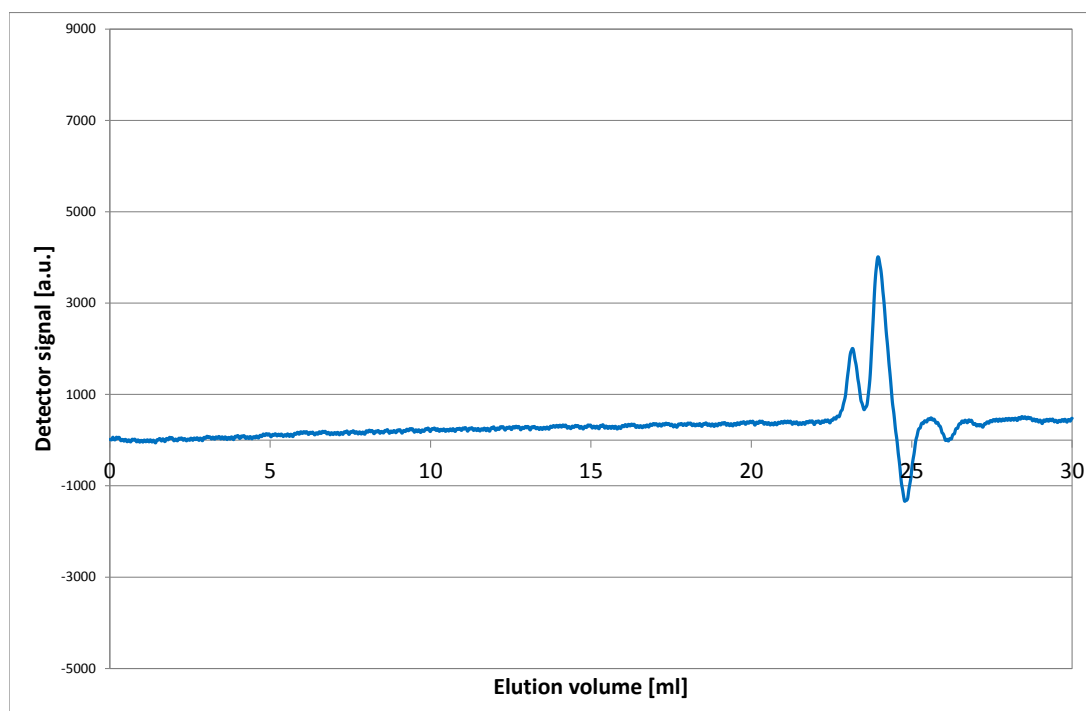
Figure 4.43.: Chromatogram of the eluent THF, artifacts elute at approx. 23 to 25 ml

4.5.2.10. Ratio of Hydrodynamic Volume to Molecular Mass

Usually, polystyrene standards with different chain lengths are used for calibration, the styrene monomer unit is shown in Figure 4.44.

(a) Polystyrene

(b) Decalin
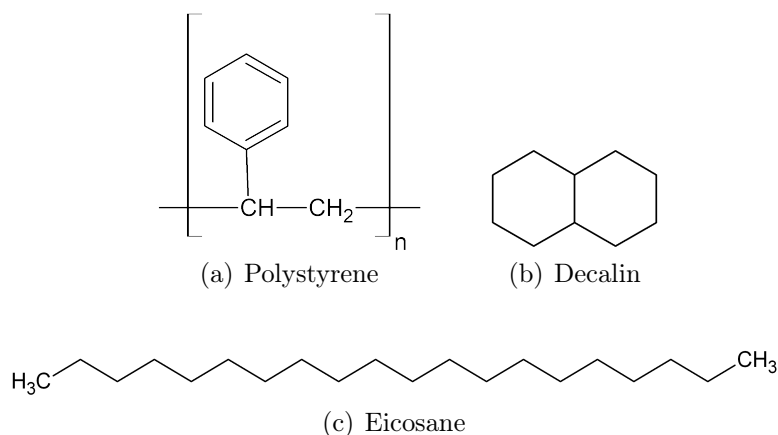
(c) Eicosane

Figure 4.44.: Structural formulas of molecules with different ratios: Polystyrene is used for calibration, pyrene has a lower and eicosane has a higher ratio of hydrodynamic volume to molecular mass than polystyrene

These polystyrene standards have a certain ratio of hydrodynamic volume to molecular mass, they may be convoluted in the solvent. In the pyrolysis oils, molecules with both lower (mostly) and higher ratio of hydrodynamic volume to molecular mass are found.

Two examples are shown in Figure 4.44, with decalin having a lower ratio and eicosane having a higher ratio than polystyrene. The weight of compounds with a lower ratio may be underestimated, whereas the weight of compounds with a higher ratio may be overestimated.

Figure 4.45 shows the elution chromatograms of decalin and eicosane, comparing their measured with their calculated elution volumes. Figure 4.46 shows the chromatograms and the actual molecular masses.
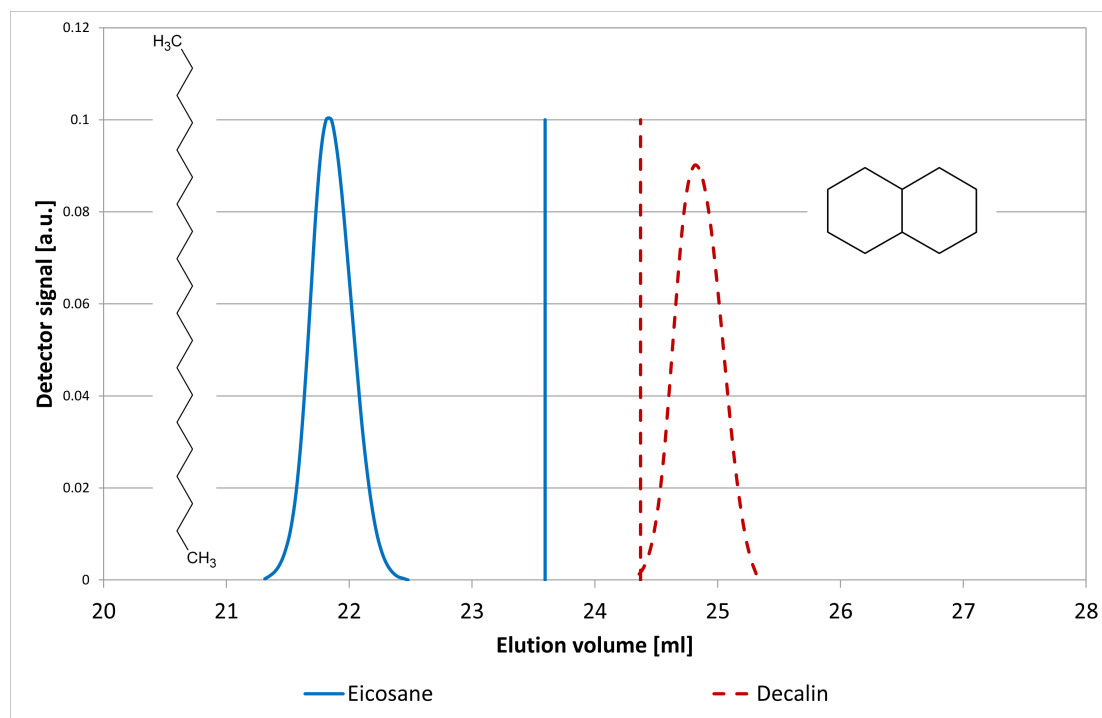
Figure 4.45.: Elution chromatograms of eicosane and decalin and their calculated elution volumes

Table 4.13 lists the calculated molecular masses of the peak maxima, the M_n and M_w and the actual molecular masses of the two substances.

It is obvious that the molecular mass of substances with a higher ratio of hydrodynamic volume to molecular mass compared to the polystyrene standards is overestimated, while the molecular mass of substances with a lower ratio is underestimated.
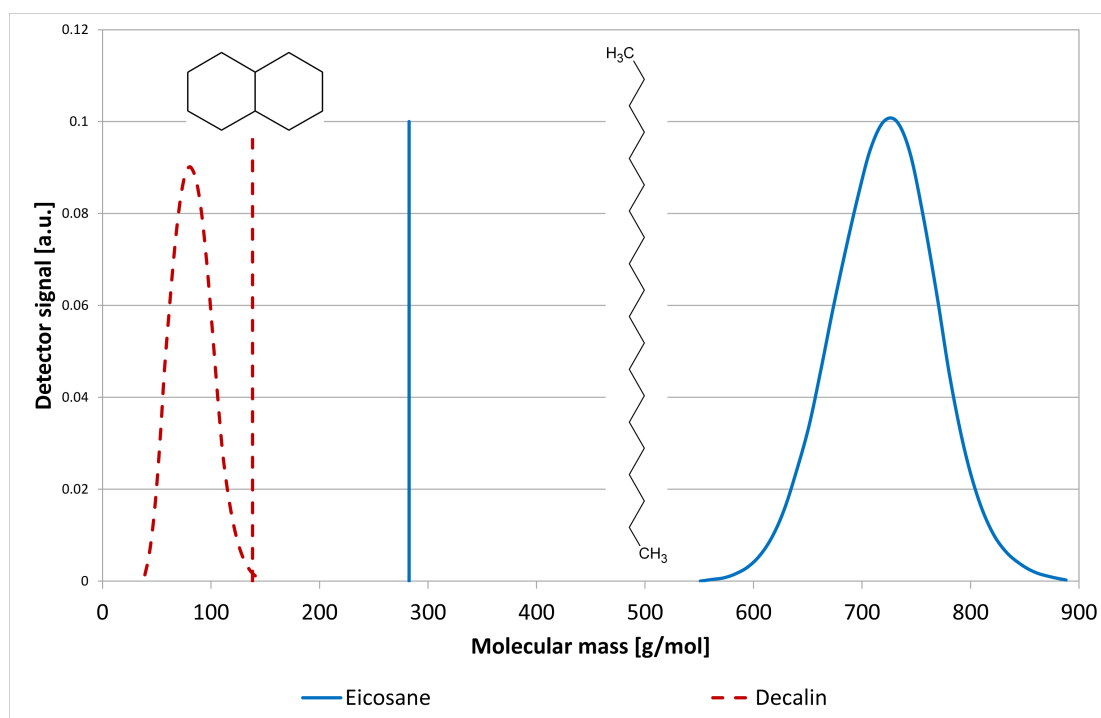
Figure 4.46.: Chromatograms of eicosane and decalin with their actual molecular masses

Table 4.13.: Actual, measured and calculated molecular masses and retention times of eicosane and decalin

Substance	t_R	MM	M_n	M_w	Actual MM	t_R
	via GPC	via GPC			from[30]	pred. w. Cal1
	[min]	[g/mol]	[g/mol]	[g/mol]	[g/mol]	[min]
Eicosane	21.8	732.0	716	720	282.55	23.60
Decalin	24.8	81.3	75	80	138.25	24.37

For the analysis of pyrolysis oils, the influence of this ratio on the elution times is problematic. Many different substances with either a higher, a lower, or a comparable ratio of hydrodynamic volume to molecular mass compared to the polystyrene standards are present in the oils.

Since the oils are a mixture of all these substances, it is not possible to distinguish between compounds eluting at the time expected according to this ratio, and between compounds that elute too early or too late compared to the polystyrene standards.

4.5.2.11. Adsorption on the Columns

GPC cannot be used for the analysis of substances containing a high amount of cyclic aromatic hydrocarbons, polycyclic aromatic hydrocarbons, PAHs, or polycyclic hydrocarbons.

The PAHs are very apolar, hence they stay on the apolar column rather than being transported by the more polar eluent. For that reason, they elute very late, and according to the calibration with the polystyrene standards, wrong molecular masses would be attributed to the PAHs.

The comparison of measured and calculated to actual molecular masses of various PAHs is listed in Table 4.14. These findings are visualized in Figure 4.47 and Figure 4.48.

Table 4.14.: Measured and actual molecular masses of some PAHs

Substance	t_R	MM	Actual MM	t_R
	via GPC	via GPC	from[30]	predicted with Cal1
	[min]	[g/mol]	[g/mol]	[min]
Anthracene	25.5	27.4	178.229	24.13
Decalin	24.8	81.3	138.25	24.37
Fluoranthene	25.8	15.9	202.25	23.99
Naphthalene	26.1	9.5	128.171	24.44
Perylene	26.5	3.6	252.309	23.74
Phenanthrene	25.9	13.4	178.229	24.13
Pyrene	26.1	9.5	202.25	23.99
Tetralin	25.6	21.8	132.202	24.41

Furthermore, tailing of the peaks is observed for all substances that have at least one aromatic ring. So tailing is an indication of adsorption behavior of apolar compounds on the apolar columns.

Various PAHs may be contained in the pyrolysis oils. Especially the products of coal liquefaction contain a high amount of PAHs. For that reason, no molecular masses are attributed to the elution volumes of the CL products.

The detector signals are always plotted over the elution volumes. By only plotting the elution volumes, the errors that would be introduced by attributing the elution volumes of PAHs to molecular masses based on a calibration with polystyrene standards can be avoided.

When comparing the results of different CL experiments, the utilization of the chromatograms with the elution volumes on the x-axis is perfectly viable and meaningful.
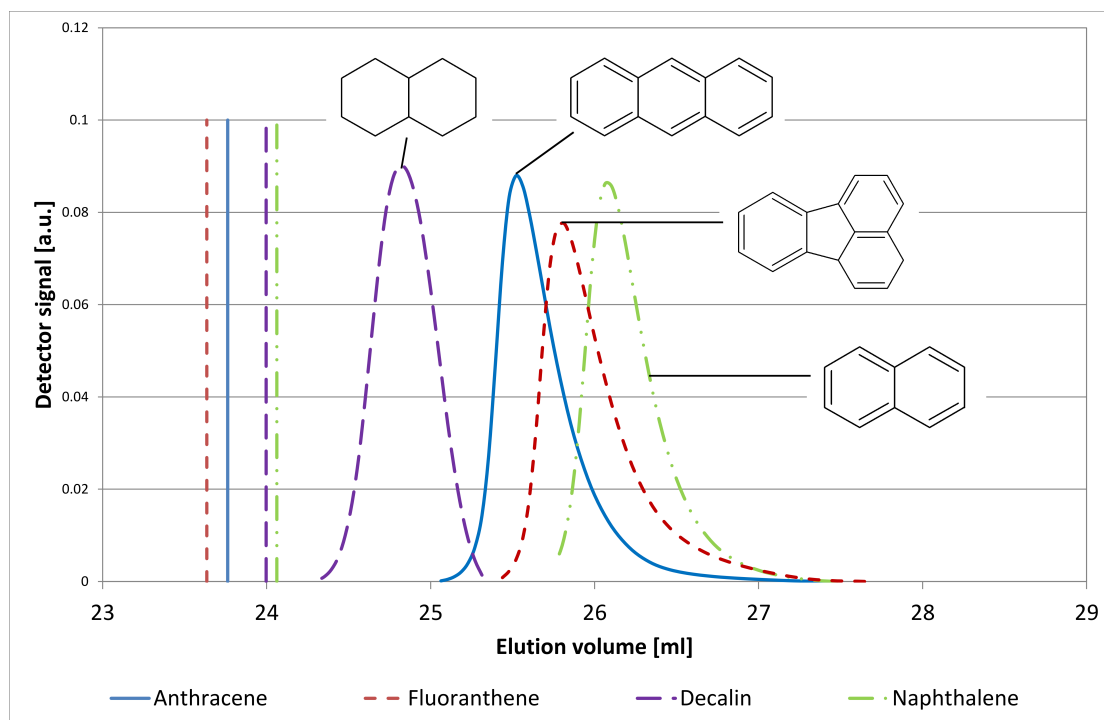
Figure 4.47.: Measured and actual elution volume of various cyclic hydrocarbons
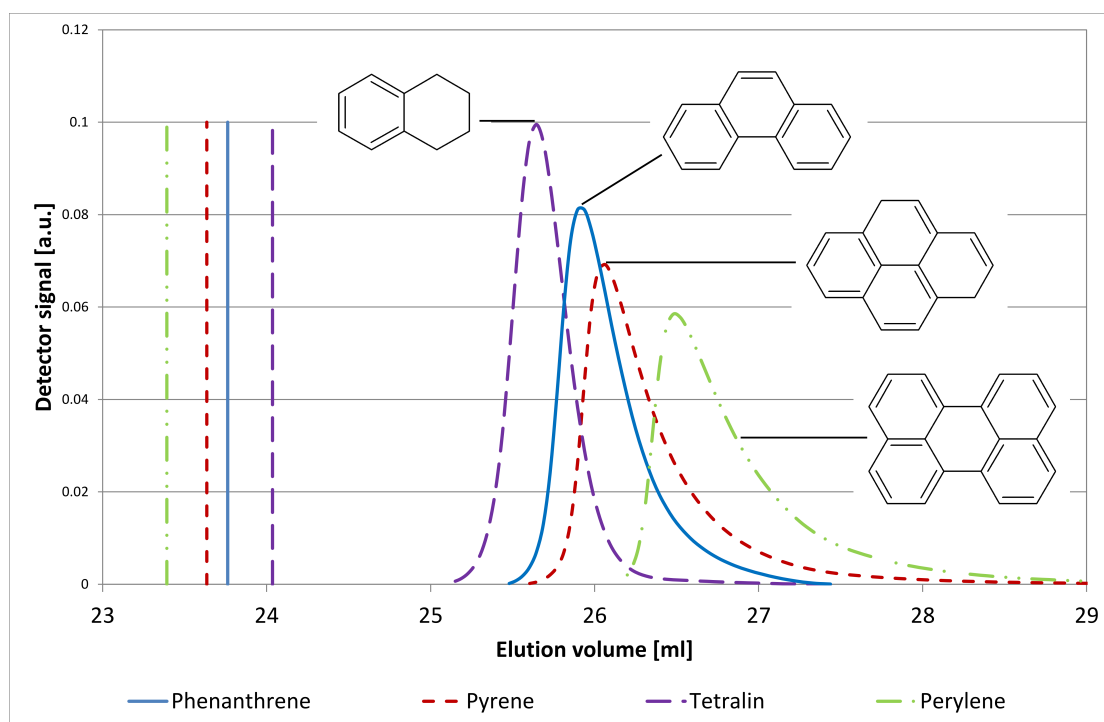
Figure 4.48.: Measured and actual elution volume of various cyclic hydrocarbons

4.5.2.12. Comparison of Chromatograms within the Same Series of Experiments

Despite all these pitfalls, it is possible to compare chromatograms within the same series of experiments when analyzed carefully. Examples for the comparison of spectra of products from both hydrodeoxygenation and coal liquefaction experiments are given below.

Comparison of Chromatograms of Hydrodeoxygenation

Figure 4.49 shows an overview of some of the experiments conducted for hydrodeoxygenation. Raney-Nickel is used as a catalyst in all the experiments presented. The stirring speed is always 500 rpm.

In a first series, mild hydrodeoxygenation at 250 °C and a H_2 pressure of 100 bar and deep hydrodeoxygenation at 300 °C and 150 bar are carried out, both for 2 hours. These two experiments are represented with red diamonds in Figure 4.49. In a second series of experiments, the deep hydrodeoxygenation experiments are carried out for different periods of time in order to optimize the reaction time. These experiments are depicted with blue squares.
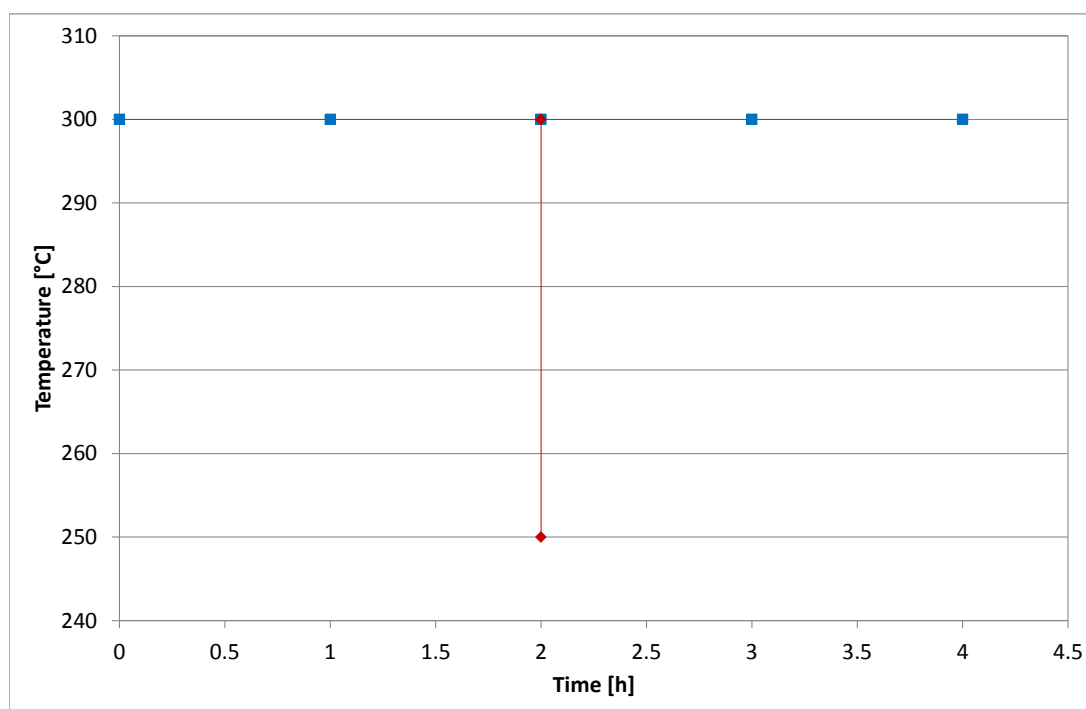
Figure 4.49.: Overview of the parameters of some of the hydrodeoxygenation experiments with Raney-Nickel - red diamonds: comparison of mild and deep hydrodeoxygenation, blue squares: deep hydrodeoxygenation for different reaction times

Figure 4.50 shows the chromatograms of the mild HDO and the deep HDO experiments.
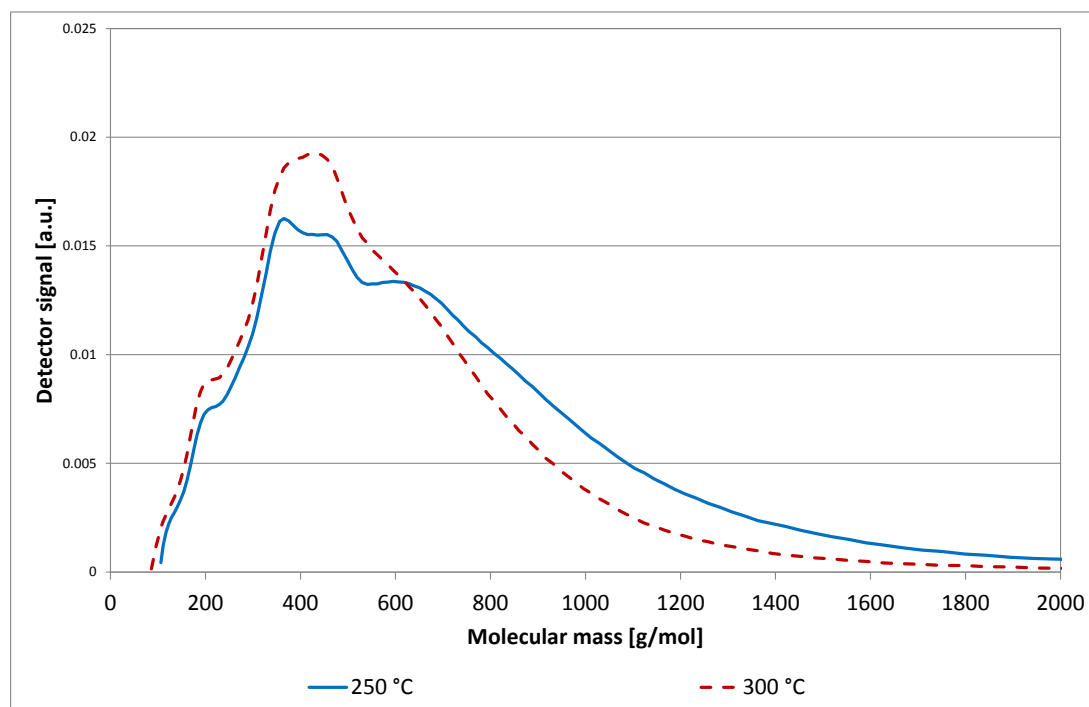
Figure 4.50.: Chromatograms of mild (250 °C, bottom phase) and deep (300 °C, top phase) HDO products

After both experiments, the products are separated in a separatory funnel into a top organic phase, an aqueous phase and a bottom organic phase. The top phase obviously has a lower density than water, while the bottom phase has a higher density.

For the mild HDO, the chromatogram of the bottom phase is shown, whereas for the deep HDO, the chromatogram of the top phase is shown. It is known that the bottom phase tends to contain more compounds with higher molecular masses. Furthermore, the oxygen content of the bottom phase tends to be lower than the oxygen content of the top phase. Thus, the top phase contains more smaller, oxygenated compounds and the functional groups are different.

From the comparison of the chromatograms, it seems that the deep HDO product contains more compounds in the range from approx. 200 to 600 g/mol and less compounds larger than 600 g/mol. However, these observations should be regarded with caution. Although the feed and the reaction conditions for both experiments are very similar, the top phase and the bottom phase are different. They probably contain compounds with different functional groups, which may

show different behavior on the GPC columns. Both phases may contain substances whose molecular masses might be overestimated or underestimated.

Furthermore, these different chemical functionalities may have different refractive indices and response factors concerning their detection. So it is likely that the deep HDO product contains more compounds in the range from approx. 200 to 600 g/mol and less compounds larger than 600 g/mol, but this interpretation should not be the sole way to analyze and compare these two products.

In Figure 4.51, the chromatograms of the reaction time series for deep HDO are shown. For all the products, the bottom phases are shown. It is assumed that they are very similar concerning functional groups and these chromatograms can be compared to each other.
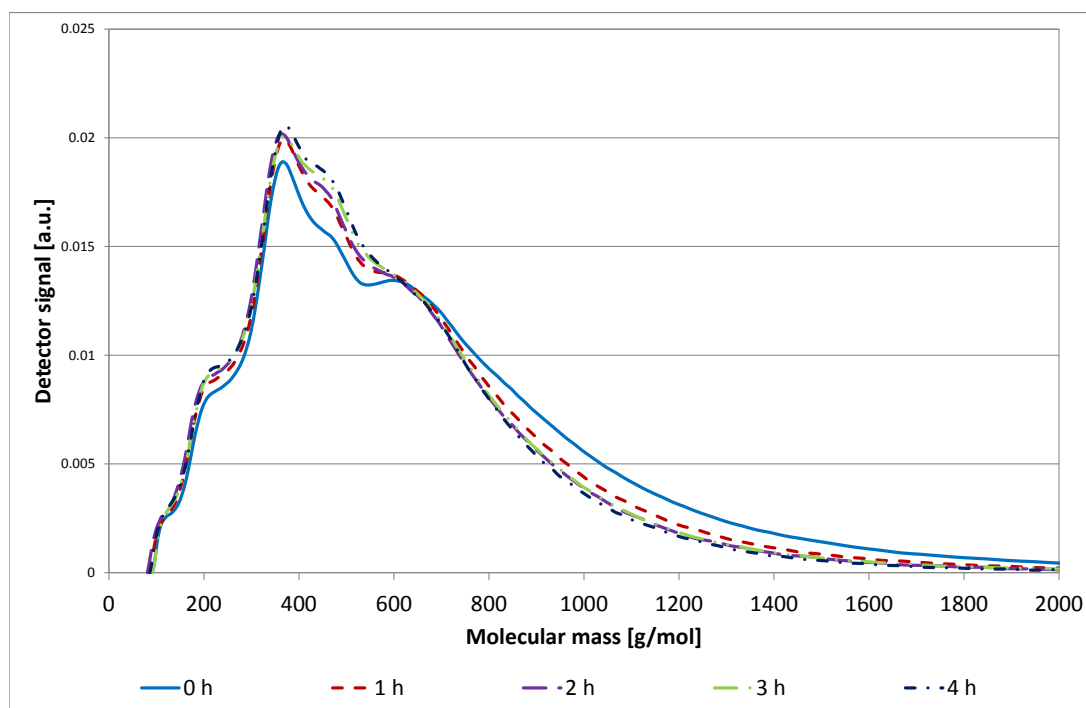
Figure 4.51.: Chromatograms of deep HDO products comparing different reaction times

The first experiment is stopped as soon as the reaction temperature is attained. Probably, the amount of substances in the range from the peak maximum to approx. 600 g/mol is lower, while the amount of substances with a higher molecular mass than 600 g/mol seems to be higher than for all the other experiments.

All the other chromatograms are very similar. So concluding only from the GPC analyses, it seems that the products obtained after only one hour of reaction time are the same as the products obtained for 2, 3 and 4 hours of reaction time. So

in the future, even shorter reaction times than 1 hour should be investigated according to the comparison of GPC results.

To sum up, the products of similar experiments can be compared. The feed should be similar, as well as reaction conditions like temperature, pressure and stirring speed. It is acceptable to compare products who are expected to have a similar chemical composition and contain compounds with similar functional groups. Otherwise, like when comparing the top phase with the bottom phase, caution should be exercised for the interpretations.

Comparison of Chromatograms of Coal Liquefaction

Figure 4.52 shows an overview of some of the experiments of coal liquefaction. Two different types of experiments are conducted. At first, after the reactor is loaded with bio-char, solvent and optionally catalyst, a H_2 pressure of 50 bar is set while heating.

When the final reaction temperature is attained, there are two different options: either more hydrogen is supplied, setting the H_2 pressure at the final reaction temperature to 180 bar H_2, or no more hydrogen is supplied. The reactions where hydrogen is supplied are called continuous experiments, while the reactions with no further hydrogen supply are called non-continuous.
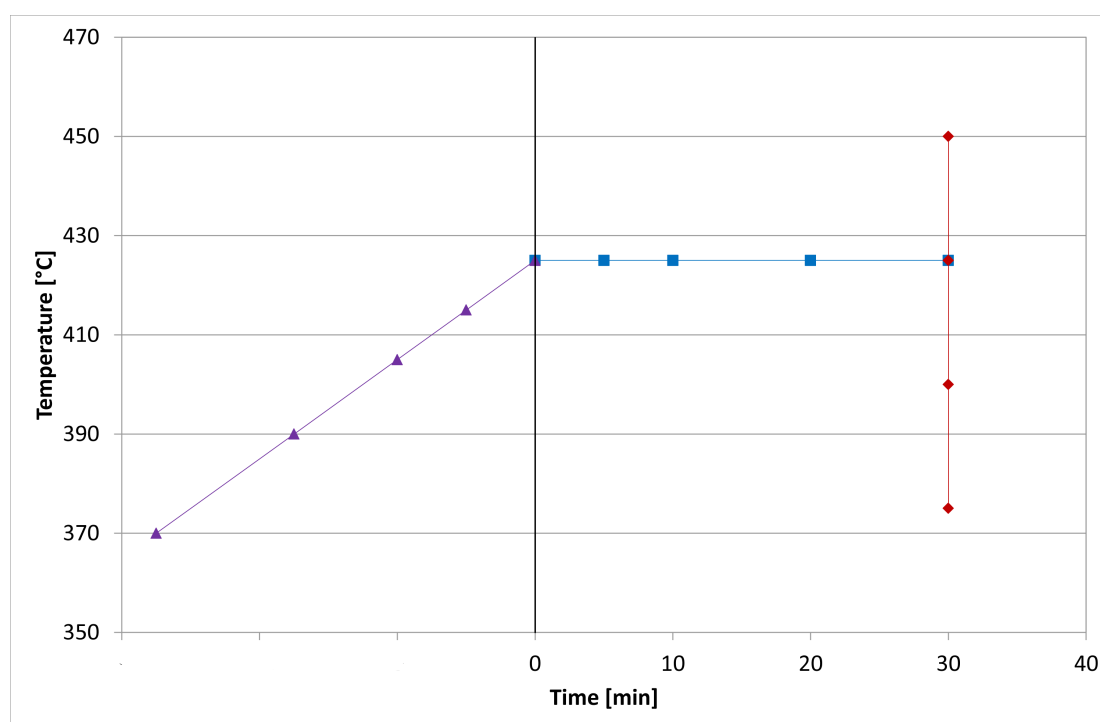
Figure 4.52.: Overview of some of the coal liquefaction experiments - purple triangles: heating series, blue squares: time series, red diamonds: temperature series

In Figure 4.52, the heating phase is shown with purple triangles. The aim of these experiments is to investigate the obtained products when the heating is carried out only up to a certain temperature, to see if reactions already start earlier. The heating phase is interrupted at 370, 390, 405, and 415 °C, respectively.

Another series of experiments are isothermal experiments which are conducted to analyze the reaction time. When the final reaction temperature of 425 °C is attained, the reactions are conducted for 0, 5, 10, 20 and 30 minutes, respectively. These series help to investigate how fast changes occur and how long the reactions should be conducted.

These experiments, as well as the next series, are conducted both continuously and non-continuously, as explained above. The isothermal experiments are shown with blue squares.

For the last series of experiments, the final reaction temperature is varied. It is investigated if the coal liquefactions can be conducted at lower temperatures, or if higher temperatures are necessary. It is desired to optimize the reaction temperature. Experiments are carried out at 375, 400, 425 and 450 °C, respectively. This series is also conducted both continuously and non-continuously. It is depicted with red diamonds.

The following figures show the GPC chromatograms of all the series explained above and shown in Figure 4.52.
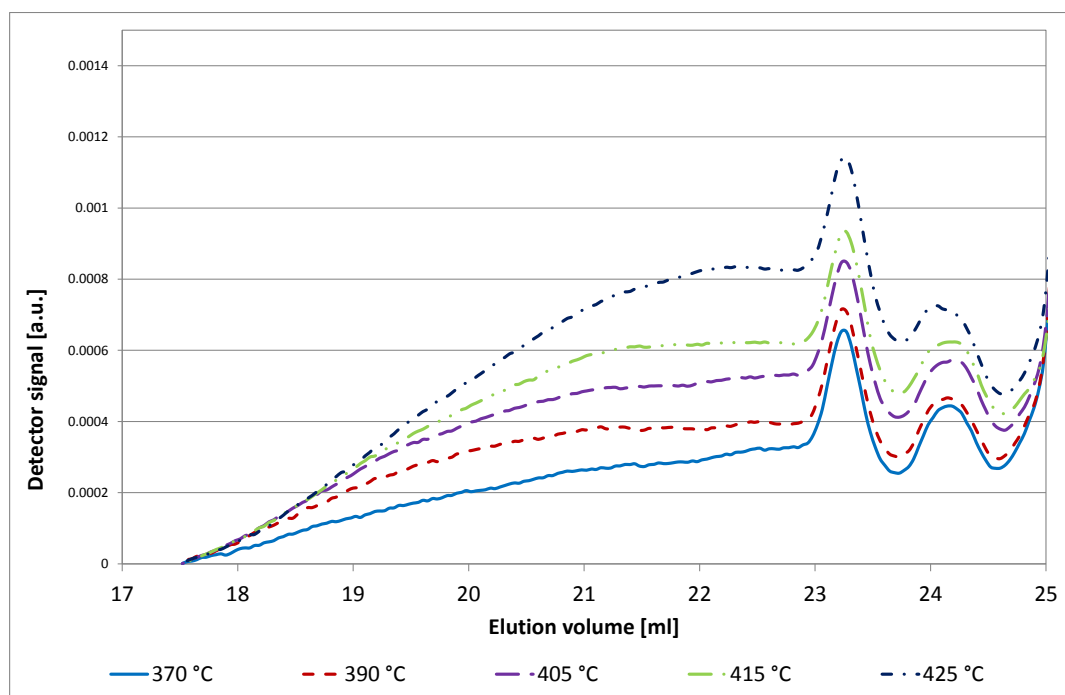
Figure 4.53.: Chromatograms of the heating series

In Figure 4.53, the GPC chromatograms of the heating series are compared. It is obvious that the chromatograms are very similar. Probably the same compounds are formed and the same conversions occur when higher temperatures are reached, because the shape of the peaks does not change. These compounds, eluting between 17.5 and 24.5 ml, are probably formed in higher amounts the more the temperature increases, because the peaks heights increase.

Furthermore, it is probable that no major changes in functional groups occur, because the peaks do not shift in elution time, and their shape does not change. Figure 4.54 and Figure 4.55 show the GPC chromatograms of the series investigating the ideal reaction temperature.

The experiments are conducted for 30 minutes. All temperature experiments are conducted both continuously, supplying more hydrogen, and non-continuously. Figure 4.54 shows the non-continuous series, and Figure 4.55 shows the continuous series.
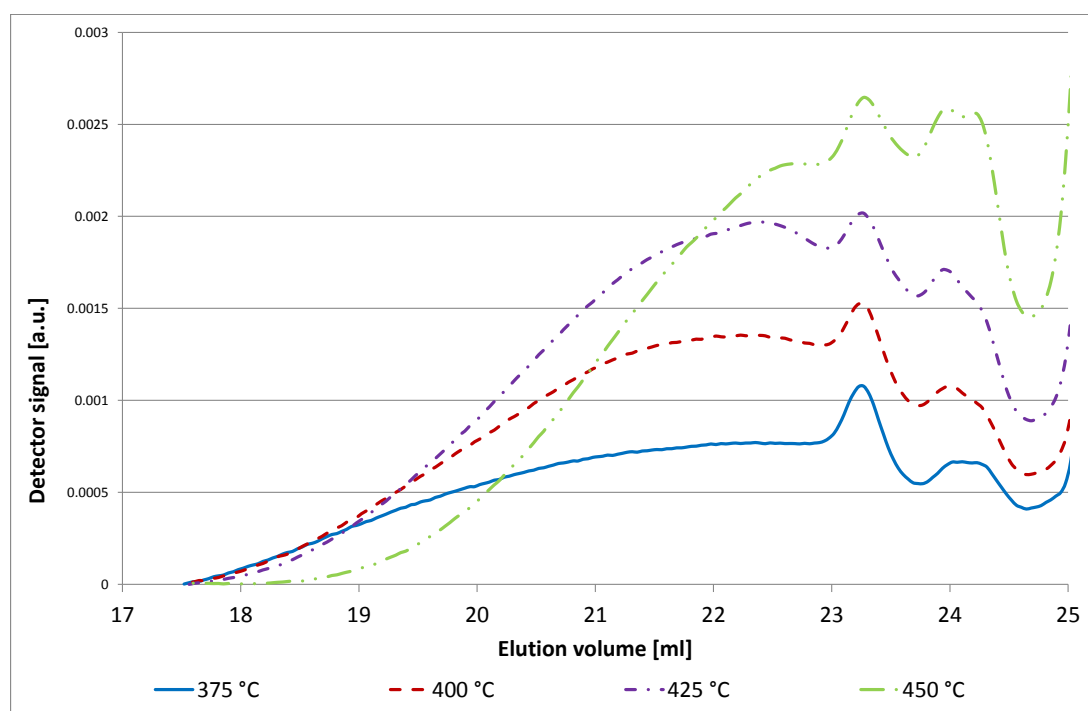
Figure 4.54.: Chromatograms of the temperature series, non-continuous experiments

For both series, the chromatograms are very similar. It is seen that the amount of compounds eluting between 17.5 and 24.5 ml increases with increasing reaction temperatures. Furthermore, the slope at early elution times shifts to higher elution times with increasing temperature. This trend probably means a shift to

lower molecular masses with higher reaction temperatures.

All the trends are observed for both the continuous and non-continuous series. Thus, a further supply of hydrogen is not necessary as the chromatograms of the continuous experiments are very similar to the experiments where no further hydrogen is supplied. So probably the same reactions occur, and the extra hydrogen supplied in the continuous experiments cannot be used.
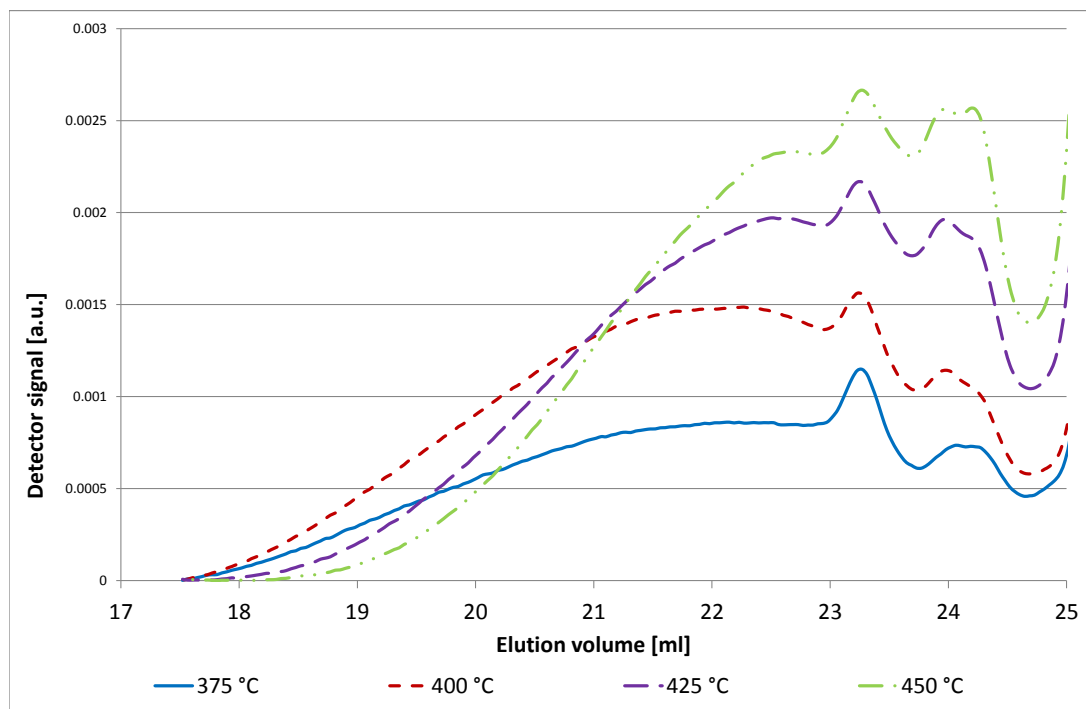
Figure 4.55.: Chromatograms of the temperature series, continuous experiments

Figure 4.56 and Figure 4.57 depict the results of the series with different reaction times. The reactions are carried out at 425 °C, and stopped after 0, 5, 10, 20 and 30 minutes, respectively.

Figure 4.56 shows the non-continuous experiments, Figure 4.57 shows the continuous series. Basically, the same trends as above are observed.

There are obviously no major changes in functional groups, as the positions and shapes of the peaks do not change, and there is a small shift to lower molecular masses with longer reaction times, because the slope at approx. 18.5 ml shifts a little to later elution volumes. This trend is a little more pronounced in the continuous series.
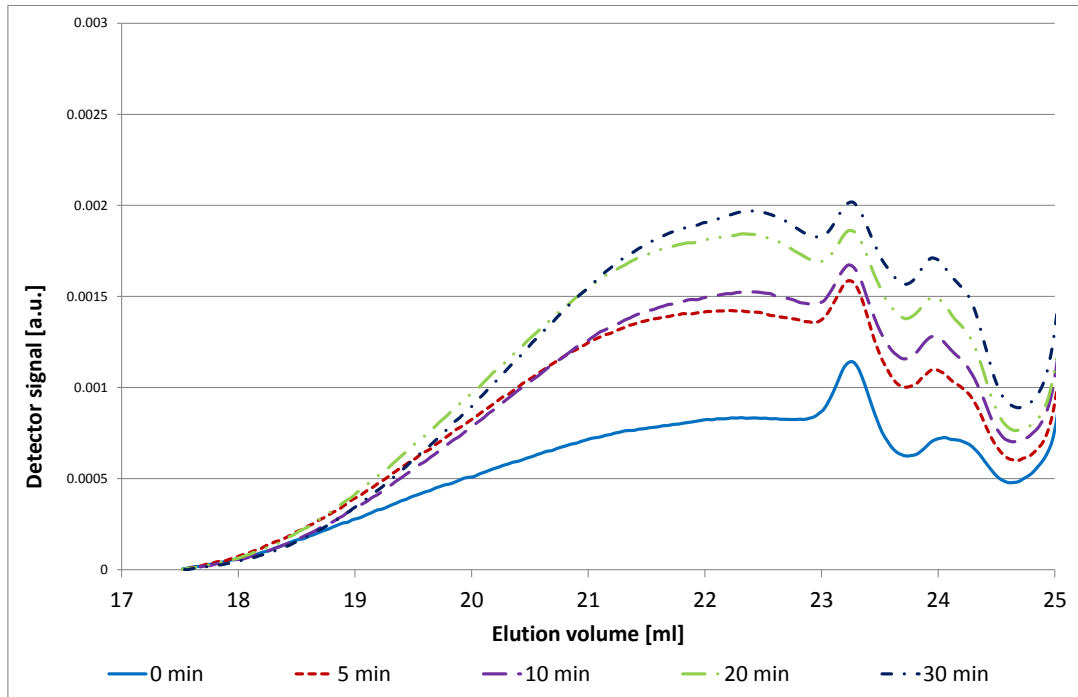
Figure 4.56.: Chromatograms of the time series, non-continuous experiments
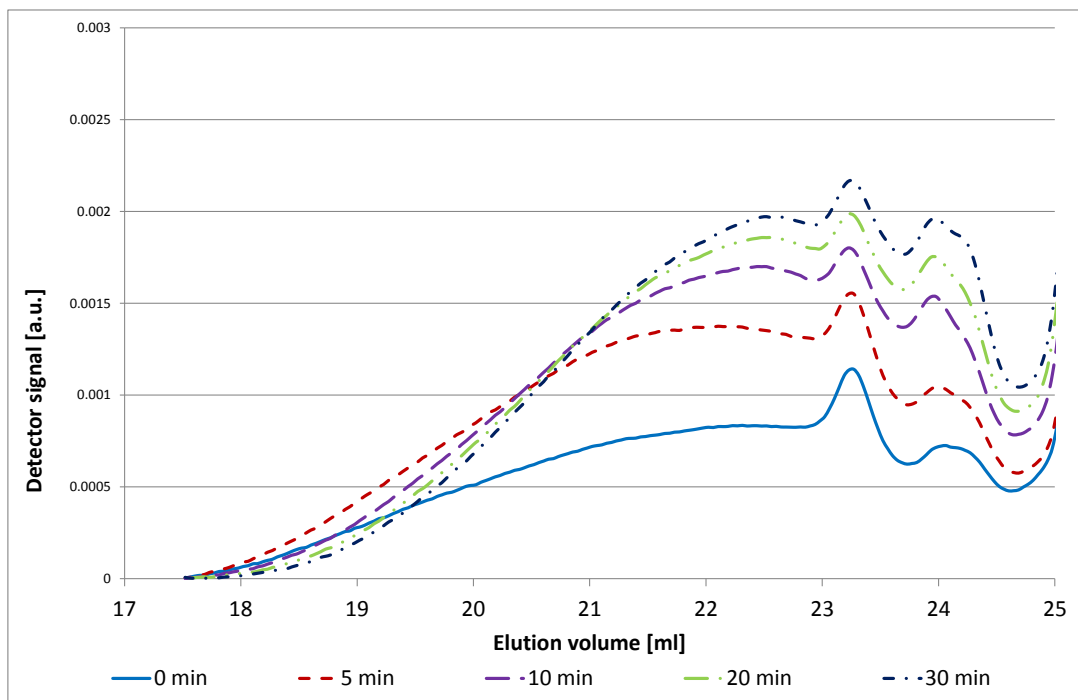
Figure 4.57.: Chromatograms of the time series, continuous experiments

To sum up, for the time series as well as for the temperature series, no major differences are observed in the chromatograms between the continuous and the non-continuous experiments. This observation means that the additionally-supplied hydrogen cannot be used. A possibility for further experiments can be the investigation of transport phenomena in the reaction mixture. For these investigations, the stirring speed could be varied, and the ratio of bio-char to solvent can be varied, thus changing the viscosity.

Furthermore, with these experimental series, it is shown that GPC is a useful tool to compare different products. Unfortunately, no quantitative statements can be made, and the chromatograms have to be interpreted with caution. However, if the experiments are similar concerning feed, reaction time, conditions like pressure, temperature and stirring speed, it is possible to compare the spectra and draw conclusions.

5. Summary

The present work describes:

- the implementation of the gel permeation chromatography, GPC, analysis system for the analysis of pyrolysis oils samples

- the investigation of the storage stability and aging behavior of pyrolysis oil, hydrodeoxygenated oil and coal liquefaction oil.

For the implementation of the GPC analysis system, the eluent is chosen to be tetrahydrofuran with 0.1 vol% trifluoroacetic acid, in order to always protonate all molecules. The eluent flow is set to 1 ml/min and the analysis time is set to 30 min per sample.

The processing of the data is developed: a calibration is used to relate the elution volume to the molecular mass, the integration boundaries are chosen, a horizontal baseline is drawn and the detector signal is standardized to compensate for different sample concentrations.

The calibration is carried out with polystyrene standards with a weight average mass M_w of 162 g/mol, 360 g/mol, 570 g/mol, 972 g/mol and 1890 g/mol; the calibration curve is a cubic function. The measurements and the data processing are always done in exactly the same way in order to keep results comparable.

Furthermore, it is found that the GPC columns age and foul over time, leading to earlier elution volumes. New calibrations should compensate for this effect. However, it is found that the elution volume of the polystyrene calibration standards shift more over time than the elution volumes of the actual samples. For that reason, the first calibration is always used for all samples, and samples of the same experimental series are measured within a short time span.

Moreover, various non-idealities are observed:

- Quantification of mass fractions of bio-oils is not possible, since compounds with different detection behavior are present. Some compounds have a very high refractive index and response factor α concerning the detection, yielding a very high signal when contained in small amounts. Some other compounds have a very low refractive index and response factor α, yielding a very small signal.
  It is not possible to tell whether a given peak is caused by a major compound yielding a small signal or a minor compound yielding a high signal.

- If the ratio of hydrodynamic volume to molecular mass of a molecule is smaller than the ratio of the polystyrene standards, the molecular mass of this substance will be underestimated. If the ratio is larger, the molecular mass will be overestimated.

- Apolar compounds tend to adsorb on the apolar columns packing rather than eluting with the polar eluent at the elution time they are expected to. Thus, they elute too late and their molecular mass is underestimated.

However, it is shown that GPC chromatograms of the same series of experiments can be compared in order to draw conclusions. Furthermore, it is possible to relate the elution volumes of the pyrolsis oils and the hydrodeoxygenated pyrolysis oils to the molecular mass.
In order to investigate the long-term stability of bio-oils, five experiments are conducted:

- two pyrolysis experiments

- one hydrodeoxygenation experiment

- two coal liquefaction experiments.

All the organic product phases are collected. They are stored in tightly closed glass bottles at room temperature in a dark box. The following analyses are carried out for the products of pyrolysis and hydrodeoxygenation:

- gas chromatography-mass spectroscopy measurements, GC-MS

- GPC measurements

- viscosity measurements

- acid concentration measurements

- pH-value measurements

- water content measurements

For the coal liquefaction products, only GPC analyses are carried out. All the analyses are done daily in the first week of storage, then weekly and later fortnightly.

In the case of the pyrolysis oils, the GC-MS investigations show a small decrease

of various molecules over time. The GPC measurements show a decrease in low-molecular mass compounds and a shift towards higher molecular masses. Moreover, the viscosity increase rate is 0.2 mPa s/d in the first week of storage, and then decreases to a rate of only 0.03 mPa s/d, which is approx. an order of magnitude lower.

The investigation of the acid concentration, pH-value and water content do not show any distinct trends within the variation of the experimental data. Thus, the pyrolysis oils are stable regarding acidity and water content, and no phase separation is observed during the storage time.

For the hydrodeoxygenated oil, the following trends are observed: According to GC-MS measurements, the concentration of some molecules exhibits a small increase over time, which may also be caused by sampling and measurement deviations.

The GPC measurements show the same trends as for the pyrolysis oils, but not as pronounced. Thus, concerning molecular mass, the hydrodeoxygenation step does stabilize the pyrolysis oils. However, the viscosity increase rate is higher with 0.5 mPa s/d. It does not change over storage time but stays constantly high. Regarding acid concentration, pH-value and water content, again no changes are observable.

Finally, in the case of the coal liquefaction products, the GPC chromatograms also show a shift to higher molecular masses and a decrease of the low molecular mass fractions.

6. Bibliography

[1]D. Mohan, C. U. J. Pittman, and P. H. Steele, "Pyrolysis of wood/biomass for bio-oil: a critical review", Energy & Fuels **20**, 848–889 (2006).

[2]D. Fengel and G. Wegener, "Wood - chemistry, ultrastructure and reactions", in (Verlag Kessel, 2003) Chap. Chemical Composition and Analysis of Wood, 26–65.

[3]D. Fengel and G. Wegener, "Wood - chemistry, ultrastructure and reactions", in (Verlag Kessel, 2003) Chap. Cellulose, 66–105.

[4]D. Fengel and G. Wegener, "Wood - chemistry, ultrastructure and reactions", in (Verlag Kessel, 2003) Chap. Polyoses (Hemicelluloses), 106–131.

[5]D. Fengel and G. Wegener, "Wood - chemistry, ultrastructure and reactions", in (Verlag Kessel, 2003) Chap. Lignin, 132–181.

[6]N. Schwaiger, V. Witek, R. Feiner, K. Zahel, A. Pieber, P. Pucher, E. Ahn, B. Chernev, H. Schroettner, P. Wilhelm, and M. Siebenhofer, "Formation of liquid and solid products from liquid phase pyrolysis", Bioresource Technology **124**, 90–94 (2012).

[7]N. Schwaiger, R. Feiner, K. Zahel, A. Pieber, V. Witek, P. Pucher, E. Ahn, P. Wilhelm, B. Chernev, H. Schroettner, and M. Siebenhofer, "Liquid and solid products from liquid-phase pyrolysis of softwood", Bioenerg. Res. **4**, 294–302 (2011).

[8]N. Schwaiger, "Reaktionstechnische analyse für die optimierung der flüssigphasen-pyrolyse", PhD thesis (Graz University of Technology, 2011).

[9]P. Mortensen, J.-D. Grunwaldt, P. Jensen, K. Knudsen, and A. Jensen, "A review of catalytic upgrading of bio-oil to engine fuels", Applied Catalysis, A: General **407**, 1–19 (2011).

[10]H. Pucher, N. Schwaiger, R. Feiner, P. Pucher, L. Ellmaier, M. Derntl, T. Glatz, L. Steiner, J. Redlinger-Pohn, A. Toth, A. Prettner, and M. Siebenhofer, "Catalytic hydrodeoxygenation of dehydrated liquid phase pyrolysis oil", unpublished, 2013.

[11]R. H. Venderbosch, A. R. Ardiyanti, J. Wildschut, A. Oasmaa, and H. Heeres, "Stabilization of Biomass-derived Pyrolysis Oils", J. Chem. Technol. Biotechnol. **85**, 674–686 (2010).

[12] J. Wildschut, F. H. Mahfud, R. H. Venderbosch, and H. J. Heeres, "Hydrotreatment of Fast Pyrolysis Oil using Heterogeneous Noble-Metal Catalysts", Ind. Eng. Chem. Res. **48**, 10324–10334 (2009).

[13] F. De Miguel Mercarder, P. Koehorst, H. Heeres, S. R. Kersten, and J. Hogendoorn, "Competition between hydrotreating and polymerization reactions during pyrolysis oil hydrodeoxygenation", AIChE Journal **57**, 3160–3170 (2011).

[14] J. G. Speight, "The chemistry and technology of coal", in, edited by H. Heinemann, 3rd ed., Chemical Industries 132 (CRC Press, 2013) Chap. Classification, 37–58.

[15] J. G. Speight, "The chemistry and technology of coal", in, edited by H. Heinemann, 3rd ed., Chemical Industries 132 (CRC Press, 2013) Chap. An Organic Sediment, 59–100.

[16] J. Jones, M. Pourkashanian, C. Rena, and A. Williams, "Modelling the relationship of coal structure to char porosity", Fuel **78**, 1737–1744 (1999).

[17] S. Vasireddy, B. Morreale, A. Cugini, C. Song, and J. J. Spivey, "Clean liquid fuels from direct coal liquefaction: chemistry, catalysis, technological status and challenges", Energy Environ. Sci. **4**, 311–345 (2011).

[18] J. G. Speight, "The chemistry and technology of coal", in, edited by H. Heinemann, 3rd ed., Chemical Industries 132 (CRC Press, 2013) Chap. Liquefaction, 545–578.

[19] T. Kaneko, F. Derbyshire, E. Makino, D. Gray, and M. Tamura, *Coal liquefaction* (Wiley-VCH Verlag GmbH & Co. KGaA, 2005).

[20] J. P. Diebold, *A review of the chemical and physical mechanisms of the storage stability of fast pyrolysis bio-oils*, tech. rep. (National Renewable Energy Laboratory NREL, Stefan Czernik, 2000).

[21] A. Streitwieser, C. Heathcock, and E. Kosower, *Introduction to organic chemistry*, edited by P. Corey, 4th ed. (Macmillan Publishing Compnay, 1992).

[22] A. Oasmaa and E. Kuoppala, "Fast pyrolysis of forestry residue. 3. storage stability of liquid fuel", Ener **17**, 1075–1084 (2003).

[23] A. Oasmaa and C. Peacocke, *Properties and fuel use of biomass-derived fast pyrolysis liquids*, edited by M. Pullinen (VTT PUBLICATIONS 731, 2010).

[24] R. N. Hilten and K. C. Das, "Comparison of three accelerated aging procedures to assess bio-oil stability", Fuel **89**, 2741–2749 (2010).

[25] *ASTM E2009 - 08 Standard Test Method for Oxidation Onset Temperature of Hydrocarbons by Differential Scanning Calorimetry*, American Society for Testing and Materials, (2002) http://www.astm.org/Standards/E2009.htm.

[26] M. Otto, "Analytical Chemistry - A Modern Approach to Analytical Science", in, edited by R. Kellner, J.-M. Mermet, M. Otto, M. Valcárcel, and H. Widmer (Wiley-VCH Verlag GmbH & Co. KGaA, 2004) Chap. 21 - Chromatography, 523.

[27] E. Hoekstra, S. R. Kersten, A. Tudos, D. Meier, and K. J. Hogendoorn, "Possibilities and pitfalls in analyzing (upgraded) pyrolysis oil by size exclusion chromatography (sec)", Journal of Analytical and Applied Pyrolysis 91, 76–88 (2011).

[28] T. Glatz, "Aufbereitung von produkten aus der flüssigphasenpyrolyse in minireaktoren", MA thesis (Graz University of Technology, 2013).

[29] M. Otto, "Analytical Chemistry - A Modern Approach to Analytical Science", in, edited by J.-M. Mermet, M. Otto, M. Valcárcel, R. Kellner, and H. Widmer, 2nd ed. (Wiley-VCH Verlag GmbH & Co. KGaA, 2004) Chap. Basic Statistics, 91–120.

[30] D. R. Lide, ed., *Crc handbook of chemistry and physics*, 84th ed. (CRC Press, 2003).

A. Appendix

Table A.1.: Calibration curve coefficients

	a	b	c
Hydroxypropanone	-0.7811359	6058.776	506355.1
Cyclopentanol	-1.151606	9449.285	1172875
1,2-Propanediol	-1.030303	8179.182	1814255
Furfural	-1.251033	8566.401	808939.1
γ-Butyrolactone	-0.4455992	4364.079	515157.6
2-Hydroxy-3-methyl-2-cyclopenten-1-one	-0.9360017	9601.331	504999.7
Phenol	-1.721259	11065.22	1422216
Guaiacol	-1.383553	10063.13	1561159
2,6-Xylenol	-1.789921	11942.95	2125590
2-Methoxy-4-methylphenol	-1.573043	10993.64	1735628
2-Methoxy-4-propylphenol	-1.795652	11691.59	2091075
Isoeugenol	-1.101758	9261.718	1867282
Levoglucosan	-0.662466	8338.851	-15077.1

Table A.2.: List of chemicals

Substance	Purity [%]	Company
1,2-Propanediol	99.5	SAFC
2,6-Xylenol	100	Merck
2-Hydroxy-3-methyl-2-cyclopenten-1-one	98	Merck
2-Methoxy-4-methylphenol	99	Aldrich
2-Methoxy-4-propylphenol	99	Sigma-Aldrich
Anthracene	99	Fluka
Cyclopentanol	99	Aldrich
Decalin	98	Merck
Fluoranthene	99	Aldrich
Furfural	100	Merck
γ-Butyrolactone	99	Aldrich
Guaiacol	99.5	Merck
Hydroxypropanone	90	Aldrich
Isoeugenol	99	Sigma-Aldrich
Levoglucosan	100	Merck
Naphthalene	100	Aldrich
Perylene	99	Fluka
Phenanthrene	96	Sigma
Phenol	99.5	Merck
Polystyrene	100	PSS
Pyrene	99	Aldrich
Sodium hydroxide	0.1 M	Roth
Tetrahydrofuran	99.9	Roth
Tetralin	98	Merck
Toluene	100	Roth
Trifluoroacetic acid	99.5	Merck